

REPORT DOCUMENTATION PAGE

AFOSR-TR-97

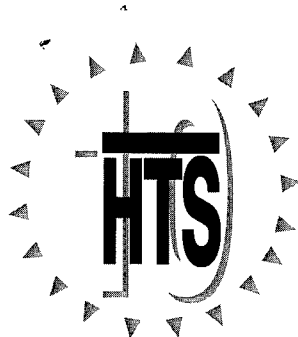
97

0085

Sources
of this
Jefferson

Public reporting burden for this collection of information is estimated to average 1 hour per response, including gathering and maintaining the data needed, and completing and reviewing the collection of information, collection of information, including suggestions for reducing this burden, to Washington Headquarters Service, Davis Highway, Suite 1204, Arlington, VA 22202-4302, and to the Office of Management and Budget, Paper

1. AGENCY USE ONLY (Leave blank)		2. REPORT DATE	3. REPORT TYPE AND DATES COVERED FINAL REPORT 15 Feb 96 - 14 Aug 96	
4. TITLE AND SUBTITLE TENTH ANNIVERSARY HTS WORKSHOP ON PHYSICS, MATERIALS AND APPLICATIONS			5. FUNDING NUMBERS 61102F 2305/GS	
6. AUTHOR(S) Professor Chu			7. PERFORMING ORGANIZATION NAME(S) AND ADDRESS(ES) University of Houston Texas Center for Superconductivity Houston Science Center Houston, TX 77204-5932	
8. AUTHOR(S)			9. SPONSORING / MONITORING AGENCY NAME(S) AND ADDRESS(ES) AFOSR/NE 110 Duncan Avenue Suite B115 Bolling AFB DC 20332-8050	
10. SPONSORING / MONITORING AGENCY REPORT NUMBER F49620-96-1-0048			11. SUPPLEMENTARY NOTES	
12a. DISTRIBUTION / AVAILABILITY STATEMENT APPROVED FOR PUBLIC RELEASE: DISTRIBUTION UNLIMITED			12b. DISTRIBUTION CODE	
13. ABSTRACT (Maximum 200 words) Tenth Anniversary HTS Workshop on Physics, Materials and Applications was held 12-16 March 1996 in Houston, Texas				
<p>19970218 078</p>				
14. SUBJECT TERMS			15. NUMBER OF PAGES	
17. SECURITY CLASSIFICATION OF REPORT UNCLASSIFIED			16. PRICE CODE	
18. SECURITY CLASSIFICATION OF THIS PAGE UNCLASSIFIED		19. SECURITY CLASSIFICATION OF ABSTRACT UNCLASSIFIED		20. LIMITATION OF ABSTRACT



ABSTRACTS
10th Anniversary HTS Workshop
on Physics, Materials and Applications

March 12-16, 1996
Doubletree Hotel at Allen Center
Houston, Texas

Workshop Sponsors



Air Force Office
of Scientific Research



Apple Computers



Department of Energy

EPRI

Electric Power
Research Institute

Electric Power Research Institute



Global Services

Houston Chronicle

Houston Chronicle



National Science Foundation



Texas Center for Superconductivity
at the University of Houston



University of Houston

Organizing Committees

International Advisory Committee

P. W. Anderson (Princeton U), J. G. Bednorz (IBM Zürich), P. Chaudhari (IBM Yorktown Heights), M. L. Cohen (UC Berkeley), R. C. Dynes (UC San Diego), T. H. Geballe (Stanford U), K. Kitazawa (U Tokyo), M. V. Klein (U Illinois, Urbana-Champaign), B. Raveau (U Caen), J. R. Schrieffer (NHFML, Florida State U), S. Tanaka (ISTEC), M.-K. Wu (National Tsing Hua U), Z. X. Zhao (Chinese Academy of Sciences)

Program Committee

Co-Chairs: B. Batlogg (AT&T Bell Labs), W. K. Chu (TCSUH), D. Gubser (NRL)

U. Balachandran (Argonne), B. Batlogg (AT&T Bell Labs), M. Cardona (Max Planck Inst.), W. K. Chu (TCSUH), T. Claeson (Chalmers U of Technology), G. W. Crabtree (Argonne), J. Daley (DOE), F. de la Cruz (Centro Atómico Bariloche), G. Deutscher (Tel Aviv U), Ø. Fischer (U Geneva), H. Freyhardt (U Göttingen), H. Fukuyama (U Tokyo), J. B. Goodenough (UT Austin), P. M. Grant (EPRI), R. L. Greene (U Maryland), D. U. Gubser (NRL), R. A. Hawsey (Oak Ridge), H. C. Ku (National Tsing Hua U), D. C. Larbalestier (U Wisconsin, Madison), A. Lauder (DuPont), W.-Y. Liang (U Cambridge), K. K. Likharev (SUNY Stony Brook), A. P. Malozemoff (ASC), D. E. Peterson (Los Alamos), R. Ralston (MIT Lincoln Lab), C. N. R. Rao (Indian Institute of Science), T. M. Rice (ETH Hönggerberg), J. M. Rowell, T. R. Schneider (EPRI), D. T. Shaw (SUNY Buffalo), R. Sokolowski (IGC), C. S. Ting (TCSUH), M. Tachiki (Tohoku U, Sendai), H. Weinstock (AFOSR), H. Wickman (NSF), S. A. Wolf (NRL)

Local Committee

Co-Chairs: A. L. de Lozanne (UT Austin), D. G. Naugle (Texas A&M), K. Salama (TCSUH)

Workshop Secretary: S. W. Butler

W. K. Chu (TCSUH), A. L. de Lozanne (UT Austin), P.-H. Hor (TCSUH), A. Ignatiev (TCSUH), A. J. Jacobson (TCSUH), D. G. Naugle (Texas A&M U), K. Salama (TCSUH), C. S. Ting (TCSUH), J. C. Wolfe (TCSUH), Q. Xiong (U Arkansas, Fayetteville)

ABSTRACTS

10th Anniversary HTS Workshop on Physics, Materials and Applications

Co-Chairs: C. W. Chu & K. A. Müller

March 12-16, 1996
Doubletree Hotel at Allen Center
Houston, Texas

Contents

KEYNOTE ADDRESS	"Public Support for Science – Public Roles for Scientists," N. Lane	10
BANQUET ADDRESS	"Nanoscience and Technology," R. Smalley	10
PLENARY SESSIONS	11
Plenary Session 1	11
PL1.1	"The Development of Superconductivity Research in Oxides," K. A. Müller	11
PL1.2	"Superconductivity Above 90 K and Beyond," C. W. Chu	11
Plenary Session 2	11
PL2.1	"The Role of Vertex Corrections to the Pairing Interaction in Spin Fluctuation Superconductors," J. R. Schrieffer	11
PL2.2	"Superconductor and Semiconductors," Shoji Tanaka	11
Plenary Session 3	12
PL3.1	"Superconducting Electronics – The Next Decade," John M. Rowell	12
Plenary Session 4	12
PL4.1	"The Symmetry of the Order Parameter in the Cuprate Superconductors," Anthony J. Leggett, Nigel D. Goldenfeld and James F. Annett	12
PL4.2	"HTS Technology: The Road from Research to Applications," Carl Rosner	13
Plenary Session 5	13
PL5.1	"Critical Current Limiting Mechanisms in High Temperature Superconductor Conductor Forms," David C. Larbalestier	13
Plenary Session 6	14
PL6.1	"Applications of HTS to Electronics-A DoD Perspective," Stuart A. Wolf	14

Plenary Session 7	14
PL7.1 "Collective Behavior of Vortices in Superconductors," G. W. Crabtree , W. K. Kwok, U. Welp, J. A. Fendrich, H. G. Kaper, G. K. Leaf, A. E. Koshelev and V. M. Vinokur	14
CONCURRENT SESSIONS	15
Session A: HTS Properties	15
A.1 "Normal State Resistivity of Superconducting LaSrCuO in the Zero-Temperature Limit," Yoichi Ando , Gregory S. Boebinger, Albert Passner, Tsuyoshi Kimura, Jun-ichi Shimoyama and Kohji Kishio	15
A.2 "Transport Properties of Overdoped HTS at High Fields and Low Temperatures," Michael S. Osofsky , Robert J. Soulen, Jr., Stuart A. Wolf, Jean-Marc Broto, Harison Rakoto, Jean-Claude Ousset, Gilbert S. Coffe, Salomon Askenazy, Patrick Pari, Ivan Bozovic, James N. Eckstein, Gary F. Virshup, Joshua L. Cohn, S. Mao and Phillip Oswald	15
A.3 "'Spin Gap' Effects on the Charge Dynamics of HTSC," S. Uchida , K. Takenaka and K. Tamasaku	15
A.4 "Raman Spectroscopy of High T_c Superconductors," Manuel Cardona	15
A.5 "Magnetic and Structural Properties and Phase Diagrams of $Sr_2CuO_2Cl_2$ and Lightly-Doped $La_{2-x}Sr_xCuO_{4+\delta}$," David C. Johnston	16
A.6 "Enhanced Magnetic Response in the Superconducting State of $La_{1.86}Sr_{0.14}CuO_4$," Gabriel Aeppli	16
A.7 "Correlations Between T_c and n_s/m^* in High- T_c Cuprates," Y. J. Uemura	16
Session B: Bulk Applications	16
B.1 "Bulk Applications of HTS Wire," A. P. Malozemoff	16
B.2 "Progress and Issues in HTS Power Cables," Aldo F. Bolza	16
B.3 "125 hp HTS Synchronous Motor Design and Preliminary Test Results," David Driscoll	16
B.4 "Superconducting Homopolar Motor Demonstration," D. Gubser , L. Toth, M. Superczynski and D. Waltman	17
B.5 "Superconducting Magnetic Bearing and Its Application in Flywheel Kinetic Energy Storage," Z. Xia, K. B. Ma, R. Cooley, P. Fowler and W. K. Chu	17
B.6 "High Temperature Superconducting Fault Current Limiter," E. M. W. Leung	17
B.7 "Development of Technologically-Useful Superconducting Wires at 20K," David T. Shaw , T. Haugan, J. Ye, F. Wong, S. Patel and L. Motowidlo	17
Session C: Symmetry	17
C.1 "Josephson Tunneling Between a Conventional Superconductor and $YBa_2Cu_3O_{7-\delta}$," R. C. Dynes , A. G. Sun, A. S. Katz, A. Truscott, Solomon Woods, Don Gajewski, Sueng-Ho Han, M. B. Maple, B. W. Veal, C. Gu, J. Clarke, R. Kleiner, R. Summer, E. Dantsher and B. Chen	17
C.2 "Half-Integer Flux Quantum Effect and Pairing Symmetry in Cuprate Superconductors," C. C. Tsuei and John R. Kirtley	18
C.3 "Intrinsic SIS Josephson Junction in Bi-2212 and Symmetry of Cooper Pair," Keiichi Tanabe , Yoshikazu Hidaka, Shin-ichi Karimoto and Minoru Suzuki	18
C.4 "Magnetic Raman Scattering in Cuprate Antiferromagnetic Insulators and Doped Superconductors," Girsh E. Blumberg and Miles V. Klein	18
C.5 "STM Observation of the Vortex Lattice in $YBa_2Cu_3O_7$," I. Maggio-Aprile, Ch. Renner, A. Erb, E. Walker and Ø. Fischer	18
C.6 "Determination of the Pairing State of High- T_c Superconductors Through Measurements of the Transverse Magnetic Moment," Allen M. Goldman	19
C.7 "Excitation Gap in the Normal and Superconducting State of Underdoped Cuprate Superconductors," Z.-X. Shen	19
C.8 "Single Grain Boundary Josephson Junction Devices - New Insights from Basic Experiments," Jochen Mannhart , H. Hilgenkamp and B. Mayer	19
C.9 "What Does d-Wave Symmetry Tell Us About the Pairing Mechanism?," Kathryn Levin	19
C.10 "Impurity States in a d -Wave Superconductor," Marcel Franz , Catherine Kallin and John A. Berlinsky	19
Session D: HTS Materials	20
D.1 "Phase Stability, Defects, and Formation of $HgBa_2Ca_{n-1}Cu_nO_{2n+2+\delta}$," Y. Y. Xue , R. L. Meng, Q. Xiong, Q. M. Lin, I. Rusakova and C. W. Chu	20
D.2 "Stabilisation of New HTcS Cuprates and Oxycarbonates: From the Bulk Materials to the Thin Films," B. Raveau	20
D.3 "Quantum Spin Ladder Oxides," Mikio Takano	20
D.4 "Normal State Transport Properties of Tl-2201 Single Crystals," Allen M. Hermann , William Kiehl and Rafael Tello	20
D.5 "Superconductive Sr_2RuO_4 and Related Materials," Yoshiteru Maeno and Toshizo Fujita	21

D.6	"Electronic Phase Separations in $\text{La}_2\text{CuO}_{4+\delta}$," Pei-Herng Hor , Zu Gang Li, Hung Hsu Feng, Zhong Y. Yang, Alejandro Hamed and Shaw-Tsong Ting, S. Bhavaraju, J. F. DiCarlo and Allan J. Jacobson	21
D.7	"Borocarbide and Other Unusual Intermetallic Compounds," Robert J. Cava	21
D.8	"Strong Flux Pinning, Anisotropy and Microstructure of $(\text{Hg,Re})\text{M}_2\text{Ca}_{n-1}\text{Cu}_n\text{O}_y$ ($\text{M}=\text{Ba,Sr}$)," Jun-ichi Shimoyama , Koichi Kitazawa and Kohji Kishio	21
D.9	"Observations Relating to the Apical Bond in High T_c Oxides: Mercury Cuprates and Cupro-oxyfluorides," Peter P. Edwards	21
D.10	"A View on HTS Performances Under Magnetic Fields from the Key Term 'Anisotropy Factor,'" Koichi Kitazawa , Hiroshi Ikuta, Jun-ichi Shimoyama, Masayuki Okuya, Satoshi Watauchi and Kohji Kishio	21
Session E: HTS Theory I		22
E.1	"Numerical Results and the High T_c Problem: From Ladders to Planes," David J. Scalapino	22
E.2	"Spin Fluctuations, Magnetotransport and $d_{x^2-y^2}$ Pairing in the Cuprate Superconductors," David Pines	22
E.3	"Quantitative Explanation of 10 Peculiar Behaviors of High- T_c Superconductors Using 'Anyon' Approach to the t-J Hamiltonian," R. B. Laughlin	22
E.4	"Cuprate Ladder Compounds," T. M. Rice	22
E.5	"Charge Inhomogeneity and High Temperature Superconductivity," Victor J. Emery and Steven A. Kivelson	22
E.6	"Phase String and Superconductivity in the t-J Model," Z. Y. Weng	22
E.7	"Gauge Theory of the Normal State Properties of High- T_c Cuprates," Naoto Nagaosa	23
E.8	"Superconductivity in the Cuprates as a Consequence of Antiferromagnetism and a Large Hole Density of States," Elbio R. Dagotto , Alexander Nazarenko and Adriana Moreo	23
E.9	"Superconductivity and the Square Fermi Surface," Alan H. Luther	23
E.10	"A Possible Primary Role of the Oxygen Polarizability in High Temperature Superconductivity," M. Weger and M. Peter	23
E.11	"A Complete Pairing Mechanism in Superconductivity," J. D. Fan and Y. M. Malozovsky	23
Session F: HTS Processing		24
F.1	"Progress of HTS Bismuth-Based Tape Application," Ken-ichi Sato	24
F.2	"Strong Flux Pinning in RE123 Grown by Oxygen-Controlled Melt Process," Noriko Chikumoto and Masato Murakami	24
F.3	"IBAD Deposition of Thick Film Superconductors," Dean E. Peterson , Paul Arendt, Xin Di Wu and Stephen R. Foltyn	24
F.4	"Fabrication of $\text{HgBa}_2\text{Ca}_2\text{Cu}_3\text{O}_{8+\delta}$ Tape," R. L. Meng , B. Hickey, Y. Q. Wang, L. Gao, Y. Y. Sun, Y. Y. Xue and C. W. Chu	24
F.5	"New Process to Control Critical Currents of $\text{Nd}_{1-x}\text{Ba}_{2-x}\text{Cu}_3\text{O}_{7-\delta}$," Yuh Shiohara , M. Nakamura, Y. Yamada, T. Hirayama and Y. Ikuhara	24
F.6	"Improvement of Flux Pinning in High Temperature Superconductors by Artificial Defects," Harald W. Weber	25
F.7	"HTS Conductors: Challenges and Progress," Leszek Motowidlo, Robert S. Sokolowski, Pradeep Haldar and Venkat Selvamanickam	25
F.8	"A Novel Approach to High Rate Melt-Texturing in 123 Superconductors," Kamel Salama	25
F.9	"Processing and Properties of Ag-Clad BSCCO Superconductors," U. Balachandran , Anand N. Iyer, R. Jammy and P. Haldar	25
F.10	"Grain Boundary Misorientation Distributions and Percolation in HTS Conductors," D. M. Kroeger , A. Goyal and E. D. Specht	26
Session G: HTS Theory II		26
G.1	"Current Fluctuations in Copper-Oxide Metals," Chandra M. Varma	26
G.2	"Aspects of D-Wave Superconductivity," Kazumi Maki , Ye Sun and Hyekeyung Won	26
G.3	"Ginzburg-Landau Theory of Superconductors with $d_{x^2-y^2}$ Symmetry," C. S. Ting , Y. Ren and J. H. Xu	26
G.4	"Inside HT_c Superconductors: An Electronic Structure View," Arthur J. Freeman and Dmitri L. Novikov	26
G.5	"Energy Spectrum and 'Intrinsic' T_c of the Cuprates: Effects of Pair-Breaking, Pressure, and Non-Adiabaticity," Vladimir Z. Kresin , Stuart A. Wolf and Yurii N. Ovchinnikov	27
G.6	"Localized States as an Explanation of Some Properties of Cuprates," Michel Cyrot	27
G.7	"Thermopower of the Cuprates Under High Pressure," J. B. Goodenough and J.-S. Zhou	27
G.8	"Hole Spectrum in Three Band Model," Lev P. Gor'kov and Pradeep Kumar	27
G.9	"Quasiparticles, Strong-Coupling Regime and Fermi Liquid Theory Breakdown," Alvaro Ferraz and Yoshi Ohmura	27
Session H: Film & Applications		28
H.1	"Synthesis of Novel High- T_c Superconductors by Atomic-Layer Epitaxy," Ivan Bozovic and James N. Eckstein	28

H.2	"Very High Growth Rates of High Quality YBCO Under Photo-Assisted MOCVD," Alex Ignatiev , Q. Zhong and P. C. Chou	28
H.3	"Ultrafast Superconductor Digital Electronics," Konstantin K. Likharev	28
H.4	"In-Plane and C-Axis Linear and Nonlinear Microwave Response of Cuprate Superconductors," S. Sridhar	28
H.5	"Fabrication of Highly Textured Superconducting Thin Films on Polycrystalline Substrates Using Ion Beam Assisted Deposition," Quan Xiong , Sergio Afonso, F. T. Chan, Kai Y. Chen, G. J. Salamo, G. Florence, Simon Ang, W. D. Brown and L. Schaper	29
H.6	"Biaxially Textured YBaCuO Thick Films on Technical Substrates," Herbert C. Freyhardt , Jürgen Wiesmann, Klaus Heinemann, Jörg Hoffmann, Jürgen Dzick, Alexander Usokin, Francesco Garcia-Moreno and Sybille Sievers	29
H.7	"Fabrication of High Quality Hg-1223 Thin Films Using Rapid Thermal Hg-Vapor Annealing," Judy Z. Wu , Sangho Yun, Steve C. Tidrow and Don Eckart	29
H.8	"Near-Term Commercialization of HTS Technology at Conductus," Randy Simon	29
Session I: Properties & Theory		30
I.1	"Enhancements of HTS Conductor Critical Currents by Splayed Columnar Tracks from Fission Fragments," Martin P. Maley , Hugo F. Safar, Lev N. Bulaevskii, Jeffrey O. Willis, Jin H. Cho, Yates J. Coulter and Stephen Flesher	30
I.2	"New Aspects of Vortex Dynamics," Anne van Otterlo , Vadim Geshkenbein and Gianni Blatter	30
I.3	"Numerical Studies on the Vortex Motion in High- T_c Superconductors," Z. D. Wang	30
I.4	"Effects Of 5.8 GeV Pb Irradiation on Magnetic Vortex Dynamics of Bi (2212 and 2223) Tapes," Y. Fukumoto, Y. Zhu, Q. Li, Masaki Suenaga , T. Kaneko, K. Sato, K. Shibutani and Ch. Simmon	30
I.5	"Phonon Anomaly in High Temperature Superconducting YBa ₂ Cu ₃ O _{7-δ} Crystals," R. P. Sharma , Z. H. Zhang, J. R. Liu, R. Chu, T. Venkatesan and W. K. Chu	30
I.6	"Unusual Magnetic Field Dependence of the Electrothermal Conductivity in Cuprate Superconductors," Jeffrey A. Clayhold , Y. Y. Xue, C. W. Chu, J. N. Eckstein and I. Bozovic	31
I.7	"Electrodynamical Properties of High- T_c Superconductors Studied with Angle Dependent Infrared Spectroscopy," D. van der Marel and A. Menovsky	31
I.8	"Transport in the ab-Plane of HTSC, New Results," Thomas Timusk	31
I.9	"Properties of Li-Doped La ₂ CuO ₄ ," Zachary Fisk , J. L. Sarrao, P. C. Hammel, Y. Yoshinari and J. D. Thompson	31
I.10	"Structures and Excitations in Monolayer Copper Oxides," Robert J. Birgeneau	31
I.11	"Recent Neutron Scattering Results on YBa ₂ Cu ₃ O _{7-δ} ," Herb A. Mook , Pengcheng Dai, Gabriel Aeppli, F. Dogan and K. Salama	31
Session J: Materials & Properties		32
J.1	"The Electronic Structure of the High Temperature Superconductors as Seen by Angle-Resolved Photoemission," Juan Carlos Campuzano , Hong Ding, Michael Norman, Mohit Randeria and Takashi Takahashi	32
J.2	"Microwave Measurements of the Penetration Depth in High T_c Single Crystals," Walter N. Hardy , Saeid Kamal, Ruixing Liang, Douglas A. Bonn, Chris C. Homes, Dimitri Basov and Tom Timusk	32
J.3	"Specific Heat of YBa ₂ Cu ₃ O _{7-δ} ," Kathryn A. Moler , David L. Sisson, Aharon Kapitulnik, David J. Baar, Ruixing Liang and Walter N. Hardy	32
J.4	"Specific Heat of HTS in High Magnetic Fields," Alain R. Junod	32
J.5	"Thermodynamic Evidence on the Superconducting and Normal State Energy Gaps in La _{2-x} Sr _x CuO ₄ and Y _{0.8} Ca _{0.2} Ba ₂ Cu ₃ O _{6+x} ," John W. Loram , K. A. Mirza, J. R. Cooper, N. Athanassopoulou, W. Y. Liang and Jeffery L. Tallon	33
J.6	"Scattering Time: A Unique Property of High- T_c Cuprates," Ichiro Terasaki , Yoshibumi Sato and Setsuko Tajima	33
J.7	"Heat Transport in High- T_c Perovskites - Effect of Magnetic Field," Ctirad Uher	33
J.8	"Thermoelectric Power: A Simple, Highly Instructive Probe of High- T_c Superconductors," Jeffrey L. Tallon	33
J.9	"High Pressure Study on Hg-Based Cuprates," F. Chen , X. D. Qiu, Y. Cao, L. Gao, Q. Xiong, Y. Y. Xue and C. W. Chu	33
J.10	"Structural Control of Transition Temperature and Flux Pinning in High- T_c Superconductors," James D. Jorgensen	34
J.11	"The Effect of Pressure on Superconducting Copper Mixed Oxides," Massimo Marezio	34
Session K: Vortex, etc.		34
K.1	"Thermodynamic Vortex-Lattice Phase Transitions in BSCCO," Eli Zeldov	34
K.2	"Pancake Vortices in High-Temperature Superconducting Thin Films," John R. Clem , Maamar Benkraouda and Thomas Pe	34
K.3	"Correlation Lengths in the Flux Line Lattice of Type-II Superconductors," Peter L. Gammel	34

K.4	"Magnetoresistivity of Thin Films of the Electron-Doped High T_c Superconductor $Nd_{1.85}Ce_{0.15}CuO_{4\pm\delta}$," Jan Hermann, Marcio C. de Andrade, Carmen C. Almasen, M. Brian Maple , Wu Jiang, Sining N. Mao and Richard L. Greene	35
K.5	"Comparative Study of Vortex Correlation in Twinned and Untwinned $YBa_2Cu_3O_{7-\delta}$ Single Crystals," Esteban Righi, Francisco de la Cruz , Daniel Lopez, Gladys Nieva, W. K. Kwok, J. A. Fendrich, G. W. Crabtree and L. Paulius	35
K.6	"High-Pressure Raman Study of the Mercury-Based Superconductors and the Related Compounds," In-Sang Yang and Hye-Gyong Lee	35
K.7	"Very High Trapped Fields: Cracking, Creep and Pinning Centers," Roy Weinstein , Charles C. Foster and Victor Obot	35
K.8	"Local Texture, Current Flow, and Superconductive Transport Properties of Tl1223 Deposits on Practical Substrates," D. K. Christen	35
K.9	"Muon Spin Rotation Studies of Magnetism in $La_{2-x}Sr_xCuO_4$ and $Y_{1-x}Ca_xBa_2Cu_3O_5$," Christof Niedermayer, Joseph I. Budnick and Bernhard Christian	36
K.10	"X-Ray Search for CDW In Single Crystal $YBa_2Cu_3O_{7-\delta}$," Peter Wochner, E. Isaacs, Simon Moss , Paul Zschack, J. Giapintzakis and D. M. Ginsberg	36

Session L: Film & Properties **36**

L.1	"HTS SQUIDS and Their Applications," John Clarke	36
L.2	"SQUID Imaging," John R. Kirtley , Chang C. Tsuei and Kathryn A. Moler	37
L.3	"Imaging of Superconducting Vortices with a Magnetic Force Microscope," Alex de Lozanne, Chun Che Chen , Qinyou Lu, Caiwen Yuan, David A. Rudman, James N. Eckstein and Marco Tortonese	37
L.4	"Electronic Eyes Based on Dye/Superconductor Assemblies," John T. McDevitt , David C. Jurbergs, Steven M. Savoy, S. Eames and J. Zhao	37
L.5	"The Search for Broken-Time-Reversal-Symmetry in High- T_c Superconductors: Status Report," Aharon Kapitulnik	37
L.6	"Pressure Effect on the Superconducting and Normal-State Properties for the YBCO/PBCO Superlattice," J. G. Lin , M. L. Lin, H. C. Yang, Z. J. Huang and C. Y. Huang	37
L.7	"Magnetocardiography in a Magnetically Noisy Environment Using High- T_c SQUIDS," John H. Miller, Jr. , Nilesh Traishawala, James Claycomb and Ji-Hai Xu	38
L.8	"Pinning and Anisotropy Properties of High- T_c Microcrystals by Miniaturized Torquemeter," C. Rossel , P. Bauer, D. Zech, J. Hofer and H. Keller	38
L.9	"HTS Materials for High Power rf and Microwave Applications," Dean W. Face , Charles Wilker, Zhi-Yaun Shen and Philip S. W. Pang	38
L.10	"High-Accuracy Specific-Heat Study on $YBa_2Cu_3O_7$ and $Bi_2Sr_2CaCu_2O_8$ Around T_c in External Magnetic Fields," Andreas Schilling , Oliver Jeandupeux, Cristoph Wälti, Anne van Otterlo and Hans-Rudolf Ott	38

POSTER SESSIONS **39**

Poster Sessions 1A : HTS Theory, Experiment, Material, & Properties **39**

P1A.1	"Anomalous Charge-Excitation Spectra in t-J and Hubbard Models," T. K. Lee , Y. C. Chen, R. Eder, H. Q. Lin, Y. Ohta and C. T. Shih	39
P1A.2	"Exact Diagonalization Study of the Single Hole t-J Model on a 32-Site Lattice," P. W. Leung and Robert J. Gooding	39
P1A.3	"Electronic Properties of the Layered Cuprates," Nejat Bulut	39
P1A.4	"Electron-Spin Diffusion Constant as Diagnostics for Spin-Charge Separation in the Metallic Cuprates," Qimiao Si	39
P1A.5	"Magnetic Frustration and Spin-Charge Separation in 2D Strongly Correlated Electron Systems," William Putikka	39
P1A.6	"Magnetic Excitation in High- T_c Cuprates," Hiroshi Kohno , Bruce Normand and Hidetoshi Fukuyama	40
P1A.7	"Thermodynamics of d-Wave Pairing in Cuprate Superconductors," S. P. Kruchinin	40
P1A.8	"Coupled States in Electron-Phonon System of HTSC Crystals," S. P. Kruchinin and A. M. Yaremko	40
P1A.9	"Neutron Scattering: A Signature of the Gap Symmetry in High- T_c Superconductors," Andreas Bill , Vladimir Hizhnyakov and Ernst Sigmund	40
P1A.10	"Anisotropy of the Gap Induced by Unscreened Long Range Interactions," Vladimir Hizhnyakov, Andreas Bill and Ernst Sigmund	40
P1A.11	"Boundary Effects and the Order Parameter Symmetry of HTC Superconductors," Safi R. Bahcall	40
P1A.12	"The Ginzburg-Landau Equations for d-Wave Superconductors with Nonmagnetic Impurities," C. S. Ting, W. Xu and Y. Ren	41
P1A.13	"Inter-Band Pairing: Resolution of Observed d-Wave and s-Wave Tunneling with Isotropic s-Wave Pairing," Jamil Tahir-Kheli	41
P1A.14	"Effects of Impurity Vertex Correction on NMR Coherence Peak of Conventional Superconductors," Han-Yong Choi	41
P1A.15	"Comparison of Three-Band and t-t'-J Model Calculations of the One-Hole Spectral Function in an Antiferromagnet with Photoemission Experiments," George Reiter and Oleg A. Starykh	41
P1A.16	"c-Axis Electronic Structure and Transport in Copper-Oxides," Joseph M. Wheatley and J. R. Cooper	41
P1A.17	"Paramagnetic Meissner Effect and Time Reversal Non-Invariance from Spin Polarization," Alpo Kallio , Viktor Sverdlove and Martti Rytivaara	41

P1A.18	“Hall-Effect Scaling and Chemical Equilibrium in Normal States of High- T_c Superconductors,” Alpo Kallio , Viktor Sverdlove and Carolina Honkala	42
P1A.19	“Spin-Susceptibility of Strong Correlated Bands in Fast Fluctuating Regime,” Mikhail Eremin	42
P1A.20	“Pairing Instability and Anomalous Response in an Interacting Fermi Gas,” Y. M. Malozovsky and J. D. Fan	42
P1A.21	“The Connections of the Experimental Results of Universal Stress Experiments and of Thermal Expansion Measurements and the Mechanisms of Microscopic Dynamics Process on CuO_2 Planes,” Dawei Zhou	42
P1A.22	“Phenomenology: What the Data Say,” John D. Dow	43
P1A.23	“Current Instabilities in Reentrant Superconductors,” David Frenkel and Jeffrey Clayhold	43
P1A.24	“Time-Window Extension for Magnetic Relaxation from Magnetic-Hysteresis-Loop Measurements,” Qianghua Wang, Xixian Yao, Z. D. Wang and Jian-Xin Zhu	43
P1A.25	“Numerical Study of Washboard Effect in High- T_c Superconductors,” Z. D. Wang and K. M. Ho	43
P1A.26	“Vortex Vacancy Motion as the Origin of the Hall Anomaly,” Ping Ao	44
P1A.27	“Vortex Dynamics in Superfluids: Cyclotronic Motion,” Ertugrul Demircan , Ping Ao and Niu Qian	44
P1A.28	“Zero-Bias (Tunneling-)Conductance Peak (ZBCP) as a Result of Midgap <u>Interface</u> States (MISs) – Model Calculations,” Chia-Ren Hu	44
Poster Sessions 1B: HTS Theory, Experiment, Material, & Properties		44
P1B.1	“Low Temperature Scanning Tunneling Microscopy and Spectroscopy of the CuO Chains in $\text{YBa}_2\text{Cu}_3\text{O}_{7-x}$,” David J. Derro , Tamotsu Koyano, Alex Barr, John T. Markert and Alex L. de Lozanne	44
P1B.2	“Momentum Dependence of the Superconducting Gap of $\text{Bi}_2\text{Sr}_2\text{CaCu}_2\text{O}_8$,” J. C. Campuzano, Hong Ding , M. R. Norman, M. Randeria, A. F. Bellman, D. Ginsberg, T. Yokoya, T. Takahashi, H. Katayama-Yoshida, T. Mochiku and K. Kadowaki	44
P1B.3	“Use of Tricrystal Microbridges to Probe the Pairing State Symmetries of Cuprate Superconductors,” John H. Miller, Jr., Jiangtao Lin , Zhongji Zou and Quan Xiong	45
P1B.4	“Ground State of Superconducting LaSrCuO in 61-Tesla Magnetic Fields,” Gregory S. Boebinger , Yoichi Ando, Albert Passner, Masayuki Okuya, Tsuyoshi Kimura, Jun-ichi Shimoyama, Kohji Kishio, Kenji Tamasaku, Noriya Ichikawa, Shin-ichi Uchida, Igor E. Trofimov, Fedor F. Balakirev and P. Lindenföld	45
P1B.5	“Behavior of ScN and ScS Contacts Under Microwave Irradiation,” Alexei B. Agafonov , Dimitriy A. Dikin, Andrei L. Solovjov and Vitaly M. Dmitriev	45
P1B.6	“Electronic Raman Scattering in $\text{YBa}_2\text{Cu}_4\text{O}_8$ at High Pressure,” Tao Zhou , Karl Syassen and Manuel Cardona	45
P1B.7	“Raman Scattering on $\text{HgBa}_2\text{Ca}_{n-1}\text{Cu}_n\text{O}_{2n+2+\delta}$ ($n=1,2,3,4,5$) Superconductors,” Xingjiang Zhou , Manuel Cardona, C. W. Chu and Q. M. Lin	46
P1B.8	“Anisotropy of Thermal Conductivity of YBCO and Selectively Doped YBCO Single Crystals,” Partick F. Henning , Jack E. Crow and Gang Cao	46
P1B.9	“Thermal Conductivity of High- T_c Superconductors,” Michel Houssa and Marcel Ausloos	46
P1B.10	“Dielectric Anomaly of $\text{La}_{2-x}\text{Sr}_x\text{CuO}_4$ Film at $x=1/4^n$,” Masanori Sugahara	46
P1B.11	“Angular Dependence of the c-Axis Normal State Magnetoresistance in Single Crystal $\text{Tl}_2\text{Ba}_2\text{CuO}_6$,” Nigel E. Hussey , John R. Cooper and Joe M. Wheatley	46
P1B.12	“Hall Effect and Magnetoresistance in Normal State in LaSrCuO ,” Fedor F. Balakirev , Sabyasachi Guha, Igor E. Trofimov and Peter Lindenföld	47
P1B.13	“The Effect of Sr Impurity Disorder on the Magnetic and Transport Properties of $\text{La}_{2-x}\text{Sr}_x\text{CuO}_4$, $0.02 \leq x \leq 0.05$,” Robert J. Gooding , Robert J. Birgeneau and Noha M. Salem	47
P1B.14	“Mössbauer Studies of $\text{Re}_{1.85}\text{Sr}_{0.15}\text{CuO}_4$ T” Phase,” Ada Lopez, Elisa Baggio-Saitovitch, Mauricio A. C. de Melo, Dalber Sánchez , Izabel A. Souza and Jochen Litterst	47
P1B.15	“Observation of a Pair-Breaking Field in $\text{RENi}_2\text{B}_2\text{C}$ Compounds,” Dalber R. Sánchez , Elisa Baggio-Saitovitch, Hans Mickitz, Magda B. Fontes and Sergey L. Bud’ko	47
P1B.16	“Pressure Effects on T_c of $\text{HgBa}_2\text{Ca}_{n-1}\text{Cu}_n\text{O}_{2n+2+\delta}$ with $n \geq 4$,” Y. Cao , X. D. Qiu, Q. M. Lin, Y. Y. Xue and C. W. Chu	47
P1B.17	“Effect of High Pressure on the Normal State Resistivity of Yttrium Doped Bi-2212 System,” S. Natarajan and S. Ravikumar	48
P1B.18	“Strong Overdoping, Similar Depression of T_c by Zn and Ni Substitution and Departure from the Universal Thermopower Behaviour in $(\text{Ca}, \text{La})\text{-1:2:3}$,” Dan Goldschmidt and Yakov Eckstein	48
P1B.19	“Nonlinear Dynamics in the Mixed State of High Temperature Superconductors,” Mark W. Coffey	48
P1B.20	“The Drude Model of Transport Properties in Pure, Pr- and Ca-Doped $\text{RBa}_2\text{Cu}_3\text{O}_{7-\delta}$ Systems,” W. Y. Guan	48

P1B.21	"Anomalous Pr Ordering and Filamentary Superconductivity for the Pr2212 Cuprates," Huan-Chiu Ku , Y. Y. Hsu, S. R. Lin, D. Y. Hsu, J. F. Lin, Y. M. Wan and Y. B. You	49
P1B.22	"Superconductivity and Structural Aspects of $Y_{1-x}Ca_xBa_2Cu_3O_{7-\delta}$ with Variable Oxygen Content," V. P. S. Awana, J. Albino Aguiar , S. K. Malik, W. B. Yelon and A. V. Narlikar	49
P1B.23	"Superconducting Properties of Nb Thin Films," Ana Luzia V. S. Rolim, J. C. de Albuquerque, E. F. da Silva, Jr., J. Marcilio Ferreira and J. Albino Aguiar	49
P1B.24	"On the Thickness Dependence of Irreversibility Line in $YBa_2Cu_2O_{7-x}$ Thin Films," Pablo Menezes and J. Albino Aguiar	49
P1B.25	"Twin Structures in Large Grains of $YB_2Cu_3O_{7-\delta}$ as Affected by the Dispersion and Volume Fractions of Y_2BaCuO_5 ," Manoj Chopra, Siu-Wai Chan , V. S. Boyko, R. L. Meng and C. W. Chu	49
P1B.26	"Electromagnetic Coupling of Melt-Textured $YBa_2Cu_3O_{6+x}$ Bicrystals," Michael B. Field , David C. Larbalestier, Apurva S. Parikh and Kamel Salama	50

Poster Sessions 1B-cont: HTS Theory, Experiment, Material, & Properties 50

P1B.27	"Evaluation of Overdoping Effect in $Y_{1-x}Ca_xBa_2Cu_3O_{7-\delta}$ Films," Cheng-Chung Chi, Chih-Lung Lin , Yea-Kuen Lin and Weiyan Guan	50
P1B.28	"Mixed-State Hall Effect Studies in High- T_c Superconducting ($YBa_2Cu_3O_{7-\delta}$) $_n$ ($PrBa_2Cu_3O_{7-\delta}$) $_m$ Superlattices," Kebin Li , Yuheng Zhang and H. Adrian	50
P1B.29	"Correlation Between Phonon-Drag Thermopower and T_c in Superconducting (Bi-Pb) SrCaCuO Thin Films," J. E. Rodríguez , A. Mariño and J. Giraldo	51
P1B.30	"Thermoelectric Power of Superconducting Alloys YNi_2B_2C and $LuNi_2B_2C$," J. H. Lee, Y. S. Ha, Y. S. Song, Y. W. Park and Y. S. Choi	51
P1B.31	"Electronic Structure and Magnetic Properties of $RENi_2B_2C$ (RE=Pr, Nd, Sm, Gd, Tb, Dy, Ho, Tm, Er)," Zhi Zeng, Elisa Baggio-Saitovitch , Diana Guenzburger and D. E. Ellis	51
P1B.32	"The Magnetic Properties of the Quaternary Intermetallics $RNiBC$ (R=Er, Ho, Tb, Gd, Y)," Julio Cesar Trochez, Elisa Baggio-Saitovitch and Mohammed El Massalami	51
P1B.33	"Related Y-Ba-Cu-O Superconducting Oxides Containing Oxyanions," Rosa Scorzelli, Elisa Baggio-Saitovitch and Angel Bustamante Dominguez	51
P1B.34	"Physical Properties of Infinite-Layer and T' -Phase Copper Oxides," John T. Markert , Ruiqui Tian and Christopher Kuklewicz	52
P1B.35	"Magnetic and Structural Properties of Nd_2CuO_4 ," Yurii G. Pashkevich	52
P1B.36	"One-Phonon Absorption Caused by Magnetic Ordering in the Nd_2CuO_4 ," Yurii G. Pashkevich , Vitalli V. Pishko, Vadim V. Tsapenko and Andrei V. Eremanko	52
P1B.37	"Superconducting Phases in the Sr-Cu-O System," Z. L. Du , Y. Cao, Y. Y. Sun, L. Gao, Y. Y. Xue and C. W. Chu	52
P1B.38	"Superconductivity in $Sr_2YRu_{1-x}Cu_xO_6$ System," Maw-Kuen Wu, Dah-Chin Ling , Chao-Yi Tai and Jun-Lin Tseng	53
P1B.39	"Synthesis and Properties of the $La_{2-x}Cs_xCuO_4$ Superconducting Oxides," Maw-Kuen Wu, Shyang-Roeng Sheen , Chen-Hui Hung and Jeng Shong Shih	53
P1B.40	"Magnetic Properties of $HgBa_2Ca_{0.86}Sr_{0.14}Cu_2O_{6-\delta}$," Sung-Ik Lee , Mun-Seog Kim, Seong-Cho Yu and Nam H. Hur	53
P1B.41	"Photoexcited Carrier Relaxation in Metallic $YBa_2Cu_3O_{7-\delta}$: A Probe of Electronic Structure," Tomaz Mertelj	53
P1B.42	"Superstructure of Potential Created by Impurity Oxygen Ions and its Effect on Resistive and Spectral Characteristics of 1-2-3 HTSC," V. Eremanko , I. Kachur, A. Ratner and V. Shapiro	53
P1B.43	"Photostimulation of Critical Temperature, Critical Current and Normal State Conductivity in Epitaxial $Y-Ba-Cu-O$ Films Nonsaturated by Oxygen," V. Eremanko , V. Piryatinskaya, O. Prikhod'ko and V. Shapiro	54
P1B.44	"Magnetic Field Effects on Superconducting Nb/Al/Nb Multilayer," Maw-Kuen Wu, Ming-Jye Wang , Cheng-Chung Chi and Ching-Shuan Huang	54
P1B.45	"Resistive Transitions of HTS Under Magnetic Fields: Influence of Fluctuations and Viscous Vortex Motion," E. Silva , R. Fastampa, M. Giura, R. Marcon and S. Sarti	54
P1B.46	"Vortex Phase Transition Critical Parameters in Single Crystals of YBCO - Apparent Translational Order Dependence," Brandon Brown and Janet Tate	54
P1B.47	"Discontinuous Onset of the c -Axis Vortex Correlation at the Melting Transition in $YBa_2Cu_3O_{7-\delta}$," Esteban Righi, Daniel Lopez , Gladys Nieva, Francisco de la Cruz, W. K. Kwok, J. A. Fendrich, G. W. Crabtree and L. Paulius	54
P1B.48	"Longitudinal Superconductivity and Percolation Transition of the Vortex Lattice," C. A. Balseiro and E. G. Jagla	55
P1B.49	"Vortex Phase Transition in $Bi_2Sr_2CaCu_2O_7$ Single Crystals and the Doping Level Dependence," Hiroshi Ikuta , Satoshi Watauchi, Jun-ichi Shimoyama and Kohji Kishio	55

P1B.50	“Oxygen Dependence of First-Order Melting Transition Lines in $\text{Bi}_2\text{Sr}_2\text{Ca}_2\text{Cu}_2\text{O}_{8+x}$ Single Crystals,” Ting Wei Li , Peter H. Kes, Boris Khaykovich, Eli Zeldov and Marcin Konczykowski	55
P1B.51	“Flux Pinning by Ti Doping in $\text{Bi}_2\text{Sr}_2\text{Ca}_1\text{Cu}_2\text{O}_{8+x}$ Single Crystals,” Ting Wei Li , Peter H. Kes, Alois A. Menovsky, Jaap J. M. Franse and Henny W. Zandbergen	55
P1B.52	“Meissner Holes in Remagnetized Superconductors,” V. K. Vlasko-Vlasov , U. Welp, G. W. Crabtree, D. Gunet, V. I. Nikitenko, V. Kabanov and L. Paulis	55
P1B.53	“Formation of $\text{HgBa}_2\text{Ca}_2\text{Cu}_3\text{O}_{8+\delta}$ with Additions Under Ambient Conditions,” B. Hickey , R. L. Meng, Y. Cao, Y. Q. Wang, Y. Y. Sun, Y. Y. Xue and C. W. Chu	56
P1B.54	“Single Crystals of $\text{HgBa}_2\text{Ca}_{n-1}\text{Cu}_n\text{O}_{2n+2+\delta}$ Compounds: Growth at 10 kbar Gas Pressure and Properties,” Janusz Karpinski , Hansjörg Schwer, Kazimir Conder, Roman Molinski and Ingmar Meier	56
P1B.55	“X-Ray Single Crystal Structure Analysis of $\text{HgBa}_2\text{Ca}_{n-1}\text{Cu}_n\text{O}_{2n+2+\delta}$ Compounds,” Hansjörg Schwer , Janusz Karpinski and Christophe Rossel	56
P1B.56	“Large Bi-2212 Single Crystals Prepared by Traveling Solvent Floating Zone Method,” Yu Huang, Kow-Wei Yeh and Joy Fang	56
P1B.57	“Growth and Characterization of $\text{Bi}_2(\text{Sr}_{1-x}\text{Ca}_x)_3\text{Cu}_2\text{O}_8$ Single Crystals with Various x-Values,” Yu Huang , Kow-Wei Yeh and Joy Fang	56
P1B.58	“Study of the Crucible Reactivity in the BSCCO Melt,” Maw-Kuen Wu, Mei-Hui Huang and Yu Huang	57
P1B.59	“Preparation and Structure Characterization of the $\text{PrBa}_2\text{Cu}_4\text{O}_8$ Compound,” Shyang-Roeng Sheen, Ju-Chun Huang , Maw-Kuen Wu and Tsong-Jen Lee	57
P1B.60	“Intercalation and Staging Behavior in Superoxygenated $\text{La}_2\text{CuO}_{4+\delta}$,” Barrett O. Wells , Robert J. Birgeneau, Fang-Cheng Chou, Marc A. Kastner, Young S. Lee, Gen Shirane, John M. Tranquada, David C. Johnson, Yasuo Endoh and Kazu Yamada	57
P1B.61	“In-Plane Ordering in Phase-Separated and Staged Single Crystal $\text{La}_2\text{CuO}_{4+\delta}$,” Xiozhong Xiong , Peter Wochner and Simon C. Moss	57
P1B.62	“Microstructural Changes of YBCO Induced by Lanthanide Doping,” Irene Rusakova , Ru-Ling Meng, Pierre Gautier-Picard and C. W. Chu	57
P1B.63	“Formation Mechanisms of Y124 Stacking Fault and Ba-Cu-O Platelet Structure in Melt-Textured Y-Ba-Cu-O System,” Chang-Joong Kim, Gye-Won Hong , Ki-Baik Kim and Il-Hyun Kuk	58
P1B.64	“Fractal Grain Boundaries in Composite $\text{YBa}_2\text{Cu}_3\text{O}_{7-\delta}/\text{Y}_2\text{O}_3$ Resulting from a Competition Between Growing Grains: Experiments and Simulations,” Nicolas Vandewalle, Marcel Ausloos , N. Mineur and R. Cloots	58
P1B.65	“TEM Study of Low-Angle Grain Boundaries in Polycrystalline YBCO,” Maria Mironova , Guoping Du, Sathyamurthy Srivatsen, Irene Rusakova and Kamel Salama	58

Poster Session 2: HTS Bulk Processing, Characterization & Application 58

P2.1	“Phase Relations in the Bi_2O_3 -CaO-CuO and Bi_2O_3 -CaO-SrO Systems at 750° to 1000° in Pure Oxygen at 1 atm,” Chi-Fo Tsang, James K. Meen and Don Elthon	58
P2.2	“Subsolidus Pressure-Temperature Phase Relations in CaO-CuO to 30 kbar,” Jürgen Sander, Arne Schmitz, James K. Meen and Don Elthon	58
P2.3	“Liquidus Phase Relations in the Bismuth-Rich Portion of the Bi_2O_3 -SrO-CaO-CuO System at 1 Atm in Pure Oxygen,” Marie-Laure Carvalho , Karine L. Senes , James K. Meen and Donald Elthon	59
P2.4	“Phase Equilibria in the La_2O_3 -SrO-CuO System at 950°C and 10-30 kbar,” Joel Geny , James K. Meen, and Don Elthon	59
P2.5	“Y123 Superconductor via in-situ Reaction/Deoxidation of a Submicrometer Precursor Containing $\text{BaCuO}_{2.5}$,” Shome Sinha	59
P2.6	“Stability Study of $\text{Hg}_{1-x}\text{Ba}_2\text{Ca}_{n-1}\text{Cu}_n\text{O}_{2n+2+\delta}$ With $n \leq 6$,” Q. M. Lin , Y. Y. Sun, Y. Y. Xue and C. W. Chu	59
P2.7	“Synthesis of Hg-1212 Using the Precursor Prepared by Sol-Gel Technique,” Arumugam Thamizhavel , Ramasamy Jayavel and C. Subramanian	60
P2.8	“Effects of Heating Process on the Superconducting Property and Microstructure of BPSCCO Materials,” Yi-Da Chiu , Chin-Hai Kao and Maw-Kuen Wu	60
P2.9	“Control of 211 Particle Dispersion And J_c Property In Melt-Textured YBCO Superconductor,” Yuh Shiohara and Akihiko Endo	60
P2.10	“Partial-Melt Processing of Bulk MgO-Whisker Reinforced $(\text{Bi,Pb})_2\text{Sr}_2\text{Ca}_2\text{Cu}_3\text{O}_{10-x}$ Superconductor,” J. S. Schön and S. S. Wang	60
P2.11	“Strain Tolerance of Superconducting Properties of Bulk MgO-Whisker-Reinforced HTS BPSCCO Composite,” G. Z. Zhang , M. S. Wong and S. S. Wang	60
P2.12	“Electro-Mechanical Properties of Jointed BPSCCO Composites,” C. Vipulanandan and G. Yang	61
P2.13	“Magnetic Levitation Transportation System by Top-Seeded Melt-Textured YBCO Superconductor,” In-Gann Chen , Jen-Chou Hsu and Gwo Jann	61
P2.14	“High- T_c Ceramic Superconductors for Rotating Electrical Machines: From Fabrication to Application,” Athanasios G. Mamalis , Ildiko Kotsis, Istvan Vajda, Andras Szalay and George Pantazopoulos	61

Poster Session 3: HTS Film Processing, Characterization & Application 61

P3.1	"Molecular Level Control of the Interfacial Properties of High- T_c Superconductor Structures and Devices," John T. McDevitt, Rung-Kuang Lo, Jianai Zhao, Jason Ritchie , Chad A. Mirkin and Kaimen Chen	61
P3.2	"Crystal Engineering of Chemically Stabilized, Cation Substituted $YBa_2Cu_3O_{7-\delta}$ Thin Film Structures," John T. McDevitt and Ji-Ping Zhou	62
P3.3	"Electrochemical Molten Salt Deposition of 77K Superconducting $EuBa_2Cu_3O_{7-x}$," Horng-Yi Tang , Chuen-Shen Lee and Jeng-Lin Yang	62
P3.4	"An Improved Procedure for Fabricating YBCO Step-Edge Junctions on MgO Substrates," Hsiao-Mei Cho , Hong-Chang Yang and Heng-Er Horng	62
P3.5	"Directly Coupled DC-SQUIDS of YBCO Step-Edge Junctions Fabricated by a Chemical Etching Process in Mixed Acids," Junho Gohng , Christelle Dosquet and Jo-Won Lee	62
P3.6	"Growth of Epitaxial $LaAlO_3$ and CeO_2 Films Using Sol-Gel Precursors," Shara S. Shoup , Mariappan Parantharam, David B. Beach and Eliot D. Specht	62
P3.7	"Study of the In-Plane Epitaxy of Bi-Epitaxial Superconducting Grain Boundary Junctions," Maw-Kuen Wu, Mei-Yen Li , Hui-Ling Kao and Cheng-Chung Chi	63
P3.8	" <i>in situ</i> Deposition of Thallium Cuprate and Other Thallium-Containing Oxides," Kirsten E. Myers , Dean W. Face and Dennis J. Kountz	63
P3.9	"Growth of Superconducting Epitaxial $Tl_2Ba_2CuO_{6+\delta}$ Thin Films with Tetragonal Lattice and Continuously Adjustable Critical Temperature," Zhifeng Ren , Chang An Wang and Jui H. Wang	63
P3.10	"Transport Critical Currents of Bi-2212 Tapes Prepared by Sequential Electrolytic Deposition," Lelia Schmirgeld-Mignot , Fabrice Legendre and Pierre Régnier, Hugo Safar and Martin Maley	63
P3.11	"Role of Constituents on the Behavior of Composite BPSCCO Tapes," S. Salib , M. Mironova and C. Vipulanandan	64
P3.12	"Ion Channeling Studies in YBCO Thin Film at Low Temperature," Xingtian Cui , Zuhua Zhang, Quark Chen, Jiarui Liu and Wei-Kan Chu	64
P3.13	"Current Transport Across YBCO-Au Interfaces," Regina Dömel Dittmann , Matthias Grove and Michael Bode	64
P3.14	"Surface Characterization of Superconductive $Nd_1Ba_2Cu_3O_y$ Thin Films Using Scanning Probe Microscopes," Wu Ting , M. Badaye, R. Itti, T. Morishita, N. Koshizuka and S. Tanaka	64
P3.15	"Direct Measurement of the Magnus Force in YBCO Films," X-M. Zhu , Eric Bäckström and Bertil Sundqvist	65
P3.16	"Interface Roughness Effect on Differential Conductance of High- T_c Superconductor Junctions," Jian-Xin Zhu , Z. D. Wang and D. Y. Xing	65
P3.17	"Modern Magneto-Optical Techniques for Superconductors," V. I. Nikitenko , V. K. Vlasko-Vlasov, G. W. Crabtree and U. Welp	65
P3.18	"Magneto-Optical Study of Flux Penetration and Critical Current Densities in [001] Tilt $YBa_2Cu_3O_{7-\delta}$ Thin Film Bicrystals," A. A. Polyanskii , A. Gurevich, A. E. Pashitski, N. F. Heinig, R. D. Redwing, J. E. Nordman and D. C. Larbalestier	65
P3.19	"Monolithic Terminations for Multifilamentary BSCCO Wires," Yuan Kai Tao , Chin-Hai Kao and Maw-Kuen Wu	65
P3.20	"A Preliminary Study of the Joining of BPSCCO Superconducting Tape," Chin-Hai Kao , Yuan Kai Tao and Maw-Kuen Wu	66
P3.21	"Mutual High-Frequency Interaction of High T_c Josephson Junctions," Marian Darula , Gerhard Kunkel and Stephan Beuven	66
P3.22	"Magnetocardiography in an Unshielded Clinical Environment Using High- T_c SQUIDS," Nilesh Tralshawala , James R. Claycomb, John H. Miller, Jr., Krzysztof Nesteruk, Ji-Hai Xu and David R. Jackson	66
P3.23	"High- T_c Superconducting r_f Receiver Coils for Magnetic Resonance Imaging," Jaroslav Wosik , Krzysztof Nesteruk, Lei-Meng Xie, Piotr Gierlowski, Cheng Jiao and John H. Miller, Jr.	66
P3.24	"Investigation of the Microwave Power Handling Capability of High- T_c Superconducting Thin Films," Jaroslav Wosik , Dawei Li, Lei-Meng Xie, Irene Rusakova, John H. Miller and Stuart A. Long	67

PRESENTING AUTHOR INDEX 68

KEYNOTE ADDRESS

Wednesday, March 13, 1:30-2:20 p.m., La Salle Ballroom A & B

"Public Support for Science – Public Roles for Scientists," **N. Lane**, National Science Foundation, 4201 Wilson Boulevard, Arlington, Virginia 22230

The American Dream is about opportunities, aspirations, and a better quality of life. In the past, science has provided an important pathway to that dream. Whether or not this will continue to be true is a question of great concern – especially considering the possibility of a one-third cut in the Federal investment in R&D by the year 2002. In essence, this nation is getting ready to run an experiment it has never done before – to see if we can dramatically reduce the federal investment in R&D and still be a world leader in the 21st century. Science can only be funded if the electorate and their representatives are convinced of its value and contribution. In this new environment, leadership from the science community requires a much more public and civic persona, and a more active presence by scientists outside research labs and academia.

BANQUET ADDRESS

Thursday, March 14, 8 p.m., La Salle Ballroom A & B

"Nanoscience and Technology," **R. Smalley**, Department of Chemistry, Rice University, P. O. Box 1892, Houston, Texas 77251

PLENARY SESSIONS

PLENARY SESSION 1

Tuesday, March 12, 10:20-11:40 a.m., La Salle Ballroom A & B
Chairs: J. R. Shrieffer, K. Kitazawa

PL1.1 10:20-11:00

"The Development of Superconductivity Research in Oxides," **K. A. Müller**, University of Zürich, Physics Department, Winterthurerstrasse 190, CH-8057 Zürich, Switzerland and IBM Zürich Research Laboratory, Säumerstrasse 4, CH-8803 Rüschlikon, Switzerland

Starting with the first observation of superconductivity in an oxide, namely SrTiO₃, the history of its development is traced. Basically, and consecutively, three kinds of oxide superconductors have been found: Compounds with normal transition-metal conduction bands, oxides with cations exhibiting charge disproportionation, and finally the cuprates with large coulomb on-site repulsion, U. The doped La₂CuO₄ was the first oxide discovered in this new class of materials. The discussion will then lead over to a characterization of the high-T_c materials concerning their main physical properties.

PL1.2 11:00-11:40

"Superconductivity Above 90 K and Beyond," **C. W. Chu**, Department of Physics and Texas Center for Superconductivity at the University of Houston, Houston, TX 77204-5932

The discoveries of high temperature superconductivity, in La_{2-x}Ba_xCuO₄ at 35 K in 1986 and in YBa₂Cu₃O₇ (YBCO) at 93 K in 1987, have been considered one of the most exciting developments in modern physics, with profound technological implications. I shall first briefly describe some events in the long search for intermetallic superconductors with a high transition temperature (T_c) which have had a significant bearing on our work on the non-intermetallic YBCO. I will recall crucial steps taken in 1986 when the seminal observation was made by Bednorz and Müller, which led to the exciting discovery in 1987 by the groups in Houston and Huntsville. Efforts to raise the T_c over the last 10 years are to be summarized, and the future prospects for a T_c above the current record (134 K in HgBa₂Ca₂Cu₃O_{8+δ} at ambient and 164 K under high pressure) will be contemplated.

This work is supported in part by NSF, EPRI, the State of Texas through the Texas Center for Superconductivity at the University of Houston, and the T. L. L. Temple Foundation. This material was also prepared with the support of the U. S. Department of Energy, Grant No. DE-FC-48-95R810542. However, any opinions, findings, conclusions, or recommendations expressed herein are those of the authors and do not necessarily reflect the views of DoE.

PLENARY SESSION 2

Tuesday, March 12, 1:20-2:40 p.m., La Salle Ballroom A & B
Chairs: Z. X. Zhao, M. L. Cohen

PL2.1 1:20-2

"The Role of Vertex Corrections to the Pairing Interaction in Spin Fluctuation Superconductors," **J. R. Schrieffer**, National High Magnetic Field Laboratory and Department of Physics, Florida State University, Tallahassee, FL 32306

A key feature of the BCS theory is the requirement that one pair dressed rather than bare fermionic excitations. While in low temperature superconductors, the dressed excitations correspond to Landau's quasi particles, the corresponding one hole spectral function A is anomalous in HTS materials. In the context of a spin fluctuation approach, the vertex function G determining the coupling between the dressed excitations is also anomalous since A and G are related by Ward's identity which is a consequence of spin rotation invariance. The physical reason why G and the pairing potential are strongly suppressed as the antiferromagnetic spin fluctuations grow as a function of doping will be explained in terms of a spin deformation potential, analogous to that for the electron phonon coupling. Implications for the validity of present spin fluctuation approaches will be discussed.

PL2.2 2-2:40

"Superconductor and Semiconductors," **Shoji Tanaka**, Superconductivity Research Laboratory, ISTEK

Great success of semiconductor technology is based on the enormous efforts on the material science of semiconductors in the past fifty years. And the quality of material reached the limit of material control.

In the science on high-T_c superconductors, the material science on those materials has just begun recently. In order to realize the possible future applications, it seems to be necessary to introduce the semiconductor technology in this field as much as possible. To do that, the quality of materials must be close to that of semiconductors.

In this talk, the similarities and the differences between both technologies are discussed, and recent progress on the research and developments in high-T_c superconductors are shown. Single crystal growth, high quality thin film formations and surface and boundary problems are discussed.

PLENARY SESSION 3

Tuesday, March 12, 3-3:40 p.m., La Salle Ballroom A & B

Chair: M.-K. Wu

PL3.1 3-3:40

"Superconducting Electronics – The Next Decade," **John M. Rowell**, John Rowell Inc., 102 Exeter Drive, Berkeley Heights, New Jersey 07922

The past decade of worldwide research into the properties and applications of the high temperature superconducting materials has resulted in a technology that is adequate to enable a number of products. These include SQUIDS for medical, NDE, geophysics and research instrument applications, RF and microwave filters for both current cellular and tomorrow's PCS communications systems, and coils for NMR and MRI machines. In most cases these will add to, rather than replace, the established products made possible by the more mature LTS technology, for example MEG-SQUID instruments and the voltage standard.

The next decade is clearly the one in which the superconducting electronics industry has to grow. It is most likely that the growth will be for products that are already in some stage of development. The challenges to growth are no longer predominantly the superconducting materials technology itself. Ten years ago, even five years, there was no technology, now there is enough to be useful.

Many of the challenges are in what might be termed associated or supporting technologies. For example, if the industry is to be large, film manufacture must be cost effective. Refrigerators reaching 50K or so will have to be accepted without reservations by the customers. So reliable, small and inexpensive coolers will be a necessity. Similarly, new substrates are very desirable, and must be produced in adequate volumes at lower cost.

I will try to outline some of these industry needs in the associated technologies, and will also discuss aspects of the superconducting technology itself that will continue to require further research.

PLENARY SESSION 4

Wednesday, March 13, 8:40-10 a.m., La Salle Ballroom A & B

Chairs: M. Tachiki, P. M. Grant

PL4.1 8:40-9:20

"The Symmetry of the Order Parameter in the Cuprate Superconductors," **Anthony J. Leggett** and Nigel D. Goldenfeld, Department of Physics, University of Illinois, 1110 West Green Street, Urbana, IL 61801, and James F. Annett, Department of Physics, University of Bristol, Royal Fort, Tyndall Ave., Bristol BS8 1TL, United Kingdom

The symmetry of the Cooper-pair internal wave function (order parameter) under the operations of the relevant crystal group is an important clue to possible microscopic mechanisms of superconductivity in the cuprates. We review the currently available experimental evidence concerning this symmetry, with particular emphasis on the Josephson experiments of the last three years. We particularly stress (a) the relevance of thermodynamic considerations in constraining possible forms of the order parameter; (b) the importance, in interpreting the Josephson experiments, in distinguishing those conclusions which rely on symmetry arguments alone from those which require additional assumptions about the form of matrix elements, etc.; and (c) the fact that in the analysis of experiments of this type performed on YBCO the complications associated with the orthorhombic anisotropy and bilayer structure of this material are very largely irrelevant. We conclude that while there is no single choice of order parameter which is compatible with all the existing experiments, the choice which is consistent with by far the largest fraction is the so-called $d_{x^2-y^2}$ state.

PL4.2 9:20-10

"HTS Technology: The Road from Research to Applications," **Carl Rosner**, Intermagnetics General Corporation, 450 Old Niskayuna Rd., P. O. Box 461, Latham, New York 12110-0461

The momentous and unexpected discoveries of higher temperature superconductors (HTS) in several types of ceramic materials during the 1986/87 period, led originally to the initiation of almost unprecedented levels of multi-disciplinary research efforts in many scientific and industrial laboratories around the world. These efforts were fueled not only by the enormously wide-ranging scientific merits of the discoveries but also by the new technological and novel product applications potential that could be envisioned for the electronic, communications, electronic power and medical equipment industries to name a few. That such expectations were in the realm of possibilities seemed confirmed by the impact being made through on-going utilization of several metallic material based superconductors discovered decades earlier. Among many important research applications, also in higher-energy physics, the use of these metallic or LTS superconductors made possible the commercialization of an important multi-billion dollar worldwide MRI medical diagnostic equipment industry utilizing superconductive magnets.

Now, almost ten years later, much of the earlier HTS research effort continues to deal with exciting challenges and noteworthy accomplishments that reinforce the potential of novel, energy efficient, HTS based applications. The time-scale, however, is more likely to match the extended periods of typically 15-25 years for the transition of research results to be developed as economically viable into the main stream of novel applications and industrial commerce. Several such HTS based feasibility demonstrations, now underway, are discussed as well as the likely impact these and other research and development efforts will have on the application of HTS technology in the 21st Century.

PLENARY SESSION 5

Thursday, March 14, 8:30-9:10 a.m., La Salle Ballroom A & B

Chair: T. H. Geballe

PL5.1 8:30-9:10

"Critical Current Limiting Mechanisms in High Temperature Superconductor Conductor Forms," **David C. Larbalestier**, Applied Superconductivity Center, University of Wisconsin, Madison, WI 53706

Widespread use of HTS materials for large scale applications requires high values of critical current density and polycrystalline conductor forms. Such conductors have a complex hierarchy of current limiting barriers, varying in length scale and in underlying mechanism. All present day applications utilize conductors made from the Bi-Sr-Ca-Cu-O compounds, which have shown great progress in recent times. We discuss some of the principal current limiting mechanisms in these complex materials, describing recent experiments that identify different regimes of current limiting behavior, utilizing results from both BSCCO and YBCO bicrystals, polycrystals and real conductor forms. Starting from the smallest scale we can identify the influence of flux pinning within the grains, of the effect of different types of grain boundary or colonies of boundaries, of second phase particles, cracks, and periodic variations of the filament cross-section. These will be described, utilizing various microscopies (Magnet-optical, transmission and scanning electron and light), and transport and magnetization measurements. Magneto optical imaging is particularly valuable since it explicitly shows that current flow is percolative and that the local current density is highly variable. The complexity of the current limiting mechanisms is responsible for the difficulty of developing processing schemes that are both completely reliable and simultaneously optimum. We conclude by describing some of the processing strategies most useful for optimizing the overall critical current density.

PLENARY SESSION 6

Friday, March 15, 8:30-9:10 a.m., La Salle Ballroom B

Chair: B. Batlogg

PL6.1

8:30-9:10

"Applications of HTS to Electronics-A DoD Perspective," **Stuart A. Wolf**, Naval Research Laboratory, Code 6340, 4555 Overlook Avenue SW, Washington, DC 20375

Over the last decade there have emerged many electronic applications of HTS technology which have important military as well as commercial implications. Examples of these include space communications, terrestrial wireless communications, radar, surveillance, countermeasures, and medical applications. I will review many of the efforts in this area that have been supported by the DoD, and, in particular, by ARPA which has invested well over \$200M on this technology. In addition, I will review the efforts to develop cryocoolers to support the HTS technology. Cooler development was required to insure the overall acceptance of cryogenic systems employing superconducting electronics.

PLENARY SESSION 7

Saturday, March 16, 8:40-9:20 a.m., La Salle Ballroom B

Chair: C. Y. Huang

PL7.1

8:40-9:20

"Collective Behavior of Vortices in Superconductors," **G. W. Crabtree**¹, W. K. Kwok¹, U. Welp¹, J. A. Fendrich¹, H. G. Kaper², G. K. Leaf², A. E. Koshelev¹ and V. M. Vinokur¹, ¹Materials Science and ²Mathematics and Computer Science Divisions, Argonne National Laboratory, Argonne, IL 60439

Magnetic vortices in superconductors display an unusually wide range of equilibrium and non-equilibrium collective behavior. The equilibrium behavior includes liquid, lattice, and glassy phases, and the non-equilibrium behavior includes driven steady states characteristic of plastic and elastic flow. An introduction to the possible static and dynamic states will be followed by a presentation of recent experiments and numerical simulations which illuminate the nature of the collective behavior. First-order melting is observed in clean crystals of $\text{YBa}_2\text{Cu}_3\text{O}_7$ by transport and magnetization measurements showing a well-defined entropy discontinuity. The nature of the dynamic phases in model superconductors is explored with large-scale simulations of the time-dependent Ginzburg-Landau equations. These simulations show distinct dynamic states in the plastic and elastic flow regimes characterized by different symmetries exhibited in the positions and velocities of the vortices.

Supported by the US DOE, contract #W-31-109-ENG-38 (GWC, WKK, UW, HGK, GKL, VMV) and by the US NSF Science and Technology Center for Superconductivity, contract #DMR91-20000 (JAF, AEK).

CONCURRENT SESSIONS

CONCURRENT SESSIONS A & B

Wednesday, March 13, 10:20 a.m. - 12:40 p.m.

SESSION A: HTS Properties

Chairs: M. V. Klein, R. L. Greene

La Salle Ballroom B

A.1 10:20-10:40

"Normal State Resistivity of Superconducting LaSrCuO in the Zero-Temperature Limit," **Yoichi Ando**, Gregory S. Boebinger and Albert Passner, AT&T Bell Laboratories, 600 Mountain Avenue, ID-208, Murray Hill, NJ 07974, and Tsuyoshi Kimura, Jun-ichi Shimoyama and Kohji Kishio, Department of Applied Chemistry, University of Tokyo, Hongo 7-3-1, Bunkyo-ku, Tokyo 113, Japan

It is believed that the unusual properties of the normal-state resistivity reflect the electronic structure that underlies high- T_c superconductivity, although direct measurement of the low temperature limiting behavior is typically obscured by the onset of superconductivity. With the use of a pulsed magnetic field of 61 T, we have suppressed the superconductivity in $La_{2-x}Sr_xCuO_4$ single crystals and measured the normal-state ρ_{ab} and ρ_c down to ^3He temperatures [1]. Most noteworthy, in underdoped crystals with $x = 0.08$ ($T_c = 20$ K) and $x = 0.13$ ($T_c = 35$ K), we find insulating behavior in which both ρ_{ab} and ρ_c diverge as $\ln(1/T)$ over a wide range of temperatures below T_c . Furthermore, in contrast to the strong temperature dependence of the anisotropy ratio ρ_c/ρ_{ab} observed above T_c , we find that ρ_c/ρ_{ab} is essentially constant over the temperature range of the logarithmic divergence, suggesting an unusual anisotropic 3D transport in underdoped samples.

[1] Y. Ando, G. S. Boebinger, A. Passner, T. Kimura, and K. Kishio, Phys. Rev. Lett. 75, 4662 (1995).

A.2 10:40-11

"Transport Properties of Overdoped HTS at High Fields and Low Temperatures," **Michael S. Osofsky**, Robert J. Soulen, Jr. and Stuart A. Wolf, Naval Research Laboratory, Code 6344, Washington, DC 20375-5343, Jean-Marc Broto, Harison Rakoto, Jean-Claude Ousset, Gilbert S. Coffe and Salomon Askenazy, S.N.C.M.P., Complexe Scientifique de Rangueil - INSA, 31077 Toulouse Cedex, France, Patrick Pari, Centre d'Etude de l'Etat Condense, 91191 Gif-sur-Yvette, France, Ivan Bozovic, James N. Eckstein and Gary F. Virshup, Ginzton Research Center, MS K-124, Varian Associates, 3075 Hansen Way, Palo Alto, CA 94304, Joshua L. Cohn, Department of Physics, P. O. Box 248046, James L. Knight Physics Building, Room 309, University of Miami, Coral Gables, FL 33124, S. Mao, Center for Superconductivity Research, Department of Physics, University of Maryland, College Park, MD 20742, and Phillip Oswald, Clarendon Laboratory, Oxford University, Parks Road, Oxford OXI 3PU, United Kingdom

The Upper critical field curve, $H_{c2}(T)$, of the Bi-Sr-Cu-O system has been extracted from resistance measurements performed in pulsed ($H < 35\text{T}$) and dc ($H < 15\text{T}$) magnetic fields at temperatures down to 65mK. The thin film samples were grown layer by layer on SrTiO₃ using MBE and had $T_c \approx 15\text{K}$. These measurements show H_{c2} diverging as a function of temperature down to 65mK ($T/T_c = 0.005!$) where its value is five times that expected in a conventional superconductor. Measurements of thermoelectric power and the shape of the $R(T)$ curve indicate that the system is overdoped. This result contrasts with similar measurements on optimally doped NdCeCuO which show conventional behavior. The results will be discussed in the context of the theory of Ovchinnikov and Kresin.¹

I. Y. N. Ovchinnikov and V. Z. Kresin, Phys. Rev. B 52, 3075 (1995)

A.3 11-11:20

"Spin Gap' Effects on the Charge Dynamics of HTSC," **S. Uchida**, K. Takenaka and K. Tamasaku, Department of Superconductivity, University of Tokyo, Yayoi 2-11-16, Bunkyo-ku, Tokyo 113, Japan

The spin gap is a phenomenon characteristic of high- T_c cuprates in the underdoped regime. Recently it has been revealed that characteristic changes take place in the charge transport below a certain temperature T^* which corresponds to the opening of the spin gap.

The scattering rate for the in-plane charge transport is significantly reduced below T^* and as a consequence a Drude peak is isolated from the mid-IR band in the optical conductivity spectrum.

The out-of-plane (c -axis) charge transport is severely blocked below T^* over a fairly wide frequency region. A pseudogap develops in the c -axis optical conductivity spectrum as temperature is lowered which is connected with the semiconducting temperature dependence of the c -axis resistivity.

A.4 11:20-11:40

"Raman Spectroscopy of High T_c Superconductors," **Manuel Cardona**, Department of Solid State Research, Max Planck Institute, Solid State Research, Heisenbergstr. 1, D-70569 Stuttgart, Germany

Raman spectroscopy has proven to be an excellent technique for basic investigations and characterization of high T_c superconductors. A review and recent results covering the following topics will be presented

1. Scattering by phonons and superconducting gaps
2. Electronic scattering and superconducting gaps
3. Scattering by crystal field excitations in materials with rare earth ions.

Emphasis will be placed on basic information concerning the elusive mechanism of high T_c superconductivity as well as on applications for structural characterization.

A.5 11:40-12

"Magnetic and Structural Properties and Phase Diagrams of $\text{Sr}_2\text{CuO}_2\text{Cl}_2$ and Lightly-Doped $\text{La}_{2-x}\text{Sr}_x\text{CuO}_{4+\delta}$," **David C. Johnston**, Department of Physics and Astronomy, Iowa State University, Ames, IA 50011

The evolution of the structural and magnetic properties with doping are reviewed for the systems $\text{Sr}_2\text{CuO}_2\text{Cl}_2$, $\text{La}_2\text{CuO}_{4+\delta}$ and $\text{La}_{2-x}\text{Sr}_x\text{CuO}_4$. In the first system, a Heisenberg to XY-like crossover is found upon cooling towards the Néel temperature $T_N = 256$ K.¹ In the second system, macroscopic phase separation occurs for $0.01 < \delta < 0.06$,² and the superconducting compounds with $\delta > 0.06$ have a staged structure.³ In the third system, in the antiferromagnetic region $0 < x < 0.02$ the effective spins of the localized (below ~ 30 K) doped holes freeze into a spin-glass state below $T_f = (815 \text{ K})x$, whereas at higher temperatures we infer that the doped holes become delocalized and segregate into walls separating undoped domains.⁴ Other work will also be reviewed.

1. B. J. Suh, F. Borsa, L. L. Miller, M. Corti, D. C. Johnston and D. R. Torgeson, Phys. Rev. Lett. **75**, 2212 (1995).
2. P. G. Radaelli, J. D. Jorgensen, R. Kleb, B. A. Hunter, F. C. Chou and D. C. Johnston, Phys. Rev. B **49**, 6239 (1994).
3. B. O. Wells, R. J. Birgeneau, F. C. Chou, Y. Endoh, D. C. Johnston, M. A. Kastner, Y. S. Lee, G. Shirane, J. M. Tranquada and K. Yamada, Z. Phys. B (accepted).
4. F. Borsa, P. Carretta, J. H. Cho, F. C. Chou, Q. Hu, D. C. Johnston, A. Lascialfari, D. R. Torgeson, R. J. Gooding, N. M. Salem and K. J. E. Vos, Phys. Rev. B **52**, 7334 (1995).

*Work supported by the USDOE under Contract No. W-7405-Eng-82

A.6 12-12:20

"Enhanced Magnetic Response in the Superconducting State of $\text{La}_{1.86}\text{Sr}_{0.14}\text{CuO}_4$," **Gabriel Aeppli**, NEC Research Institute, Inc., 4 Independence Way, Princeton, New Jersey 08540

A.7 12:20-12:40

"Correlations Between T_c and n_s/m^* in High- T_c Cuprates," **Y. J. Uemura**, Physics Department, Columbia University, New York, NY 10027

Following the discovery of high- T_c cuprates, we found interesting correlations between T_c and n_s/m^* (superconducting carrier density / effective mass) by performing muon spin relaxation (μSR) measurements of the magnetic field penetration depth λ . In this talk, I would like to review recent developments in the study of these correlations, together with my current picture for their interpretation. We will consider following features: (A) There is a linear relation $T_c \propto n_s/m^*$ in the underdoped region, with a universal slope for most of the cuprates. (B) In the YBCO 123 compound, the increase of n_s/m^* at the $T_c = 90$ K "plateau" can be ascribed to the contribution of the chains. (C) In the overdoped Tl2201 and Hg1201 systems, n_s/m^* decreases with increasing carrier doping (i.e., decreasing T_c), suggesting the coexistence of superconducting and normal carriers in the ground state. (D) The pseudo-gap results found in the underdoped region by conductivity, NMR, neutron and specific heat measurements suggest a formation of singlet-spin correlations in the normal state above T_c . (A) and (D) can be viewed as a signature of Bose-Einstein condensation of

"pre-formed" pairs in the underdoped region. The system is expected to cross-over to a simple Fermi liquid with progressive doping through the overdoped region. However, (C) suggests that superconductivity in the overdoped region occurs with a microscopic phase separation, unlike the case of simple metals. Moreover, a trace of BE condensation can still be found even in the overdoped region, in the monotonic relationship between T_c and n_s/m^* . I will also discuss relevant results found in organic, doped fullerene, and other "exotic" superconductors.

SESSION B: Bulk Applications

Chairs: **R. Eaton III**, **R. A. Hawsey**

Granger A & B

B.1 10:20-10:40

"Bulk Applications of HTS Wire," **A. P. Malozemoff**, American Superconductor Corporation, Research and Development, 2 Technology Drive, Westborough, MA 01581

High temperature superconducting (HTS) wire based on a powder-in-tube process and using $\text{BiSrCaCuO} - 2223$ has been developed to a pilot manufacturing level, with current leads as the first commercial product.

DC Solenoidal magnets of several tesla have been constructed for a variety of applications, such as magnetic separation and research use. Racetrack and ring coils have been used in tests of motors producing over 100 hp. Multistrand conductors over 30m long have been constructed. HTS applications status will be reviewed.

B.2 10:40-11

"Progress and Issues in HTS Power Cables," **Aldo F. Bolza**, Pirelli Cavi S.p.A., R&D, Viale Sarca, 222, 201226-Milano, Italy

The discovery of HTS in 1986 has revitalized a great interest in SC cables and transmission systems: bearing in mind that the SC technology in LHe had proved to be technically valid but did not work economically with respect to conventional systems, the paper examines as the key opportunity for HTS the perspective of a less costly solution, cooled by LN, combined with a more effective practical performance, for various possible applications in the power system.

The practical actions originating from this interest are considered: they started and are continuing to grow in the parallel directions of both a tailored improvement of materials and technology and an increasingly detailed technical and economical analysis of the SC applications for power transmission in the grid.

The present advances for HTS cable systems are described in the perspective of a wide range of applications: some of them are already at the development stage, (like the retrofit of existing saturated lines) others are being systematically analyzed for feasibility and for the associated opportunities (like high power ac and dc links and more effective urban feeders).

The possible future evolution for materials technology and applications is finally discussed.

B.3 11-11:20

"125 hp HTS Synchronous Motor Design and Preliminary Test Results," **David Driscoll**, Reliance Electric/Rockwell Automation, 24800 Tungsten, Cleveland, Ohio 44117

B.4 11:20-11:40

"Superconducting Homopolar Motor Demonstration," **D. Gubser** and L. Toth, Naval Research Laboratory, Washington, DC, and M. Superczynski and D. Waltman, Naval Surface Warfare Center, Annapolis, MD

A homopolar motor employing magnets fabricated with high temperature superconducting (HTS) bismuth-cuprate tape conductors has been operated at temperatures of 4.2K and 28K, producing 167 hp and 122 hp, respectively in the initial tests. This is the most powerful motor ever constructed with the new HTS materials and represents a significant advance in conductor and magnet development. The magnet system in the motor contained solenoids fabricated by both American Superconductor Corporation and Intermagnetic General Corporation. The initial coils operated at 120 amperes of current with a current density of 5600 amperes/cm². Second generation coils with improved superconducting performance have recently been installed in the motor. This talk will describe the conductor and magnet developments, and the motor and motor test results.

B.5 11:40-12

"Superconducting Magnetic Bearing and Its Application in Flywheel Kinetic Energy Storage," Z. Xia, K. B. Ma, R. Cooley, P. Fowler and **W. K. Chu**, Texas Center for Superconductivity, University of Houston, Houston, TX 77204-5932

The feasibility of superconducting magnetic bearings (SMB) for industrial applications has been investigated since the discovery of high temperature superconducting materials in the late 80's. For example, Nuclear Research Center of Germany, ISTEK of Japan, DM & DP of Italy, Argonne National Lab., Boeing and others, all have the flywheel activities using HTS-magnet levitation bearings. At TcSUH, we have constructed a flywheel prototype using hybrid superconducting magnetic bearings (HSMB). The hybrid bearing design uses magnetic forces from permanent magnets for levitation and HTS in between the magnets for stabilization. A 42 lb. flywheel currently is rotated up to 6000 RPM with kinetic energy of 8 Wh. The recent rotor spin-down experiment indicates an average frictional energy loss < 1% per hour in a vacuum of 5×10^{-6} torr.

B.6 12-12:20

"High Temperature Superconducting Fault Current Limiter," **E. M. W. Leung**, Lockheed Martin Corporation

One of the most near term High Temperature Superconductor (HTS) applications is Fault Current Limiter (FCL). It is a device that can provide significant cost savings and operational efficiency increase for the power utility industry. This is especially important amid an environment of deregulation. The Lockheed Martin team, which also includes the Southern California Edison (SCE), American Superconductor Corporation (ASC), and Los Alamos National Laboratory (LANL), has been developing a 2.4 kV, 2.2 kA HTS FCL since October, 1993, under the auspices of the Department of Energy (DoE) Superconductivity Partnership Initiative (SPI) program. This two-year Phase 1 program was successfully completed in October, 1995, following a six week extensive testing at the Center Test Substation of SCE in the summer. A final report describing the development and results of the FCL unit is scheduled to commence in February, 1996. Planning effort and schedule for this new

phase will be given. A brief description of the underlying principle of a FCL and how it can benefit the power utility will also be given.

B.7 12:20-12:40

"Development of Technologically-Useful Superconducting Wires at 20K," **David T. Shaw**, T. Haugan, J. Ye, F. Wong and S. Patel, SUNY at Buffalo, Electrical & Computer Engineering, 330 Bonner Hall, Buffalo, NY 14260, and L. Motowidlo, IGC Advanced Superconductors Inc.

The fabrication of technologically-useful high temperature superconducting (HTS) wires has been hindered by the anisotropic mechanical properties and chemical phase instability of HTS materials. Successful techniques to overcome many of these problems in long-length HTS wires will be reviewed. The scale-up production of Bi-2212 tapes and the performance of these tapes, as compared to Bi-2223 wires at 20K, will be discussed.

The effects of anisotropic mechanical properties on mechanical rolling instabilities in Bi-based HTS powders will be analyzed. Theoretical and experimental studies have been carried out on two rolling configurations (rod-in-tube processing and sand-switch processing) to minimize these instabilities by increasing the shear to compressive strain ratio. Both techniques lead to a smaller degree of rolling instability, thus less sausageing and higher critical currents.

Isothermal partial-melt processing (IPMP) has been developed to stabilize the chemical phase-formation kinetics. By heat treating powder-in-tube Bi-2212 green wires in inert atmosphere (N₂ or AR), the partial-melt temperature is reduced by more than 40°C. The Bi-2212 phase is formed with less secondary phases within a relatively large temperature window (larger than 8°C). The IPMP processing of long-length Bi-2212 wires in our annular (ring-shaped) furnace will be presented.

CONCURRENT SESSIONS C & D

Wednesday, March 13, 2:40-6:20 p.m.

SESSION C: Symmetry

Chairs: **A. L. de Lozanne**, **D. G. Naugle**
La Salle Ballroom B

C.1 2:40-3

"Josephson Tunneling Between a Conventional Superconductor and $YBa_2Cu_3O_{7-\delta}$," **R. C. Dynes**, A. G. Sun, A. S. Katz, A. Truscott, Solomon Woods, Don Gajewski, Sueng-Ho Han and M. B. Maple, University of California, San Diego, B. W. Veal and C. Gu, Argonne National Lab, and J. Clarke, R. Kleiner, R. Summer, E. Dantscher and B. Chen, University of California, Berkeley

We report two experiments which are designed to extend our earlier studies on Josephson tunneling between a conventional superconductor and $YBa_2Cu_3O_{7-\delta}$. The first is a study of tunneling into the a-b direction to probe the in plane coupling of the order parameter. The second is a study of the a-c Josephson effect through measurements of the microwave induced Shapiro steps in c-axis junctions. Both experiments are consistent with earlier results which conclude that while we cannot

C.2 - C.5

exclude a $d_{x^2-y^2}$ component to the order parameter, there is substantial 1st order coupling to a conventional s-wave superconductor.

C.2 3-3:20

"Half-Integer Flux Quantum Effect and Pairing Symmetry in Cuprate Superconductors," **C. C. Tsuei** and John R. Kirtley, IBM T.J. Watson Research Center, P. O. Box 218, Yorktown Heights, NY 10598

A phase-sensitive and non-invasive test of the pairing symmetry in cuprates is important to understanding the origin of high-temperature superconductivity. Based on macroscopic quantum coherence effects arising from pair tunneling and flux quantization, a series of tricrystal experiments have been designed and carried out to probe the microscopic phase of the pair wavefunction in high- T_c cuprate superconductors. By using a high-resolution scanning SQUID microscope, and the half-integer flux quantum effect in various tricrystal geometrical configurations, we have obtained strong evidence for a d-wave pairing state in YBCO and Tl 2201. In this talk we will describe the basic tricrystal experiment and present new results. Topics to be discussed also include: symmetry independent mechanisms for the half-integer flux quantum effect, g-wave pairing symmetry, universality, and the effects of twinning, chains, bilayers, and doping on d-wave pairing symmetry.

Work done in collaboration with: M. Rupp, J. Z. Sun, A. Gupta, and M. B. Ketchen (IBM); C. C. Chi (Tsing-Hua U.); K. A. Moler (Princeton); C. A. Wang, Z. F. Ren and J. H. Wang (SUNY Buffalo); and M. Bhushan (SUNY Stony Brook).

C.3 3:20-3:40

"Intrinsic SIS Josephson Junction in Bi-2212 and Symmetry of Cooper Pair," **Keiichi Tanabe**, Superconductivity Research Laboratory, International Superconductivity Technology Center, 1-10-13 Shinonome, Koto-ku, Tokyo 135, Japan, and Yoshikazu Hidaka, Shin-ichi Karimoto and Minoru Suzuki, NTT Interdisciplinary Research Laboratory, 162 Shirakata, Tokai, Ibaraki 319-11, Japan

We have recently succeeded in observing both clear pair and quasiparticle tunneling characteristics in intrinsic junction stacks with a number of CuO_2 bilayer as few as 40 fabricated on underdoped Bi-2212 single crystals. The relatively large McCumber parameter and nearly temperature-independent junction normal resistance R_N indicate that the $\text{SrO-Bi}_2\text{O}_2\text{-SrO}$ layered block acts as a sufficiently insulating tunnel barrier in this material. These intrinsic junction stacks are of particular interest not only as candidates for electronic devices but also as a probe of order parameter in the CuO_2 bilayer, because their tunneling characteristics are expected to be insensitive to surface degradation and exactly reflect the order parameter distribution in the k_x - k_y space.

The tunneling properties are characterized by the following three points; (1) the energy gap suppression due to nonequilibrium superconductivity effect especially evident in a higher current region, (2) a large subgap conductance which exhibits a clear V^2 dependence, (3) a small $I_c R_N$ product less than 1/5 of the BCS value. Numerical calculation taking account of the nonequilibrium effect indicates that the quasiparticle current-voltage characteristics are consistent with a d-wave order parameter with a 2Δ of 50 meV.

C.4 3:40-4

"Magnetic Raman Scattering in Cuprate Antiferromagnetic Insulators and Doped Superconductors," **Girsh E. Blumberg** and Miles V. Klein, University of Illinois at Urbana-Champaign, Department of Physics, 1110 W. Green St., Urbana, IL 61801

We study antiferromagnetic (AF) interactions in cuprate superconductors and parent AF insulators by two-magnon (2M) resonance Raman excitation profile (RREP) technique.

2M RREP measurements for single layer $\text{Sr}_2\text{CuO}_2\text{Cl}_2$ and bilayer $\text{YBa}_2\text{Cu}_3\text{O}_{6.1}$ antiferromagnets reveal composite structure of the 2M line shape and strong nonmonotonic dependence of the scattering intensity on excitation energy. We analyze these data using the *triple resonance* theory of Chubukov and Frenkel (Phys. Rev. Lett., **74**, 3057 (1995)) and deduce information about magnetic interaction and electronic band parameters in these AF insulators. We study the evolution of the magnetic excitation with hole doping in $\text{YBa}_2\text{Cu}_3\text{O}_{6+\delta}$ and $\text{YBa}_2\text{Cu}_4\text{O}_8$ single crystals and find that the magnetic excitations, similar to the 2M excitations in the insulators, persist with doping and are evidence that AF fluctuations with spatial extent of at least three lattice constants are not overdamped in the underdoped superconductors. The 2M RREP shows the existence of the charge-transfer gap in the underdoped cuprates and provides information about evolution of electronic band parameters with doping.

We discuss the nature of the electronic Raman continuum. The RREP and doping studies suggest that the flat continuum, including the low-frequency continuum from which the "gap-like features" emerges, might be related to magnetic fluctuations.

C.5 4-4:20

"STM Observation of the Vortex Lattice in $\text{YBa}_2\text{Cu}_3\text{O}_7$," I. Maggio-Aprile, Ch. Renner, A. Erb, E. Walker and **Ø. Fischer**, Departement de Physique de la Matière Condensée, Université de Genève, 24 Quai E.-Ansermet, CH-1211 Genève 4, Switzerland

We have investigated the high temperature superconductor $\text{YBa}_2\text{Cu}_3\text{O}_{7-\delta}$ by scanning tunneling spectroscopy (STS). We have observed reproducible and uniform spectra in the superconducting state. These spectra are different from the isotropic BCS type spectra and also very different from the spectra we observe on $\text{Bi}_2\text{Sr}_2\text{CaCu}_2\text{O}_8$. Whereas in BSCCO the spectra are similar, though not identical, to what one would expect from a d-wave superconductor, in YBCO we observe a multiple peak structure. In the presence of a magnetic field we have succeeded to observe the vortex lattice by STS. The spectra in the vortex core of YBCO show a double peak structure which we identify with the two lowest lying localized states. The vortex cores appears elongated suggesting an a-b anisotropy of ξ of ≈ 1.5 . The vortex lattice is disordered but have locally an oblique structure which is different from the one expected from the a-b anisotropy if one assumes an hexagonal non-distorted lattice. The distortion of the vortex lattice and the anisotropy of ξ can be reconciled if we assume a square non-distorted vortex lattice.

C.6 4:40-5

"Determination of the Pairing State of High- T_c Superconductors Through Measurements of the Transverse Magnetic Moment* \ddagger ," **Allen M. Goldman**, University of Minnesota, School of Physics and Astronomy, 116 Church St. SE, Minneapolis, MN 55455

The angular dependence of the transverse magnetic moment of well-characterized single crystals of LuBaCuO, and YBaCuO, both in the form of rectangles and discs (to reduce demagnetization effects) has been studied in the nonlinear Meissner regime. Measurements were carried out using a SQUID susceptometer in which the magnetic moment of the crystals was measured along an axis perpendicular to both the field direction and the c -axis. The crystals were rotated about their c -axes which were aligned perpendicular to the direction of the field. The expected signature of d -wave pairing, a Fourier component of the transverse moment with angular period $\pi/2$ was found to be smaller than expected for pure d -wave pairing and the dependence of this component on magnetic field disagreed with the predicted functional form. The results are consistent with isotropic pairing, but do not rule out nodeless anisotropic pairing. Other properties of the crystals were similar to those of high quality YBa₂Cu₃O_{7- δ} crystals, suggesting that the negative results for d -wave pairing are not a consequence of impurity scattering or other defects.

*Work performed in collaboration with A. Bhattacharya, J. Buan, D. Grupp, C.-C. Huang, T. Jacobs, J.-Z. Liu, R. Shelton, S. Sridhar, B. Stojkovic, O. T. Valls, U. Welp, and I. Zutic

\ddagger Supported in part by the AFOSR under Grant F49620-93-1-0076, and by the Supercomputer Institute of the University of Minnesota

C.7 5-5:20

"Excitation Gap in the Normal and Superconducting State of Underdoped Cuprate Superconductors," **Z.-X. Shen**, Department of Applied Physics and Stanford Synchrotron Radiation Laboratory, McCullough Building 232, Mail Code 4055, Stanford University, Stanford, CA 94305

Angle resolved photoemission experiments reveal incidence for an energy gap in the normal state excitation spectrum of the cuprate superconductor Bi₂Sr₂CaCu₂O_{8+ δ} . This gap exists only in the underdoped samples, and disappears at the doping level where T_c is maximized. The momentum dependence and the magnitude of the gap closely resemble those of the $d_{x^2-y^2}$ gap observed in the superconducting state. We compare our data other experiments which produced results consistent with a gap in the normal state of underdoped cuprate superconductors.

C.8 5:20-5:40

"Single Grain Boundary Josephson Junction Devices - New Insights from Basic Experiments," **Jochen Mannhart**, H. Hilgenkamp and B. Mayer, IBM Research Division, Zürich Research Laboratory, Säumerstr. 4, CH-8803 Rüschlikon, Switzerland

Intrinsically non-Fraunhofer type $I_c(H)$ characteristics of single YBa₂Cu₃O_{7- x} grain boundaries provide clear evidence that these junctions are strongly influenced by the $d_{x^2-y^2}$ symmetry component of the superconducting order parameter. This

symmetry effect causes a reduction of the grain boundary critical current density by an order of magnitude at large misorientation angles. Facetting effects reduce the $I_c R_n$ product of the junctions, which no longer is a direct measure of the microscopic barrier transmission. The boundaries are electrically inhomogeneous on a length scale of 10-100 nm, which degrades the noise properties of the junctions.

C.9 5:40-6

"What Does d-Wave Symmetry Tell Us About the Pairing Mechanism?," **Kathryn Levin**, University of Chicago, The James Franck Institute, 5640 S. Ellis Ave. Chicago, Illinois 60637

Recent experiments have provided strong support for the d -wave ($d_{x^2-y^2}$) pairing symmetry, although some inconsistencies still remain. Observation of this pairing state has sometimes been cited as support for a specific (spin fluctuation) pairing mechanism. In this talk we argue that d -wave symmetry is a general consequence of superconductivity driven by repulsive interactions. Van Hove effects, deriving from the two dimensionality of the CuO₂ plane are important in stabilizing this state. We discuss problems associated with one particular realization of repulsion-driven superconductivity, the spin fluctuation pairing scenario. These problems arise in the context of neutron data. As a consequence we are driven to investigate the superconducting response in the "charge channel". By extending the original Kohn-Luttinger picture to a 2D lattice, we find that the direct Coulomb term is associated with a d -wave instability. Whether this is all or only a component of the pairing is too soon to say, but it is clear that direct Coulombic effects in the cuprates act in concert with any other underlying pairing mechanism.

Parts of this work were done in collaboration with Dongzi Liu and Jiri Maly.

C.10 6-6:20

"Impurity States in a d -Wave Superconductor," **Marcel Franz**¹, Catherine Kallin¹ and John A. Berlinsky², ¹Department of Physics & Astronomy and ²Institute for Materials Research, McMaster University, 1280 Main Street West, Hamilton, Ontario, L8S 4M1, Canada

We study the effects of impurities on the quasiparticle states in a superconductor with a $d_{x^2-y^2}$ pairing. The issue of the localization of impurity states in such superconductors has been hotly debated; arguments based on the self-consistent T -matrix approximation^a predict a lack of localization while arguments involving the scaling theory of localization^b and numerical studies of the Dirac fermion model^c find evidence for strong localization by disorder. We address this controversy within the framework of the Bogoliubov-de Gennes (BdG) theory applied to the extended Hubbard model^d with on-site repulsion and nearest neighbor attraction. Such a treatment has advantages compared to previous studies in that the impurity scattering is treated *exactly* and the model is *directly* relevant to d -wave superconductors. We carry out a fully self-consistent numerical diagonalization of the BdG equations on finite clusters containing up to 40 x 40 sites. We identify localized states by probing

their sensitivity to the boundary conditions and we investigate the detailed spatial distribution of the quasiparticle wavefunctions.

^aA. V. Balatsky *et al.*, Phys. Rev. **B51**, 15547 (1995).

^bA. Lee, Phys. Rev. Lett. **71**, 1887, (1993).

^cY. Hatsugai and P. A. Lee, Phys. Rev. **B48**, 4204 (1993).

^dT. Xiang and J. M. Wheatley, Phys. Rev. **B51**, 11721 (1995.)

SESSION D: HTS Materials

Chairs: **A. J. Jacobson, J. Crow**

Granger A & B

D.1 2:40-3

"Phase Stability, Defects, and Formation of $\text{HgBa}_2\text{Ca}_{n-1}\text{Cu}_n\text{O}_{2n+2+\delta}$," **Y. Y. Xue**, R. L. Meng, Q. Xiong, * Q. M. Lin, I. Rusakova and C. W. Chu, Department of Physics and Texas Center for Superconductivity at the University of Houston, Houston, TX 77204-5932; *Department of Physics, High Density Electronic Center, University of Arkansas, Fayetteville, AR 72701

We have studied systematically the phase stability, defect structures, and the formation of $\text{HgBa}_2\text{Ca}_{n-1}\text{Cu}_n\text{O}_{2n+2+\delta}$ [$\text{Hg-12}(n-1)n$]. It is found that the equilibrium Hg vapor pressure P_{Hg} of $\text{Hg-12}(n-1)n$ increases with n , and reaches a value almost as large as that of the impurity phase HgCaO_2 at $n = 3$; the presence of dopants such as Pb, Re, Mo, *etc.* suppresses the P_{Hg} of $\text{Hg-12}(n-1)n$; and traces of $\text{H}_2\text{O}/\text{CO}_2$ reduce the P_{Hg} of HgCaO_2 . The observations demonstrate that the addition of Pb, Re, Mo, *etc.* enhances the formation of $\text{Hg-12}(n-1)n$, whereas $\text{H}_2\text{O}/\text{CO}_2$ does the opposite. Data also show that $\text{Hg-12}(n-1)n$ is nonstoichiometric in Hg at the synthesis temperature, and various defects may occur in the HgO_δ layers. It is suggested that the occupation of the dopants at the Hg-site may change the defect structure, the formation free-energy of these defects, therefore, stabilize $\text{Hg-12}(n-1)n$. In such doping, the apical oxygen bond-length, the related disorder, and the available oxygen sites in the HgO_δ layer should change significantly. However, the optimal ambient T_c is almost the same, although the pressure effects of T_c seem to be rather different.

D.2 3-3:20

"Stabilisation of New HTcS Cuprates and Oxycarbonates: From the Bulk Materials to the Thin Films," **B. Raveau**, Laboratoire CRISMAT, ISMRA et Université de Caen, 6 Bd du Maréchal-Juin, 14050 Caen Cedex, France

The different routes to synthesize new cuprates and superconducting oxycarbonates are reviewed. Starting from the infinite layer structure (IL), the generation of oxycarbonates, oxysulfates, but also oxyborates and oxychromates is predicted. Two mechanisms, named intergrowth and shearing mechanisms can then be applied to these oxyanion compounds for the generation of new structures.

The intergrowth mechanisms applied to the thallium "1201", and bismuth "2201" structures with the oxycarbonate $\text{Sr}_2\text{CuO}_2\text{CO}_3$ (S_2CC), lead to the two series of superconducting oxycarbonates $[\text{1201}]_m [\text{S}_2\text{CC}]_n$ and $[\text{2201}]_m [\text{S}_2\text{CC}]_n$. The application of the intergrowth mechanisms to the I.L. structure and to the S_2CC

structure, allows the synthesis to the 110 K superconductors $[\text{Ba}_2\text{CuO}_2\text{CO}_3]_m [\text{CaCuO}_2]_n$, obtained in the form of thin films by laser ablation.

Starting from the intergrowth oxycarbonates, the application of shearing mechanisms along a direction transversal to the $[\text{CuO}_2]_\infty$ layers allows four series of collapsed oxycarbonates to be generated. Two classes, with the generic formulation $(\text{Tl}, \text{M})_1\text{A}_4\text{Cu}_2\text{CO}_3\text{O}_7$ and $(\text{Hg}, \text{M})_1\text{A}_4\text{Cu}_2\text{CO}_3\text{O}_7$ with $\text{A} = \text{Sr}, \text{Ba}$ form a large series of superconductors with T_c ranging from 17 K to 77 K in which $\text{M} = \text{Bi}, \text{Pb}, \text{Cr}, \text{V}$; they derive from the $[\text{1201}]_1 [\text{S}_2\text{CC}]_1$ intergrowth by a shearing phenomenon along the (001) or to (110) plane of the perovskite so that they are called (100) and (110) - collapsed "1201- S_2CC " oxycarbonates. A similar shearing phenomenon applied to the $[\text{2201}] [\text{SrCC}]_m$ series, i.e. $\text{Bi}_2\text{Sr}_2\text{CuO}_6 \cdot (\text{Sr}_2\text{CuO}_2\text{CO}_3)_m$ leads to the shear like oxycarbonate $\text{Bi}_{15}\text{Sr}_{29}(\text{CO}_3)_7\text{O}_{56}$ that does not superconduct due to the fact that the $[\text{CuO}_2]_\infty$ layers are interrupted. The fourth series correspond to $(\text{Y}, \text{Ca})_n (\text{Ba}, \text{Sr})_{2n}\text{Cu}_{3n-1}\text{CO}_3\text{O}_{7n-3}$; it results from the shearing phenomenon in the $[\text{Ba}_2\text{CuO}_2\text{CO}_3]_m [\text{CaCuO}_2]_n$ type intergrowth.

Other shearing phenomena applied to the cuprates, especially the bismuth cuprates are also described that lead for instance to the collapsed cuprate $\text{Bi}_{16}\text{Sr}_{28}\text{Cu}_{17}\text{O}_{69+\delta}$, that derives from the 2212 bismuth cuprate and can be of great interest for the creation of pinning in $\text{Bi}_2\text{Sr}_2\text{CaCu}_2\text{O}_{8+\delta}$.

D.3 3:20-3:40

"Quantum Spin Ladder Oxides," **Mikio Takano**, Institute for Chemical Research, Kyoto University, Gokasho, Uji, Kyoto-fu 611, Japan

Experimental research of a class of new cupric oxides called spin ladder compounds will be summarized, where the ladders are made from antiferromagnetic chains of $S = 1/2$ spins by connecting them together with inter-chain antiferromagnetic bonds. Hole carriers doped into even-leg ladders have been predicted to pair, and possibly superconduct. By means of high pressure synthesis at 3-6 GPa and 1200 K, typically, two kinds of 2-leg ladder compounds SrCu_2O_3 and LaCuO_2 and a 3-leg ladder compound $\text{Sr}_2\text{Cu}_3\text{O}_5$ have been prepared. Their magnetic and electrical properties will be compared with theoretical predictions.

D.4 3:40-4

"Normal State Transport Properties of Tl-2201 Single Crystals," **Allen M. Hermann**, William Kiehl and Rafael Tello, Department of Physics, University of Colorado-Boulder, P. O. Box 390, Boulder, CO 80309-0390

In this paper, we present and analyze transport properties of Tl2201 single crystals as a function of oxygen doping (and corresponding variation of T_c). Thermoelectric power (TEP) data and Hall effect results are shown in detail and discussed. Measurements both parallel to and perpendicular to the ab plane are presented. The ab -plane room-temperature TEP and Hall constants have differing signs and unusual temperature dependencies. Hall coefficients are temperature dependent and, for B.L. ab plane, the Hall data at optimal doping (high T_c) do not show the inverse Hall mobility - T^2 correlation "universality" found for most HTSC materials. Some possible explanations are offered.

We gratefully acknowledge the support of the Office of Naval Research under ONR grant number N00014-90-J-1571.

D.5 4-4:20

"Superconductive Sr_2RuO_4 and Related Materials," **Yoshiteru Maeno** and Toshizo Fujita, Department of Physics, Hiroshima University, Higashi-Hiroshima 739, Japan

Sr_2RuO_4 ($T_c=1$ K) is the only layered-perovskite superconductor known to date that does not contain copper. Extensive studies using high-quality single crystals have demonstrated that this compound serves as an ideal reference material to high- T_c cuprates: the effect of electron correlations is important, the superconductivity is highly anisotropic, and the normal state is characterized well as a nearly two-dimensional Fermi liquid.

In addition to comparing and contrasting the basic electronic states of the superconductive ruthenate and cuprates, we will also discuss the low-temperature properties of related materials, including Sr_2RhO_4 , $\text{Sr}_3\text{Ru}_2\text{O}_7$ and $\text{Sr}_2\text{CaRuO}_y$.

D.6 4:40-5

"Electronic Phase Separations in $\text{La}_2\text{CuO}_{4+\delta}$," **Pei-Herng Hor**^{1,3}, Zu Gang Li^{1,3}, Hung Hsu Feng^{1,3}, Zhong Y. Yang^{1,3}, Alejandro Hamed^{1,3}, Shaw-Tsong Ting^{1,3}, S. Bhavaraju^{2,3}, J. F. DiCarlo^{2,3} and Allan J. Jacobson^{2,3}, ¹Department of Physics, ²Department of Chemistry and ³Texas Center for Superconductivity, University of Houston, Houston, TX 77204-5932

We present the results of electrochemical, x-ray powder diffraction and thermal annealing experiments performed on $\text{La}_{2-x}\text{Sr}_x\text{CuO}_{4+\delta}$ system for $x = 0, 0.025, 0.05$ and $0 < \delta < 0.12$. We show that thermal equilibrium can be achieved in samples either annealed at 110°C or electrochemically intercalated at elevated temperatures. Under equilibrium, from constant current chronopotentiometric measurements, we observed two two-phase regions defined by, instead of oxygen excess δ , specific hole concentrations (p). A new orthorhombic phase with $p = 0.25$ is discovered and structural anomalies of $\text{La}_2\text{CuO}_{4+\delta}$ are observed at corresponding hole concentrations which define the two-phase regions in chronopotentiometric data. Our results indicate that there are electronic structures formed at some specific hole concentrations which correspond to ordered 2D arrangements of holes in the CuO_2 planes. It is suggested that the electronic phase separations, with the help of structural optimization of elastic energy, are responsible for the observed chemical phase separations around ambient temperature.

D.7 5-5:20

"Borocarbide and Other Unusual Intermetallic Compounds," **Robert J. Cava**, AT&T Bell Laboratories, 600 Mountain Avenue, Murray Hill, New Jersey 07074

D.8 5:20-5:40

"Strong Flux Pinning, Anisotropy and Microstructure of $(\text{Hg,Re})\text{M}_2\text{Ca}_{n-1}\text{Cu}_n\text{O}_y$ ($\text{M}=\text{Ba,Sr}$)," **Jun-ichi Shimoyama**, Koichi Kitazawa and Kohji Kishio, Department of Applied Chemistry, University of Tokyo, 7-3-1 Hongo, Bunkyo-ku, Tokyo 113, Japan

The chemically stable $(\text{Hg,Re})12(n-1)n$ system, found by the authors two years ago, has turned out to be a very promising material for the high field application at 77K as well as an interesting example to think of the possibility of introducing an ideal type of pinning centers by chemical means. Various characterizations have

revealed the following. The Re-doping does not deteriorate the original high- T_c of Hg-based system. The highest T_c was achieved for $n=3$ phases both in $\text{M}=\text{Ba}$ and Sr compounds and were 135K and 123K, respectively. In the $\text{M}=\text{Sr}$ compounds, Re ions substitute the Hg site and each of them introduces 4 extra oxygen atoms in the Hg-plane to form ReO_6 octahedra. Accordingly, similar structure is supposed to be formed in the $\text{M}=\text{Ba}$ compounds. We believe that the inter-layer coupling is much strengthened in the present compounds by introduction of this local structure. Substitution of Sr for Ba further reduces the inter-layer distance. These altogether are favorable to make the anisotropy of the material significantly smaller. The resulting irreversibility field has been found to be the highest ever, approximately 7T at 86K for $\text{Hg}_{0.8}\text{Re}_{0.2}\text{Ba}_2\text{Cu}_3\text{O}_y$.

D.9 5:40-6

"Observations Relating to the Apical Bond in High T_c Oxides: Mercury Cuprates and Cupro-oxyfluorides," **Peter P. Edwards**, School of Chemistry, The University of Birmingham, Edgbaston, Birmingham, B15 2TT, United Kingdom

The importance of the apical bond in High T_c solids continues to attract widespread interest and controversy. In this lecture I will give a brief review of recent work on two chemical systems in which the nature of the apical Cu-O bond will be critically assessed. These investigations encompass;

- The crystal structure of $\text{HgBa}_2\text{Ca}_2\text{Cu}_3\text{O}_{8+\delta}$ at high pressure (to 8.5 GPa), determined by neutron diffraction (Armstrong et al., *Phys. Rev. B52*, No. 17, 1 November 1995). The Cu-O apical bond here is some 2.9Å, challenging us to now define the precise meaning (and length scale) of a chemical bond in cuprate superconductors.
- A newer class of cupro-oxyfluorides, e.g. $\text{Sr}_2\text{CuO}_2\text{F}_{2+\delta}$, and variants, having a maximum T_c of some 70K; this represents the highest ever recorded value for a material with the confirmed La_2CuO_4 structure (Al-Mamouri et al., *Nature*, 369, 1994, 382). Interestingly, the apical bond is now a Cu-F bond.

D.10 6-6:20

"A View on HTS Performances Under Magnetic Fields from the Key Term 'Anisotropy Factor,'" **Koichi Kitazawa**, Hiroshi Ikuta, Jun-ichi Shimoyama, Masayuki Okuya, Satoshi Watauchi and Kohji Kishio, Department of Superconductivity, University of Tokyo, 7-3-1 Hongo, Bunkyo, Tokyo 113, Japan

One of the vital problems of the HTS materials to be overcome for the high field application is their strong tendency towards thermodynamical fluctuation of superconductivity. This tendency has its origin mainly in the weak inter-layer coupling of superconductivity. Since no HTS materials have been found outside the category of the CuO_2 layered structure, the relationship between the anisotropy and the superconducting performances and the mechanism behind it will keep to be the key problems in the HTS engineering. We report that the irreversibility field, a suitable engineering parameter to represent the extent of fluctuation, is essentially determined solely by the anisotropy factor irrespective of the specific material systems. The phase diagram in the mixed region can also be systematically discussed in terms of the anisotropy factor, including the 2D-3D crossover in the vortex structure and the melting

of its lattice. The anisotropy of each material can be chemically modified for optimization. The mechanisms of chemical control and possible future directions to improve the pinning strength are discussed.

CONCURRENT SESSIONS E & F

Thursday, March 14, 9:20 a.m. - 1 p.m.

SESSION E: HTS Theory I

Chairs: R. C. Dynes, C. S. Ting

La Salle Ballroom A & B

E.1 9:20-9:40

"Numerical Results and the High T_c Problem: From Ladders to Planes," **David J. Scalapino**, Department of Physics, UCSB, Santa Barbara, CA 93106-9530

Here we will discuss what numerical methods have told us about the pairing mechanism in doped ladders and planes with short-range antiferromagnetic correlations.

E.2 9:40-10

"Spin Fluctuations, Magnetotransport and $d_{x^2-y^2}$ Pairing in the Cuprate Superconductors+," **David Pines**, Department of Physics, University of Illinois at Urbana-Champaign, 1110 W. Green Street, Urbana, IL 61801

I use a nearly antiferromagnetic Fermi liquid (NAFL) description of planar excitations to review recent experimental and theoretical work on spin fluctuation excitations in the cuprate superconductors which establishes magnetic scaling behavior in the normal state and reconciles the results of neutron and NMR experiments on $\text{La}_{2-x}\text{Sr}_x\text{CuO}_4$ and $\text{YBa}_2\text{Cu}_3\text{O}_{6+x}$ systems. I describe the results of model NAFL calculations which make evident the causal relationship between the magnetic quasiparticle interaction, normal state magnetotransport, and the transition at high temperatures to a superconducting state with $d_{x^2-y^2}$ pairing, and discuss further recent experiments which support that pairing state.

+ Supported by NSF DMR 91-20000 Grant to the Science and Technology Center for Superconductivity

E.3 10-10:20

"Quantitative Explanation of 10 Peculiar Behaviors of High- T_c Superconductors Using 'Anyon' Approach to the t - J Hamiltonian," **R. B. Laughlin**, Department of Physics, Stanford University, Stanford, California 94305

I will show that the slope of the linear doping dependence of the optical sum rule, the depth of the pocket in the quasiparticle dispersion, the fermi velocity, the equality of the quasiparticle width and binding energy at most momenta, the 5% doping boundary to antiferromagnetic order, the 25% doping boundary to the normal metal state, the discommensuration of the magnetic susceptibility peak with doping, the size of T_c and its bell-like doping dependence, the sharp "gap mode" seen in

neutron scattering, and the occurrence of d-wave pairing symmetry are all present in simple "anyon" calculations for the t - J Hamiltonian that are reasonably controlled, consistent with known properties of the model, and not adjusted to fit the facts.

E.4 10:40-11

"Cuprate Ladder Compounds," **T. M. Rice**, Theoretische Physik, ETH Hönggerberg, 8093 Zürich, Switzerland

Ladder compounds can be achieved by breaking up the standard CuO_2 -planes into strong coupled chains to form the ladders which in turn are only weakly coupled to each other. Theoretical predictions that a clear distinction should exist in undoped compounds at low temperatures between ladders with even and odd numbers of legs have been confirmed. The even-leg ladders are spin liquids with a finite spin gap whereas the odd-leg ladders behave as effective single chain systems and have gapless excitations. The biggest interest lies in hole doping to test the prediction of hole pairing. To date only one ladder compound has been doped $\text{La}_{1-x}\text{Sr}_x\text{CuO}_{2.5}$, but this shows localization and not superconductivity at low doping¹. Estimates of the interladder coupling in this family give relatively large values and place it near the quantum critical point where the spin liquid develops antiferromagnetic order².

¹Z. Hiroi and M. Takano, Nature **377**, 41 (1995)

²B. Normand and T. M. Rice, ETH-preprint

E.5 10:40-11

"Charge Inhomogeneity and High Temperature Superconductivity," **Victor J. Emery**, Brookhaven National Laboratory, Department of Physics, Upton, NY 11973-5000, and Steven A. Kivelson, Department of Physics, UCLA, Los Angeles, CA 90095

When the condensation of a gas of fermions into a (self-bound) liquid state is frustrated by the long-range Coulomb interaction, the consequence is a large local fluctuation of the charge density, together with pairing on a high energy scale. The competition between these two effects at long length scales determines the nature of the ordered state at low temperatures. Evidence for the central role of this competition in determining the physical properties of the high temperature superconductors is provided by the delicate interplay of superconductivity, charge and spin ordering, and structural phase transformations in the La_2CuO_4 family of materials. There the gas-liquid transition corresponds to the phase separation of holes doped into an antiferromagnetic insulator. Because of the low superfluid density and poor conductivity, the critical temperature for the superconducting transition in underdoped and optimally doped materials is governed by the onset of phase coherence and not by the pairing energy scale.

E.6 11-11:20

"Phase String and Superconductivity in the t - J Model," **Z. Y. Weng**, Texas Center for Superconductivity at the University of Houston, Houston, TX 77204-5932

When a doped hole hops on an antiferromagnet, it always leaves a trace of spin mismatches on its path. Whether such a "string" effect is repairable or not through spin flips can make a great difference in low-lying charge and spin dynamics. Recently it has been rigorously shown that string effect induced by doped-holes cannot be

repaired by low-energy spin dynamics in the t - J model. Consequently many very interesting properties can be deduced from this picture. Here we focus on the discussion of superconductivity and its close correlation with anomalous spin dynamics based on a self-consistent treatment of the string effect. A comparison of our theory with experimental measurements in high- T_c cuprates will be given.

E.7 11:20-11:40

"Gauge Theory of the Normal State Properties of High- T_c Cuprates," **Naoto Nagaosa**, Department of Applied Physics, University of Tokyo, 7-3-1 Hong, Bunkyo-ku, Tokyo 113, Japan

E.8 11:40-12

"Superconductivity in the Cuprates as a Consequence of Antiferromagnetism and a Large Hole Density of States," **Elbio R. Dagotto**, Alexander Nazarenko and Adriana Moreo, National High Magnetic Field Lab and Department of Physics, Florida State University, Tallahassee, Florida 32306

A recently proposed scenario for the cuprates (Phys. Rev. Lett. **74**, 310 (1995)) is briefly reviewed. Superconductivity is caused by short-range antiferromagnetic correlations, and it appears in the $d_{x^2-y^2}$ channel. A real-space picture of the interaction between quasiparticles is helpful to visualize the d -character of the pairs. The presence of flat bands in the hole dispersion induce a robust peak in the hole density of states (DOS), which is important to boost up the critical temperature. The flat regions are produced by antiferromagnetic correlations, rather than band structure effects. When the chemical potential crosses the DOS peak, T_c is maximized explaining the presence of an optimal doping. The narrow band character of the quasiparticles is crucial for the present ideas. The evolution of the hole dispersion with hole density is also discussed.

E.9 12-12:20

"Superconductivity and the Square Fermi Surface," **Alan H. Luther**, Nordita, Blegdamsvej 17, Copenhagen, 2100, Denmark

In two dimensions, the Hubbard model at a filling of one electron per site would have a square Fermi surface, in the absence of electron-electron interactions. Switching on interactions, or adding holes, raises many questions – which can be answered exactly.

Using an exact mapping of the flat portions of the Fermi surface onto a system of 1D chains, it is possible to study the effects of interactions in detail. Interactions, either attractive or repulsive, lead to confinement of electrons to the chains. In other words, electron hopping parallel to the flat portions vanishes – the corresponding operator is irrelevant in the renormalization group sense.

In general, the system exhibits spin-charge separation. At one electron per site, there is a gap in the charge spectrum, and the spin excitations are consistent with anti-ferromagnetic spin waves. Doping away from this point, it is found that interactions stabilize the square. The circular distortion operator is irrelevant.

The paper also reports a study of the superconducting fluctuations and magnetic excitation spectrum. These results are argued to be asymptotically exact.

E.10 12:20-12:40

"A Possible Primary Role of the Oxygen Polarizability in High Temperature Superconductivity," **M. Weger**¹ and M. Peter², ¹Racah Institute of Physics, Hebrew University, Jerusalem, ²DPMC, Geneva University, Geneva

The ionic dielectric constant in superconducting cuprates is found to be very large at low frequencies, $\epsilon_0 \approx 40$ with a dispersion around $\xi_1 \approx 15$ meV. This dielectric constant has a profound effect, the material being a "doped semiconductor" rather than a "conventional" metal. Since $\epsilon_{ion} > \epsilon_{el}$ (except for very small q -values), the electron-electron interaction is shielded by the ionic polarizability, and the electronic Thomas-Fermi parameter κ_{TF} is very small. This causes the electron-phonon matrix element to be abnormally large for small values of ω ($\omega < \xi$) and for small (but not extremely small) values of ω ($\omega \approx \kappa_{TF}$). As a result, the McMillan coupling constant λ is abnormally large at small energies. We calculate the superconducting transition temperature T_c and other properties by solving the Eliashberg equations in a "very strong coupling" scenario. The maximum value of T_c in a 2-D system is given approximately by: $(T_c)_{max} = 0.1(e^2/2a_c) \cdot 1/(m/M)^{1/2} \cdot 1/(\Delta\theta)^{1/2} \cdot (\xi_1/\Omega)$ where $2a_c$ is the width of the metallic layer (a_c is the Bohr radius of the oxygen ion in the c -direction), m the band mass, M the oxygen mass, $\Delta\theta$ the scattering angle ($\approx \kappa_{TF}/k_F$), and Ω the frequency of the Cu-O stretching vibrations (≈ 40 meV). This gives a maximum value of about 200 K for parameters characteristic of the cuprates. The small value of $\Delta\theta \approx 0.3$ radians indicates forward-scattering of the electrons by the phonons. This causes a near-degeneracy between superconducting states with d -wave and s wave symmetry, the d -wave state being favored in "clean" samples. Under certain (but not all) conditions, the isotope effect is greatly compensated.

Therefore, we believe that it is possible to account for high temperature superconductivity by the BCS phonon-mediated interaction.

E.11 12:40-1

"A Complete Pairing Mechanism in Superconductivity," **J. D. Fan** and Y. M. Malozovsky, Department of Physics, Southern University and A & M College, Baton Rouge, LA 70813

A new concept of the pairing instability is introduced based on the consideration of pair Coulomb interactions in the particle-hole channel of an interacting Fermi gas. The pairing of two quasiparticles is analogous to the resonating valence binding (RVB) between two electrons in a positronium molecule-like structure (biexciton). It is a development of the conventional Cooper instability and may lead to a unified understanding of both low- and high- T_c superconductivity. It is turned out that scattering diagrams from this model allow one to evaluate the vertex part Γ_c in the charge channel. T_c is hence calculated by using the pole condition of Γ_c . It has been found that T_c can reach quite high values and presents the bell shape, and is related to the carrier density, interlayer distance, dielectric constant and electron band mass, etc.

-Supported by DOE under the grant No. DE-FG05-94ER25229 through the Science and Engineering Alliance, Inc.

SESSION F: HTS Processing

Chairs: D. T. Shaw, U. Balachandran
Granger A & B

E1 9:20-9:40

"Progress of HTS Bismuth-Based Tape Application," **Ken-ichi Sato**, Sumitomo Electric Industries, Ltd., Osaka Research Laboratory, 1-1-3, Shimaya Konohana-ku, 554, Japan

A great deal of progress on HTS bismuth-based tape application have been achieved. Especially, actual application using bismuth-based HTS tapes for large current conductors and magnets was demonstrated.

Two years stable operation of 4-sets of 2kA current leads for NbTi bending magnets in NIJI-III (synchrotron radiation equipment) proved the economic aspects and stability of HTS materials. Also, 66kV/1kArms 3-phase power cable (7-m long) prototype proved that only HTS could make a compact and large capacity power cable.

A large bore, 60 mm ϕ , magnet could generate 0.66 T at 77 K, and 3 T at 20 K, showing the actual field and size capability of HTS magnet. For large magnet application, we need high amperage and high strength tapes. High amperage tape was developed. This tape showed high amperage of $I_c=1,380$ A at 15 T and 4.2 K, and 91 A at 1 T and 77 K. For high strength tapes, silver-alloy matrix tapes could sustain 200 MPa without degradation of critical current.

E2 9:40-10

"Strong Flux Pinning in RE123 Grown by Oxygen-Controlled Melt Process," **Noriko Chikumoto** and Masato Murakami, ISTEC-SRL, 16-25 Shibaura 1-chome, Minato-ku, Tokyo 105, Japan

It had been long recognized that it is impossible to fabricate the melt-textured $REBa_2Cu_3O_7$ superconductors with light RE ions (Nd, Sm, Eu) possessing both high superconducting transition temperature (T_c) and a sharp superconducting transition, because of the heavy substitution of RE on the Ba site. However, we have recently revealed that a reduced oxygen atmosphere during melt processing is critical for the fabrication of a good RE123. Nd123 superconductor melt processed in the mixed gas of 0.1% O_2 in Ar showed a sharp superconducting transition at around 96K, while that fabricated in air showed very broad transition at 60 K.

In addition, fabricated RE123 superconductors exhibit excellent pinning properties: J_c values in a high field regions exceed those of good quality melt-processed Y123 and the irreversibility field with H/c axis reaches 8 T at 77 K. Such a strong flux pinning is likely to provided preferably distributed Nd-rich regions (low T_c regions) in the high- T_c matrix.

This work was partially supported by NEDO.

E3 10:10-20

"IBAD Deposition of Thick Film Superconductors," **Dean E. Peterson**¹, Paul Arendt², Xin Di Wu¹ and Stephen R. Foltyn¹, ¹Superconductivity Technology Center and ²Materials Technology: Polymers and Coatings, Los Alamos National Laboratory, P. O. Box 1663, Mail Stop K763, Los Alamos, NM 87545

Thick film superconducting tapes that carry substantial currents when cooled by liquid nitrogen and have a high degree of flexibility have now been shown to be feasible. The fabrication approach involves initial formation of an aligned oxide thin film on a nickel tape by using ion beam assisted deposition (IBAD). A YBCO thick film (1-2 microns) is then deposited on the buffer layer by laser ablation. Achievement of J_c (75K) of more than 1 MA/cm² with an I_c (75K) of 200 A in 2 micron thick superconducting has demonstrated the potential of this method. The critical current response of the tapes was characterized as a function of magnetic field orientation out to 19T at 75 K. Bending tests of the tapes indicated retention of 91% of the initial critical current with strains of 1% compressive and 0.5% tension. The importance of alignment of the buffer and superconductor layers is to be discussed. Opportunities for the economic manufacture of long lengths of HTS tape by this IBAD approach while maintaining high engineering J_e (77 K) values will be presented.

E4 10:20-10:40

"Fabrication of $HgBa_2Ca_2Cu_3O_{8+\delta}$ Tape," **R. L. Meng**, B. Hickey, Y. Q. Wang, L. Gao, Y. Y. Sun, Y. Y. Xue and C. W. Chu, Department of Physics and Texas Center for Superconductivity at the University of Houston, Houston, TX 77204-5932

$HgBa_2Ca_2Cu_3O_{8+\delta}$ (Hg-1223) exhibits superior superconducting properties to many other cuprate high temperature superconductors and thus is a good candidate for conductors. Unfortunately, the complex chemistry of Hg-1223 makes its fabrication as tape difficult. Therefore, we have carried out a systematic study on the formation and chemical stability of Hg-1223 and competing compounds, such as $HgCaO_2$ and $HgBaO_2$, during the synthesis of Hg-1223; on the Hg/metal reaction; and on the Hg-1223/metal-substrate interfacial reaction. By selecting Ni as the metallic-substrate with a thin buffer layer of Cr, thick tapes of Hg-1223 have been prepared with a $T_c \sim 130$ K and a $J_c \sim 2.5 \times 10^4$ A/cm² in the self-field at 77 K. The results on the preparations of the substrate and the Hg-1223 tape will be presented and discussed.

This work is supported in part by NSF, EPRI, the State of Texas through the Texas Center for Superconductivity at the University of Houston, and the T. L. Temple Foundation. This material was also prepared with the support of the U. S. Department of Energy, Grant No. DE-FC-48-95R810542. However, any opinions, findings, conclusions, or recommendations expressed herein are those of the authors and do not necessarily reflect the views of DoE.

E5 10:40-11

"New Process to Control Critical Currents of $Nd_{1-x}Ba_{2-x}Cu_3O_{7-\delta}$," **Yuh Shiohara**, M. Nakamura and Y. Yamada, SRL-ISTEC, Div. 4, 10-13 Shinonome I-Chome, Koto-ku, Tokyo, 135, Japan, and T. Hirayama and Y. Ikuhara, JFCC, 2-4-1 Mutsuno, Atsuta-ku, Nagoya, Aichi, 456, Japan

It has been reported that $Nd_{1-x}Ba_{2-x}Cu_3O_{7-\delta}$ (Nd123) superconductive oxides have higher T_c (~ 96 K) and higher J_c under high magnetic fields of several teslas than those of YBCO. A new process to control nano-scale microstructure has been developed. It has been well recognized that Nd123 crystals are nonstoichiometric compounds, namely composed of a solid solution phase, due to substitution of Nd ions with Ba ions. In this work, several different series of heat treatments in a pure

oxygen gas flow were applied to Nd123 bulk single crystals produced separately by crystal pulling. J_c -H curves with either H//a-axis or H//c-axis of obtained crystals heat treated at 340°C for 200 hrs show no anomalous peak effect. On the other hand, when two stage heat treatment (500°C for 100 hrs and 340°C for 200 hrs) was applied, J_c -H curve at 77K with H//c-axis exhibited an anomalous peak effect. Magnetic J_c value calculated at this peak field by the extended Bean's critical state model was as high as 3×10^4 A/cm² at 77K, 4T. Further annealing of the same sample (900°C for 100 hrs, quenched, 340°C for 200 hrs) resulted in disappearance of the peak effect. These results together with TEM observation confirm that a reversible solid state reaction such as spinodal decomposition modifies nano-scale microstructure of the bulk Nd123 crystal. More detailed results will be presented.

This work was supported by NEDO as a part of Industrial Science and Technology Frontier Program.

E.6 11-11:20

"Improvement of Flux Pinning in High Temperature Superconductors by Artificial Defects," **Harald W. Weber**, Atomic Institute of the Austrian Universities, Department of Low Temperature Physics and Superconductivity, Schüttelstraße 115, A-1020 Vienna, Austria

Many attempts to improve flux pinning in high temperature superconductors have been reported on, but only a few were found to be effective in all families of the cuprate superconductors. This paper is intended to review the progress achieved by introducing artificial defects by fast neutron irradiation into single crystals, textured bulk materials as well as thin films of Y-, Bi- and Tl-based cuprates.

Fast neutrons penetrate the materials in an isotropic form with a mean free path of a few cm between collisions. Therefore, the defects are arranged in a statistical manner without preferential orientation. TEM on YBCO single crystals has shown, that the most important defects produced in this way are collision cascades with roughly spherical shape and diameters of ≈ 3 nm surrounded by a strain field of the same size. Hence, the total extension of these defects is of the order of the coherence length and, therefore, ideally suited to effective pin flux lines or pancake vortices.

The beneficial effects of these defects will be demonstrated, in particular with regard to enhancements of the critical current densities and shifts of the irreversibility lines, which are especially remarkable at higher fields and at temperatures of practical interest.

E.7 11:20-11:40

"HTS Conductors: Challenges and Progress," Leszek Motowidlo and Robert S. Sokolowski, IGC Advanced Superconductors, Department of High Temperature Superconductors, 1875 Thomaston Avenue, Waterbury, CT 06704, and Pradeep Haldar and **Venkat Selvamanickam**, Intermagnetics General Corporation, Department of High Temperature Superconductors, 450 Old Niskayuna Rd., P. O. Box 461, Latham, NY 12110-0461

Since the discovery of superconductivity at temperatures well in excess of the operating range of conventional metallic (low-temperature) superconductors, the progress across the world in developing practical methods for producing high-temperature superconductors in long lengths has far exceeded expectations. This

success, particularly in the United States and Japan, has led to the early introduction of significant quantities of HTS conductors into prototype devices, such as laboratory magnets, generator coils, and power transmission cables. In spite of this rapid progress, substantial improvements in performance are still needed to realize true commercialization.

Intermagnetics has developed different processing techniques in order to produce a variety of HTS conductors suited for such varied applications as electric power and spectroscopy. The engineering challenges for several of these applications will be presented. The relative advantages of these materials in practical applications will be discussed, with emphasis placed on the economic comparisons drawn to the competitive.

E.8 11:40-12

"A Novel Approach to High Rate Melt-Texturing in 123 Superconductors," **Kamel Salama**, Department of Mechanical Engineering and Texas Center for Superconductivity, University of Houston, Houston, TX 77204-4792

Initial hurdles of processing the Y-123 compound ($Y_1Ba_2Cu_3O_x$) to satisfy high current applications were overcome by the melt texturing process developed in 1988. This process yielded pseudo-single crystals that have transport current densities of 10^5 Amp/cm² at 77 K in self field and 10^3 Amps/cm² at 77 K and in 30 T. Recently, it was found that certain RE-123 type compounds containing the rare earth element neodymium ($Nd_{1-x}Ba_{2+x}Cu_3O_{7-\delta}$) have a very high rate of recrystallization. The high rate of recrystallization causes the recombination and solidification rates to increase significantly, thus making these compounds highly suitable for the directional solidification process. By processing bars (50 mm x 5 mm x 5 mm) of these compounds through a high temperature gradient, fully textured microstructures were obtained at rates up to 50 mm/hr, and up to 100 mm/hr in case of electrophoretically coated wires. These processing rates are 50-100 times more faster than the texturing rates employed in $Y_1Ba_2Cu_3O_x$. After oxygen annealing, these textured bars have a T_c onset of 93K and a transport J_c at 77K and zero applied magnetic field, on the order of 5,000 A/cm². These results are expected to increase significantly as more progress takes place*.

*K. Salama, A. S. Parikh and L. Woolf, "High Rate Melt Texturing of $Nd_{1-x}Ba_{2+x}Cu_3O_{7-\delta}$ Type Superconductors", Applied Physics Letters, April 1996, In press.

E.9 12-12:20

"Processing and Properties of Ag-Clad BSCCO Superconductors," **U. Balachandran**, Anand N. Iyer and R. Jammy, Argonne National Laboratory, Energy Technology Division, 9700 South Cass Avenue, Argonne, IL 60439, and P. Haldar, Intermagnetics General Corporation, Latham, NY 12110

Long lengths of mono- and multifilament Ag-clad BSCCO conductors with critical current densities $> 10^4$ A/cm² at 77 K were fabricated by the powder-in-tube technique. Magneto-optical imaging techniques were used to better understand the transport current flow patterns. High- T_c magnets were assembled (by stacking pancake coils fabricated from long tapes) and tested as a function of applied magnetic field at various temperatures. A magnet that contained ≈ 2400 m of high- T_c conductor

E.10 - G.4

generated a field of 3.2 T at 4.2 K. In-situ tensile and bending characteristics of the Ag-clad conductors have been studied. Preliminary results on the in-situ bending characteristics of monofilament conductors indicate that the irreversible strain limit increases with decreasing superconductor/Ag ratio. Superconducting joints and multilayer Ag/superconductor/Ag composites have been fabricated by a novel chemical etching technique. After exposure to 1% strain, the multilayer composite retained 90% of its initial critical current at 77 K. Recent advancements in the fabrication and application of Ag-clad BSCCO superconductors will also be presented.

Work at ANL and part of the work at IGC is supported by the U.S. Dept. of Energy, Energy Efficiency and Renewable Energy, as part of a program to develop electric power technology, under Contract W-31-109-Eng-38.

E.10 12:20-12:40

"Grain Boundary Misorientation Distributions and Percolation in HTS Conductors*," **D. M. Kroeger**, A. Goyal and E. D. Specht, Metals & Ceramics Division, Oak Ridge National Laboratory, Oak Ridge, TN 37831

The importance of the grain boundary misorientation distribution and the local spatial arrangement of grains for a given macroscopic texture in determining the effective critical current density is discussed. Experimentally determined grain boundary misorientation distributions (GBMD) in high- J_c Bi-2223 power-in-tube, Tl-1223 thick films, and melt-processed Bi-2212 thick films were compared to theoretical calculations of GBMDs based on macroscopic texture. The populations of low angle boundaries were found to be much larger than expected from calculations based on their macroscopic texture. In Bi-2223 no in-plane texture was observed on any scale. In Tl-1223 thick films, although no macroscopic in-plane texture was observed, local texture resulting in "colonies" of grains with similar a -axis orientation was observed. The general view has emerged that long-range conduction in polycrystalline superconductors utilizes connected networks of low energy boundaries. Consistent with the above, high- J_c 's have been obtained in epitaxial thick films on biaxially textured, polycrystalline, substrates prepared using the ORNL's RABiT (rolling assisted biaxially textured substrates) process.

*Research sponsored by USDOE, Office of Advanced Utility Concepts under contract DE-AC05-84OR21400 with Lockheed-Martin Energy Research.

CONCURRENT SESSIONS G & H

Friday, March 15, 9:30 a.m. - 12:30 p.m.

SESSION G: HTS Theory II

Chair: K. Levin

La Salle Ballroom A

G.1 9:30-9:50

"Current Fluctuations in Copper-Oxide Metals," **Chandra M. Varma**, Lucent Technologies, AT&T Bell Laboratories, 600 Mountain Avenue, Murray Hill, New Jersey 07974

G.2 9:50-10:10

"Aspects of D-Wave Superconductivity," **Kazumi Maki** and Ye Sun, Department of Physics and Astronomy, University of Southern California, Los Angeles, CA 90089-0484, and Hyekyung Won, Physics and Interdisciplinary Center for Physical Science, Hallym University, Chunchon, 200-702, South Korea

Recent works on impurity scattering and on vortex lattice in d -wave superconductors are reviewed. Impurity scattering in the unitarity limit not only describes a rapid suppression of the superconducting transition temperature but also rapid appearance of the residual density of states as determined from specific heat and Knight shift in Zn-substituted LSCO and YBCO. In a magnetic field the fourfold symmetry of d -wave superconductor is revealed clearly. In $\mathbf{B} // c$ a square lattice tilted by 45° from the a axis is found to be most stable except in the immediate vicinity of $T = T_c$. Indeed such a vortex lattice though elongated in the a direction has been seen by SAN scattering and STM imaging from monocrystals of YBCO. In $\mathbf{B} // a-b$ the upper critical field is written as $H_{c2}(\theta, t) = H_{c2}(\pi/4, t) + \Delta H_{c2}(t) \cos^2(2\theta)$, where θ is the angle \mathbf{B} makes from the a axis. Also in the absence of Pauli paramagnetism, $H_{c2}(\pi/4, 0) \cong 650$ Tesla and $\Delta H_{c2}(0) \cong 120$ Tesla, much too large to compare with the observed value (~ 350 Tesla) in YBCO.

G.3 10:10-10:30

"Ginzburg-Landau Theory of Superconductors with $d_{x^2-y^2}$ Symmetry," **C. S. Ting**, Y. Ren and J. H. Xu, Texas Center for Superconductivity at the University of Houston, Houston, TX 77204-5932

The structures of a single vortex and vortex lattice in superconductors with $d_{x^2-y^2}$ symmetry are studied self-consistently employing the microscopically derived Ginzburg-Landau equations. Near a single vortex, we found that an s -wave component of the order parameter is always induced. The magnitude of the induced s -wave component depends on the relative strength between the on-site repulsive coulomb interaction V_s and the d -wave pairing interaction V_d . For moderate values of V_s/V_d our numerical calculation indicates that the vortex structure is always oblique except in the region of $T \rightarrow T_c$. When V_s becomes negative (attractive), the system undergoes s to $s + id$ and to d pairing transition as the value of the parameter V_d increases. We also derived the Ginzburg-Landau equations for an anisotropic d -wave superconductor. The application of these equations to study the superconductivity of YBCO will be discussed and compared with experiments.

G.4 10:30-10:50

"Inside HT_c Superconductors: An Electronic Structure View[†]," **Arthur J. Freeman** and Dmitri L. Novikov, Department of Physics and Astronomy, Northwestern University, 2145 Sheridan Road, Evanston, IL 60208-3112

From the earliest days of high- T_c research, electronic structure theory has successfully revealed the physical and chemical properties of the normal state of the cuprates. In this talk, a review is given of some striking predictions of electronic structure theory about the role of van Hove singularities (vHs) on the electronic structure and properties of the newest and highest temperature superconducting cuprates at ambient and high pressures. The results provide possible strong evidence for the role of vHs in the superconductivity of quasi-2D high T_c systems. They thus

serve to call attention to their role not only in enhancing T_c through large increases in $N(E_F)$ and Fermi surface areas, but also in possibly providing support for vHs based excitonic pairing mechanisms for superconductivity. Further, this information, derived from the understanding - expressed as an "empirical rule" - gained from the related role of doping and pressure, is used to investigate other likely systems for being made into high T_c superconductors.

† Supported by the NSF (DMR91-20000)

G.5 10:50-11:10

"Energy Spectrum and 'Intrinsic' T_c of the Cuprates: Effects of Pair-Breaking, Pressure, and Non-Adiabaticity," **Vladimir Z. Kresin**, University of California, Lawrence Berkeley Laboratory, 1 Cyclotron Road, Berkeley, CA 94720, Stuart A. Wolf, Naval Research Laboratory, Material Sciences Branch, Code 6340, Washington, D.C. 20375-5000, and Yurii N. Ovchinnikov, Landau Institute for Theoretical Physics, 2 Kosygin Str., Moscow, 11733V, Russia

A unique property of the high T_c oxides is the strong dependence of the energy spectrum on the degree of doping. One can observe two-gap structure; deviation from stoichiometry leads to a transition into the peculiar gapless regime. The value of T_c is greatly affected by an interplay between doping and pair-breaking scattering. This scattering leads to a depression of T_c relative to its "intrinsic" value.

Spin-flip scattering along with the trend to ordering of magnetic impurities leads to the "strengthening" of superconductivity as $T \rightarrow 0$; this effect is manifested in a drastic increase in the value of H_{c2} , in agreement with the experimental data. One can raise T_c above the maximum ambient pressure value by pressure-induced doping.

Apical oxygen is characterized by a non-adiabatic behavior. In addition, the magnetic moments are located on the apical oxygen site, and this allows to explain the large difference in T_c between 2201 and 1223 (or 1223) structures.

G.6 11:10-11:30

"Localized States as an Explanation of Some Properties of Cuprates," **Michel Cyrot**, Laboratoire Louis Neel, CNRS, 38042 Grenoble cedex, France

In some recent publications, we have argued that besides Fermi liquid excitations, it can exist in a doped Mott insulator, localized excitations of energy much smaller than the bandwidth or the intraatomic interaction. We show that such an hypothesis can explain the experimental findings by neutron scattering of coexistence of localized and itinerant magnetism in the superconducting cuprates. Also the optical conductivity which shows a transfer from the mid infrared to Drude peak with doping can find a reasonable explanation in the transfer of the weight of the localized states to itinerant states.

G.7 11:30-11:50

"Thermopower of the Cuprates Under High Pressure," J. B. Goodenough and **J.-S. Zhou**, MS & E Department, University of Texas at Austin, Austin, TX 78712

The temperature dependence of the thermopower of the intergrowth copper oxides is $\alpha(T) = \alpha_0 + \delta\alpha(T)$. The enhancement factor $\delta\alpha(T)$ disappears in

polaronic conductors; a $\delta\alpha(T)$ having a $T_{max} \approx 140$ K is found in the superconductors $La_{2-x}Sr_xCuO_4$, a $\delta\alpha(T) > 0$ extends into the overdoped regime; the pressure experiments show a strong correlation between T_c and $\delta\alpha(T)$ indicative of a common underlying mechanism. In underdoped $YBa_2Cu_3O_{6.7}$, the $Cu(1)O_x$ planes do not contribute to $\alpha(T)$ and pressure transfers electrons from the CuO_2 sheets to $Cu(1)O_x$ planes, which increases T_c and $\delta\alpha(T)$. In fully oxidized $YBa_2Cu_3O_{6.96}$ and $YBa_2Cu_4O_8$, the more conductive chains give a negative $\delta\alpha(T)$ that dominates the positive $\delta\alpha(T)$ of the CuO_2 sheets, and pressure increases the superconductive-pair concentration n_s in the chains but not in the sheets; it also increases the negative component in $\delta\alpha(T)$ relative to any change in the positive component. A c-axis vibration observed with Raman spectroscopy supports a vibronic coupling as the underlying mechanism responsible for $\delta\alpha(T)$ and the inducing of superconductivity in the chains.

G.8 11:50-12:10

"Quasiparticles, Strong-Coupling Regime and Fermi Liquid Theory Breakdown," **Alvaro Ferraz**, International Centre of Condensed Matter Physics, Universidade de Brasilia, Caixa Postal 04667, 70919-970 Brasilia DF, Brazil, and Yoshi Ohmura, Department of Physics, Tokyo Institute of Technology, Tokyo 152, Japan

We consider a strongly interacting electron liquid characterized by a charge parameter $Z \ll 1$. In this regime the position of the Fermi surface (S_F) is no longer sharply defined, which implies that the quasi-particle chemical potential is momentum dependent. Considering that these particles are confined in a very thin shell in momentum space around their Fermi surface, we argue that there exists more than one type of quasiparticle in the physical system. Here we construct a model which takes explicit account of this feature. It is shown that, as a result, there is a region in momentum space, away from the lower energy S_F , in which the effective interaction between quasiparticles of the same kind becomes attractive. This leads to a breakdown of the quasiparticle representation and to a new non-perturbative regime.

G.9 12:10-12:30

"Hole Spectrum in Three Band Model," **Lev P. Gor'kov**, National High Magnetic Field Laboratory, Florida State University, 1800 E. Paul Dirac Dr., Tallahassee, FL 32306, and Pradeep Kumar, Department of Theory & Math, NSF, 4201 Wilson Blvd., Arlington, VA 22230

We consider the energy spectrum of a single hole in the framework of a three band model for CuO_2 plane. The hole Hamiltonian is derived perturbatively up to the terms quadratic in the hopping matrix element between the Cu- and O- sites, as usual. By making use of the explicit symmetry of the resulting Hamiltonian we get, however, some more insight into structure of the hole bands and their renormalization due to interactions with the spin excitations of the antiferromagnetic background. The band lowest in energy turns out to be dispersionless. This fact leads to the conclusion that the spin polaronic cloud surrounding the hole, has a finite size and internal degrees of freedom. The dispersion of the hole which is a result of interaction with the spin excitations, is directly related to the dispersion of the latter. The minima of the hole spectrum are at the boundary of the magnetic unit cell. The results are discussed and compared with the ones for the t-J-model.

SESSION H: Film & Applications

Chairs: A. Lauder, J. C. Wolfe

La Salle Ballroom B

H.1 9:30-9:50

"Synthesis of Novel High- T_c Superconductors by Atomic-Layer Epitaxy," **Ivan Bozovic**¹ and James N. Eckstein², Varian Research Center, M/S K-114¹ and M/S K-214², 3075 Hansen Way, Palo Alto, CA 94304-1075

Atomic layer-by-layer molecular beam epitaxy (ALL-MBE) have been used to synthesize single-crystal thin films of cuprate superconductors and other oxides. A variety of heterostructures, multilayers and superlattices with atomically abrupt interfaces have been fabricated for electronics device applications. The samples are engineered by stacking molecular layers of different compounds, by adding or omitting atomic monolayers, and by doping within specified monolayers.

Here we will summarize our efforts to synthesize new cuprate superconductors by atomic layering. In particular, we have investigated Bi-Sr-Ca-Cu-O and La-Sr-Ca-Cu-O phases containing multiple (4-10) CuO_2 planes.

So far, the highest T_{c0} (about 75 K) was achieved in Bi-1278 compound (epitaxially stabilized by Bi-2201). Replacing the central Ca layer in Bi-1278 by Dy, one creates a bizarre compound which contains an insulating slab in the center while the outer CuO_2 layers are clearly superconducting. We have utilized such layers to fabricate *c*-axis tunnel junctions which show $I_c R_n$ as high as 10 mV.

H.2 9:50-10:10

"Very High Growth Rates of High Quality YBCO Under Photo-Assisted MOCVD," **Alex Ignatiev**, Q. Zhong and P. C. Chou, Texas Center for Superconductivity, Houston, TX 77204-5507

High quality YBCO films have been previously deposited by photo-assisted MOCVD (PhAMOCVD), however recent developments have shown the possibility of YBCO thick film deposition by PhAMOCVD at very high growth rates. YBCO films of >1mm thickness with $J_c \sim 1 \times 10^6 \text{ A/cm}^2$ have been deposited on a variety of substrates at rates of up to 8000 A per minute. The films can be either *c*-axis or *a*-axis oriented depending on growth parameters, with the *c*-axis oriented growths yielding films with rocking curve half widths of $\sim 0.28^\circ$. Quartz-halogen lamps are used as the sole energy source for the MOCVD reactor which is set up in a vertical-flow mode. The application of the PhAMOCVD technique to rapid, thick film YBCO growth is being extended to metal substrates for future use in flexible wires and tapes. Growths are underway on nickel substrates textured by ion beam assisted deposition, and on silver substrates textured by rolling. The rapid, high quality growth of YBCO thick films by PhAMOCVD can result in superconducting tape fabrication at speeds of the order of cm/min indicating the possibility for commercial production of high current YBCO wires and tapes.

H.3 10:10-10:30

"Ultrafast Superconductor Digital Electronics," **Konstantin K. Likharev**, State University of New York, Stony Brook, NY 11794-3800

I will review the recent progress in the development of superconductor digital circuits using Josephson junctions as active circuit components. In contrast to earlier, unsuccessful attempts of the practical introduction of superconductor digital electronics, the current work in the field is focused on a novel, ultrafast Rapid Single-Flux Quantum (RSFQ) logic family. The elementary cells of these circuits exchange the data in the form of short voltage pulses with quantized "area" $\int v dt = \Phi_0 \approx 2 \text{ mV}\cdot\text{ps}$. These pulses may be passed between the cells ballistically, with a velocity approaching the speed of light. This property allows to retain ultrahigh speed of operation even in complex integrated circuits. Recent experiments using an LTS (Nb/ AlO_x/Nb) technology have demonstrated the operation of a simple RSFQ circuit at frequencies up to 370 GHz. Using HTS, the maximum clock speed could reach a few THz for simple circuits and approach 1 THz for complex circuits and systems. Simple HTS RSFQ circuits have been demonstrated at temperatures up to 65 K, but the technology of fabrication of Josephson junctions using these materials should mature substantially before more complex digital HTS circuits become feasible. I will discuss in detail the challenges which should be met by the technology before the HTS digital electronics become a reality.

H.4 10:30-10:50

"In-Plane and C-Axis Linear and Nonlinear Microwave Response of Cuprate Superconductors," **S. Sridhar**, Physics Department, Northeastern University, 360 Huntington Avenue, Boston, MA 02115

Precision measurements of the penetration depth and surface impedance of cuprate superconductors are used to probe the quasi-particle density of states, scattering and order parameter symmetry in cuprate superconductors. Our latest results of the *ab*-plane penetration depth of BSCCO crystals shows a common behavior of the density of states of BSCCO and YBCO, consistent with nodes in the in-plane superconducting gap, while the *c*-axis transport is quantitatively consistent with direct hopping across weakly coupled superconducting layers [1]. These measurements resolve previous controversies between $\lambda(T)$ results on BSCCO and YBCO crystals. The role of scattering and comparisons with detailed calculations of models of *d*-wave superconductivity is considered in YBCO crystals [2], and magnetic pair-breaking caused by *Pr*-doping is shown to lead to some unusual effects on the surface impedance.

A novel switching behavior of the surface impedance of BSCCO single crystals is observed which manifests as quantized changes in surface impedance for microwave field strength changes of less than 1 mG. The non-linearity is associated with microwave critical currents driving an intrinsic Josephson junction along the *c*-axis of the crystal [3] and experimental data are compared with the dynamic microwave impedance expected for a purely *ac*-biased junction.

Work supported by NSF and AFOSR.

[1] Phys. Rev. Lett., **75**, 4526 (1995)

[2] J. Phys. Chem. of Solids, (to appear)

[3] Appl. Phys. Lett. (Submitted).

H.5 10:50-11:10

"Fabrication of Highly Textured Superconducting Thin Films on Polycrystalline Substrates Using Ion Beam Assisted Deposition," **Quan Xiong**¹, Sergio Afonso¹, F. T. Chan¹, Kai Y. Chen¹, G. J. Salamo¹, G. Florence², Simon Ang², W. D. Brown² and L. Schaper², ¹Physics Department and ²Electrical Engineering Department/High Density Electronics Center, University of Arkansas, Fayetteville, AR 72701

Tl₂Ba₂CaCu₂O₇ (Tl2212) thin films on ceramic Al₂O₃ substrates with J_c (77K) of about 10⁵ A/cm² and high quality YBCO/YSZ/SiO₂/YSZ/YBCO/LaAlO₃ multilayers with J_c (77K) of about 6x10⁵ A/cm² in the top YBCO layer have been successfully deposited for the first time. These Mirror-like, highly c-axis oriented films were grown on highly textured YSZ buffer layers, which were deposited through Ion Beam-Assisted Laser Ablation. The zero resistance temperature is 95-108K for the Tl2212 films, and 85-90K for the multilayer YBCO films. The synthesis procedure and possible applications will be discussed.

*This work is supported in part by NSF DMR 9318946, ARPA (Contract No. MDA 972-90-J-1001) through Texas Center for Superconductivity at the University of Houston.

H.6 11:10-11:30

"Biaxially Textured YBaCuO Thick Films on Technical Substrates," **Herbert C. Freyhardt**¹, Jürgen Wiesmann¹, Klaus Heinemann¹, Jörg Hoffmann¹, Jürgen Dzick¹, Alexander Usokin², Francesco Garcia-Moreno² and Sybille Sievers², ¹Institut für Metallphysik, LMM/KL and ²ZFW Göttingen GmbH, Windausweg 2, D-37073 Göttingen, Germany

High-current applications require homogeneous well textured high-temperature superconducting (HTSL) YBaCuO films of sufficient thickness deposited on technical substrates. Depending on the application in electrical engineering or power distribution systems, metallic or nonmetallic substrates will have to be selected as ribbons or sheets; e.g. Ni, Hastelloy (C22) and flexible Y-stabilized ZrO₂ (YSZ) as well as Al₂O₃+bi-YSZ. However, in particular the metallic substrates cannot be used without buffer films, which serve as a template for the YBaCuO and as a diffusion barrier.

Ion-beam assisted deposition (IBAD) was employed to grow biaxially textured buffer films of YSZ and also of CeO₂ on planar as well as curved; i.e. cylindrical, substrates.

High-quality thick YBa₂Cu₃O_{7-δ} films were produced on different moving substrates by pulsed excimer laser ablation. Two methods were used to control (to high precision) the surface temperature of the growing HTSL film, whereby the use of a quasi-equilibrium radiation heater proved to be most successful. Up to 9 μm thick films were grown on moving substrates with reduced structural degradation effects. On single crystalline SrTiO₃, critical current densities, J_c, between (3.5-1.5)x10⁶ A/cm² at 77K, 0T could be obtained, which only slightly decrease with film thickness, and J_c values of 9x10⁵ A/cm² (0T, 77K) were measured for YBaCuO on Ni with bi-YSZ buffers and of 4x10⁵ A/cm² on YSZ with bi-YSZ. The critical superconducting parameters of the films were investigated under tension and compression.

The research is supported by BMBF of Germany.

H.7 11:30-11:50

"Fabrication of High Quality Hg-1223 Thin Films Using Rapid Thermal Hg-Vapor Annealing," **Judy Z. Wu** and Sangho Yun, Department of Physics & Astronomy, University of Kansas, 1082 Malott Hall, Lawrence, Kansas 66045, and Steve C. Tidrow and Don Eckart, Department of Physical Science, US Army Research Lab, Fort Monmouth, NJ 07731

Fabrication of high-quality Hg-based cuprate HgBa₂Ca_{n-1}Cu_nO_{2n+2+δ} thin films has been hindered by high volatility and toxicity of Hg-compounds. Progress has been recently made by adoption of rapid thermal annealing of non-Hg-containing cuprate precursor films. By nearly an order of magnitude shortening of the high temperature processing period, this technique effectively reduces the formation of CaHgO₂ impurity phase and the film/substrate interface chemical reaction, the two major problems caused by the high volatility of the Hg-compounds. High-quality Hg-based cuprate thin films with zero-resistance T_c above 130 K have been obtained reproducibly using this technique. Critical current densities (J_c) at 5 K are up to 25 MA/cm² at zero field and above 2 MA/cm² at 5 Tesla. J_c up to 0.2 MA/cm² can still be maintained in the film at temperatures near 115 K. The Hg-based cuprate thin films are thus very promising for various electronic device applications.

H.8 11:50-12:10

"Near-Term Commercialization of HTS Technology at Conductus," **Randy Simon**, Conductus, Inc., 969 West Maude Avenue, Sunnyvale, CA 94086

Ten years after the initial discovery of high-temperature superconductors, Conductus has introduced or is poised to introduce commercial products based on thin-film HTS technology for three major markets: communications, healthcare and instrumentation. The first instrumentation products, based on HTS SQUIDS, were introduced to the laboratory market in 1992. The use of HTS SQUIDS for applications in geophysics, non-destructive evaluation and medicine is just beginning. In the healthcare market, superconducting receivers for magnetic resonance instruments are reaching commercialization for NMR spectrometers and are under development for use in MRI medical scanners. These receivers offer dramatic performance enhancements to magnetic resonance instruments. In communications, filter subsystems for wireless base stations are being field tested and evaluated by the telecommunications industry and could enter the commercial market this year. They have the potential to offer major economic and performance benefits to the industry. In all these markets, superconducting components of the enabling elements of high-performance subsystems. After nearly a decade of intense development, HTS technology is ready to become a significant contributor to electronic systems.

CONCURRENT SESSIONS I & J
Friday, March 15, 1:40-5:40 p.m.

SESSION I: Properties & Theory
Chairs: W.-Y. Liang, H. H. Wickman
La Salle Ballroom B
I.1 1:40-2

"Enhancements of HTS Conductor Critical Currents by Splayed Columnar Tracks from Fission Fragments," **Martin P. Maley**, Hugo F. Safar, Lev N. Bulaevskii, Jeffrey O. Willis, Jin H. Cho and Yates J. Coulter, Los Alamos National Laboratory, Superconductivity Technology Center, MS-K763, Los Alamos, NM 87545, and Stephen Fleshler, American Superconductor, 2 Technology Drive, Westborough, MA 01581

The highly successful Bi-based HTS conductors are, unfortunately, severely limited at temperatures above 30K by rapid thermally activated flux motion resulting from extreme anisotropy. It is clear that the introduction of much stronger-pinning defects will be required to permit operation at higher temperatures. Success with amorphous columnar defects produced by heavy ion irradiation has shown that linear tracks with well defined radii of 5-7 nm are most effective; but heavy ions have a small range in solid matter, making this technique infeasible for treating bulk HTS conductors. A new approach uses 0.8 GeV protons, with a range of 0.5µm in dense matter, to fission Bi nuclei in the sample. The resulting energetic fission fragments create splayed columnar tracks throughout the bulk of the conductor. We irradiated several single crystals of Bi-2212 and commercial BSCCO/Ag tape conductors with 0.8 GeV protons at several dose levels. We observed 100-fold increases in J_c measured by magnetic hysteresis on the single crystals. Direct transport measurements on the tape conductors showed substantial enhancements in J_c at 75K, reaching a record high level of 5000 A/cm² at 1.0T in a tape conductor. These results exhibit performance superior to any previously achieved and provide a proof-of-principal for the utility of this technique.

I.2 2-2:20

"New Aspects of Vortex Dynamics," **Anne van Otterlo**, Vadim Geshkenbein and Gianni Blatter, ETH-Zürich, Theoretische Physik, ETH-Hönggerberg, CH-8093 Zürich, Switzerland

We discuss the dynamics of vortices in the mixed state of Type II superconductors in terms of their equation of motion, which is derived from the microscopic BCS theory. A coherent view on vortex dynamics is obtained, in which both hydrodynamic flow around the vortex and the quasi-particles in the vortex core contribute to the forces on a vortex. The competition between these two provides an interpretation of the observed sign change in the Hall effect in superconductors with mean free path l of the order of the coherence length ξ in terms of broken particle-hole symmetry, which is related to details of the microscopic mechanism of superconductivity. Also the damping force and the several contributions to the vortex mass are discussed and compared in the dirty, clean, and superclean limits.

I.3 2:20-2:40

"Numerical Studies on the Vortex Motion in High- T_c Superconductors," **Z. D. Wang**, Department of Physics, University of Hong Kong, Hong Kong

In the framework of the Bardeen-Stephen and Nozières-Vinen approach and taking into account the backflow current due to the pinning and some other interactions, we derive a general phenomenological equation for the vortex motion in the presence of thermal fluctuations. Based on this equation, a simple analytical analysis on the dc vortex motion, particularly on the Hall effect, is introduced first. Then numerical simulation results are presented. Finally, we simulate numerically the interesting washboard effect of the moving vortex lattice. Our theoretical results are also compared with the relevant experimental observations for high- T_c superconductors.

I.4 2:40-3

"Effects Of 5.8 GeV Pb Irradiation on Magnetic Vortex Dynamics of Bi (2212 and 2223) Tapes," Y. Fukumoto, Y. Zhu, Q. Li, and **Masaki Suenaga**, Brookhaven National Laboratory, Upton, NY 11973, T. Kaneko and K. Sato, Sumitomo Electric Industries, Ltd., Konohana, Osaka, 554, Japan, K. Shibusaki, Kobe Steel, Ltd., Nishiku, Kobe, 651, Japan, and Ch. Simmon, Laboratoire CRISMAT, CNRS URA, ISMRA, Caen, France

Silver sheathed mono-core tapes of Bi(2212) and Bi(2223) were irradiated with 5.8 GeV Pb ions for fluences of 0.5, 1.0 and 2.0×10^{11} ions/cm². Detailed V-I measurements for these and virgin tapes were made as a function of applied magnetic fields H and the angle between H and the tape face for 55K-80K in liquid oxygen. The results raise some questions for the direct applicability of the Bose glass scaling theory and the commonly held mechanism for the vortex pinning in high energy heavy ion irradiated highly anisotropic superconductors such as Bi(2212) and Bi(2223). The results which may suggest these questions will be presented.

This work was supported by the US Department of Energy, Division of Materials Sciences, Office of Basic Energy Sciences, under Contract No. DE-AC02-76CH00016. Heavy ion irradiation was performed at GANIL, ISMARA, Caen, France.

I.5 3-3:20

"Phonon Anomaly in High Temperature Superconducting $YBa_2Cu_3O_{7-\delta}$ Crystals," **R. P. Sharma**², Z. H. Zhang¹, J. R. Liu¹, R. Chu¹, T. Venkatesan² and W. K. Chu¹, ¹Texas Center for Superconductivity, University of Houston, TX 77204-5932, ²Center for Superconductivity Research, University of Maryland, College Park, MD 20742

Ion Channelling investigations are made in two high quality single crystals of $YBa_2Cu_3O_{7-\delta}$. One crystal is superconducting ($T_c=92.5K$) while the other one is made non superconducting by reducing the oxygen content to an appropriate level. Channelling measurements on thermal vibration amplitude are made on both single crystals in the temperature range between 33K to 290K at close intervals. In the non-superconducting crystal, the thermal vibration amplitude versus temperature follows the Debye like behavior. In the superconducting sample, phonon anomaly in two different temperature regions are observed, one at ($T < T_c$) and the other in the temperature range between 180K-230K. In both temperature regions the thermal

vibration amplitude projected on ab plane for Cu-O rows along C direction is independent of temperature with constant value of ~ 3.5 pm and ~ 5.8 pm respectively. It is surprising to know that for superconducting state ($T < 90$ K), the constant thermal vibration amplitude ~ 3.5 pm is coincidentally in agreement with the zero point vibration calculation (3.2 pm). In this presentation we will describe the channeling method, experimental results, and our interpretation based on possible static or dynamic Jahn-Teller distortion and a normal state phase transformation.

I.6 3:20-3:40

"Unusual Magnetic Field Dependence of the Electrothermal Conductivity in Cuprate Superconductors," **Jeffrey A. Clayhold**, Y. Y. Xue and C. W. Chu, Texas Center for Superconductivity at the University of Houston, Houston, TX 77204-5932, and J. N. Eckstein and I. Bozovic, Varian Research Center, Palo Alto, CA 94304

The electrothermal conductivity, relating electric currents to thermal gradients, is, in principle, the least varied of all transport properties of superconductors in the mixed state. Nearly featureless, it should be independent of the magnetic field, independent of the vortex viscosity, and remain unchanged for pinned and unpinned vortices. It should be equal to its value in the normal state.

Microscopically, the electrothermal conductivity *should* be independent of the details of the vortex motion because it is only sensitive to the entropy and dissipation of the normal quasiparticles inside the vortex core. The apparent "featurelessness" of the electrothermal conductivity in conventional superconductors merely expresses the fact that the excitations within the vortex core can be treated as normal, non-superconducting electrons.

We have found that the situation is more complicated with the cuprate superconductors. We have measured a pronounced low-field peak of the electrothermal conductivity in $\text{YBa}_2\text{Cu}_3\text{O}_7$, $\text{Bi}_2\text{Sr}_2\text{CaCu}_2\text{O}_{8+\delta}$, and $\text{Tl}_2\text{Ba}_2\text{CaCu}_2\text{O}_{8+\delta}$. The peak narrows and moves to lower magnetic field values as the temperature is increased. In $\text{Bi}_2\text{Sr}_2\text{CaCu}_2\text{O}_{8+\delta}$ the new contribution is negative in sign, causing a sign-change of the mixed-state thermopower. Possible origins of the anomalous low-field electrothermal conductivity will be discussed.

I.7 4:4-20

"Electrodynamical Properties of High- T_c Superconductors Studied with Angle Dependent Infrared Spectroscopy," **D. van der Marel**, Solid State Physics Laboratory, University of Groningen, Nijenborgh 4, 9747 AG Groningen, The Netherlands, and A. Menovsky, University of Amsterdam, Valckenierstraat 65, 1018 XE Amsterdam, The Netherlands

From measurements of the reflectivity taken at a finite incidence angle with *s*- and *p*-polarized light we determine the dielectric function both parallel and perpendicular to the optical axis. With this technique we determine the loss function perpendicular to the layers of various single-, double- and triple-layer high T_c superconductors, for which single crystals with large dimensions in the *c*-direction are not always available. We determine the *c*-axis Josephson plasma frequency as a function of temperature. In particular we investigate experimentally the existence of a correlation between T_c and $4\hbar\omega_J$ as follows from the interlayer pair-hopping superconducting mechanism, as was recently pointed out by Anderson.

Infrared reflectivity measurements, using *p*-polarized light at a grazing angle of incidence, shown an increased sensitivity to the optical conductivity of highly reflecting superconducting materials. For the in-plane response of a $\text{La}_{1.85}\text{Sr}_{0.15}\text{CuO}_4$ single crystal in the superconducting state, we find a reduction of the optical conductivity in the frequency range below 20 meV. The observed frequency dependence excludes an isotropic *s*-wave gap, but agrees well with model calculations assuming a *d*-wave order parameter.

I.8 4:20-4:40

"Transport in the ab-Plane of HTSC, New Results," **Thomas Timusk**, McMaster University, Hamilton, Ontario, Canada

The mechanism of charge transport in the ab-plane of high temperature superconductors presents an ongoing puzzle. Far infrared spectroscopy provides a unique tool to study this problem, since it gives information about the scattering processes of charge carriers. Advances in the production of high quality thin films and untwinned single crystals have led to a clearer picture of the optical conductivity. New data will be presented on the role of the chains, the *c*-axis pseudogap, impurities and radiation damage on ab-plane scattering processes.

I.9 4:40-5

"Properties of Li-Doped La_2CuO_4 ," **Zachary Fisk** and J. L. Sarrao, National High Magnetic Field Laboratory, Florida State University, 1800 E. Paul Dirac Drive, Tallahassee, Florida 32306-3016, and P. C. Hammel, Y. Yoshinari and J. D. Thompson, MST-10, Los Alamos National Laboratory, Los Alamos, NM 87545

Li substitutes for Cu in La_2CuO_4 up to the limiting stoichiometry $\text{La}_2\text{Cu}_{.5}\text{Li}_{.5}\text{O}_4$, which has superstructure order. The effects of this in-plane hole doping on the structural and magnetic properties of La_2CuO_4 are very similar to those due to Sr-doping, except that here the holes appear to be localized. In the Cu NMR of the diamagnetic end-member $\text{La}_2\text{Cu}_{.5}\text{Li}_{.5}\text{O}_4$, the Cu nuclear spins relax via a magnetic excitation with characteristic energy 1500K.

I.10 5:5-20

"Structures and Excitations in Monolayer Copper Oxides," **Robert J. Birgeneau**, School of Science, Massachusetts Institute of Technology, 6-123 MIT, 77 Massachusetts Avenue, Cambridge, Massachusetts 02319

I.11 5:20-5:40

"Recent Neutron Scattering Results on $\text{YBa}_2\text{Cu}_3\text{O}_{7-\delta}$," **Herb A. Mook** and Pengcheng Dai, Solid State Division, Oak Ridge National Laboratory, P. O. Box 2008, Oak Ridge, TN 37831-6393, Gabriel Aeppli, AT&T Bell Labs, Murray Hill, NJ 07974, F. Dogan, Department of Materials Science and Engineering, University of Washington, Seattle, WA 98195, and K. Salama, Texas Center for Superconductivity, University of Houston, Houston, TX 77204

Both polarized and unpolarized neutrons have been used to study the magnetic fluctuations in $\text{YBa}_2\text{Cu}_3\text{O}_{7-\delta}$ with the ideally doped oxygen concentration of 6.93. $\chi(Q, \omega)$ will be shown in absolute units for both the superconducting and normal state with particular emphasis placed on the 41 meV excitation.

A new set of one-dimensional excitations has been discovered in $\text{YBa}_2\text{Cu}_3\text{O}_{6.93}$ that are not visible in the $\text{YBa}_2\text{Cu}_3\text{O}_{6.15}$. These are found to be very sharply defined in momentum space with a wavevector of 0.233 in terms of b^* . This is the wavevector expected for $2k_F$ for the Cu-O chains. These measurements will also be discussed.

SESSION J: Materials & Properties

Chair: H. C. Ku
La Salle Ballroom A

J.1 1:40-2

"The Electronic Structure of the High Temperature Superconductors as Seen by Angle-Resolved Photoemission," **Juan Carlos Campuzano** and Hong Ding, Department of Physics, University of Illinois at Chicago, 845 W. Taylor St., Chicago, IL 60607, Michael Norman, Argonne National Laboratory, Materials Science Division, 4700 S. Cass Ave., Argonne, IL 60439, Mohit Randeria, Tata Institute for Fundamental Research, Bombay, India, and Takashi Takahashi, Tohoku University, Sendai, Japan

We report measurements of the momentum dependence of the superconducting gap in $\text{Bi}_2\text{Sr}_2\text{CaCu}_2\text{O}_{8+x}$ (Bi2212) with angle-resolved photoemission spectroscopy using a dense sampling of the Brillouin zone in the vicinity of the Fermi surface. The observation of particle-hole mixing unambiguously establishes that the observed gap is in fact the superconducting gap. In the Y quadrant of the zone, where there are no complications from ghost bands caused by the superlattice, we find a gap function consistent within error bars to the form $\cos k_x - \cos k_y$, expected for a d-wave order parameter. Similar results are found in the X quadrant if the photon polarization is chosen in such a way as to enhance main band emission over that due to ghost bands. We also report on the effects of dirt and doping on the superconducting gap.

J.2 2:2-20

"Microwave Measurements of the Penetration Depth in High T_c Single Crystals," **Walter N. Hardy**, Saeid Kamal, Ruixing Liang and Douglas A. Bonn, Department of Physics, University of British Columbia, 6224 Agricultural Road, Vancouver, B. C., V6T 1Z1, Canada, Chris C. Homes, Department of Physics, Simon Fraser University, Burnaby, B. C., V5A 1S6, Canada, and Dimitri Basov and Tom Timusk, Department of Physics, McMaster University, 1280 Main Street West, Hamilton, ON, L8S 4M1, Canada

This paper summarizes the penetration depth part of our efforts to determine the intrinsic electrostatics of YBCO for the a, b and c directions, and as a function of oxygen concentration. The temperature dependence of $\lambda_i(T)$, $i = a, b, c$, is obtained by precision microwave cavity perturbation measurements on untwinned single crystals; the zero temperature values, $\lambda_i(0)$, are obtained by FAR IR reflectivity methods. For oxygen concentrations $x = 6.60, 6.95$ and 6.99 , $1/(\lambda_i(T))^2$, which is proportional to the superfluid density, shows a strong linear component at low temperatures for the a and b directions, whereas the c direction shows a much flatter dependence, even for the overdoped samples ($x = 6.99$). Near T_c , strong fluctuation effects are observed for all 3 directions. In the a and b directions the results fit easily

into the d-wave picture of superconductivity for a two-dimensional system. The significance of the unusual c-axis results will be discussed.

J.3 2:20-2:40

"Specific Heat of $\text{YBa}_2\text{Cu}_3\text{O}_{7-\delta}$," **Kathryn A. Moler**, Princeton University, Department of Physics, Princeton, NJ 08544, David L. Sisson and Aharon Kapitulnik, Department of Physics, Stanford University, CA 94305, and David J. Baar, Ruixing Liang and Walter N. Hardy, Department of Physics, UBC, Vancouver, British Columbia, V6T1Z1, Canada

We present a summary of the specific heat of $\text{YBa}_2\text{Cu}_3\text{O}_{7-\delta}$ single crystals from 2 to 10 Kelvin and from 0 to 10 Tesla, including both twinned and detwinned crystals with various oxygen doping ($7-\delta = 6.95, 6.97, \text{ and } 6.99$). The zero-field specific heat includes a linear- T term which is small compared to other $\text{YBa}_2\text{Cu}_3\text{O}_{7-\delta}$ samples, but large compared to the T^2 electronic specific heat predicted for clean lines of nodes in the gap function. This zero-field linear- T term is found to decrease with decreasing concentration of twin boundaries and oxygen vacancies δ . The specific heat is increased in a magnetic field and has a strong dependence on field orientation. Several possible field-dependent contributions are compared to the data, including a Schottky anomaly, vortex-vortex interactions, a traditional mixed-state HT term associated with vortex cores, and a \sqrt{HT} term predicted by G. Volovik for the mixed state in superconductors with lines of nodes in the gap function. The field dependence of the specific heat, according to a comparison of fits based on these possibilities, supports the existence of lines of nodes and suggests an exotic vortex structure.

J.4 2:40-3

"Specific Heat of HTS in High Magnetic Fields," **Alain R. Junod**, Université de Genève, Section de Physique, 24, quai Ernest-Ansermet, 1211 Genève 4, Switzerland

The mixed-state specific heat of extreme type-II superconductors is investigated in fields up to 16 Tesla. Uncommon behaviours are reported for classic superconductors: gaps in the mixed-state DOS for PbMo_6S_8 ($T_c = 13.9\text{K}$), non-linear $\gamma(H)$ for NbSe_2 ($T_c = 7.1\text{K}$), fluctuation broadening of the transition for $\text{Nb}_7\text{Zr}_{23}$ ($T_c = 10.8\text{K}$). In Y-123 ($T_c = 93\text{K}$), we observe below $T_c/10$ a Schottky specific heat with a field-dependent amplitude and a small T-linear contribution that is not explained by the d-wave theory. This is confirmed by entropy measurements between $T_c/2$ and T_c . In Bi-2212 ($T_c = 85\text{K}$), the mixed-state specific heat is best evaluated using magnetization measurements; again a pure d-wave term is not observed, but the mixed-state specific heat is compatible with $\lambda^{-2}(0) - \lambda^{-2}(T) \propto T^2$.

Near T_c , the distinct behaviours of the quantities $\partial(C/T)/\partial H$, $\partial(C/T)/\partial T$ and $M(H,T)$ are classified as 3D (e.g. Y-123) and 2D (e.g. Bi-2212). A crossover between both regimes is observed for the 123-phase $\text{Ca}_{0.4}\text{La}_{1.25}\text{Ba}_{1.35}\text{Cu}_3\text{O}_{7+x}$ as a function of doping. The 3D case is described by the critical exponents of the 3D-XY model ($\nu = 2/3$, $a = 0$) or by a modified lowest Landau level 3D scaling. The 2D case is not described by 2D-XY but rather by $\nu = 3/2$, $\alpha = -1$; the crossing point of the magnetization is explained by identifying $T_c = T^*$. The shape of the transition in zero field is given by a phenomenological model for $\partial(C/T)/\partial H$ valid both for low- and high-temperature superconductors. In this framework, it is shown that T_c does not change with field for Bi-2212.

J.5 3-3:20

"Thermodynamic Evidence on the Superconducting and Normal State Energy Gaps in $\text{La}_{2-x}\text{Sr}_x\text{CuO}_4$ and $\text{Y}_{0.8}\text{Ca}_{0.2}\text{Ba}_2\text{Cu}_3\text{O}_{6+x}$," **John W. Loram**, K. A. Mirza, J. R. Cooper, N. Athanassopoulou and W. Y. Liang, Interdisciplinary Research Centre in Superconductivity, University of Cambridge, Madingley Road, Cambridge CB3 0HE, and Jeffery L. Tallon, New Zealand Institute for Industrial Research, P. O. Box 31310, Lower Hutt, New Zealand

We present the electronic specific heat $\gamma(T)$ ($2 \leq T \leq 320\text{K}$) and susceptibility $\chi(T)$ ($T_c \leq T \leq 400\text{K}$) of $\text{La}_{2-x}\text{Sr}_x\text{CuO}_4$ ($0 \leq x \leq 0.45$) and $\text{Y}_{0.8}\text{Ca}_{0.2}\text{Ba}_2\text{Cu}_3\text{O}_{6+x}$ ($0.2 < x < 0.96$). Both systems exhibit a similar progression in superconducting and normal state properties with hole doping p . (i) Below T_c γ exhibits a d-wave T -dependence $\gamma = aT - \gamma_n T / \Delta_s$, where Δ_s is the d-wave gap. The coefficient a is independent of p in the underdoped region but increases dramatically on overdoping, resulting in a significant decrease in $\Delta_s(0)/T_c$. (ii) In the normal state the Wilson ratio $S/\chi T$ (where S is the electronic entropy) is close to the value expected for a non-interacting Fermi liquid. From S and χT we find an increase of ~ 0.8 fermion states per added hole within $E_F \pm 40\text{meV}$ suggesting the growth of a resonance in the DOS. With progressive underdoping a gap Δ_n develops at E_F in this quasiparticle spectrum for both systems. For $T_c < T < \Delta_n$ we find $\chi, \gamma \sim T/\Delta_n$, possibly indicating line nodes and d-wave symmetry for the normal state gap.

J.6 3:20-3:40

"Scattering Time: A Unique Property of High- T_c Cuprates," **Ichiro Terasaki**, Yoshibumi Sato and Setsuko Tajima, Superconductivity Research Laboratory, International Superconductivity Technology Center, 1-10-13, Shinonome, Koto-ku, Tokyo 135, Japan

Since the discovery of high- T_c superconductors (HTSC) it has been a central issue of recent solid-state physics to study low-dimensional systems with strong correlation. In particular, quasi-two-dimensional superconductors such as Sr_2RuO_4 and BEDT salts are good reference materials for HTSC. The most significant difference between them is the charge transport of HTSC, e.g., T -linear ab -plane resistivity and semiconducting c -axis resistivity. We have so far proposed that the anomalous transport is mainly characterized by the scattering time. In the present talk, I will introduce our recent results on (1) anomalously short scattering time along the c axis, (2) the ab -plane scattering-time enhancement in the mixed state through magnetothermopower measurements.

J.7 4-4:20

"Heat Transport in High- T_c Perovskites - Effect of Magnetic Field," **Ctirad Uher**, University of Michigan, Department of Physics, 2071 Randall Laboratory, Box 1120, Ann Arbor, MI 48109

First reports on the behavior of the thermal conductivity in high- T_c superconductors were published only a few months after the discovery by Bednorz and Müller and already from these studies it was obvious that the heat transport is rather unusual, full of surprises and quite rich in terms of information the data revealed. Its most characteristic feature, a sudden and dramatic rise in the thermal conductivity setting in at T_c and resulting in a peak near $T_c/2$, stimulated considerable

interest and much contention as to the mechanism of the heat transport. While the early reports argued in favor of the enhancement in the mean-free path of phonons due to carrier condensation as the reason for the rise in the thermal conductivity below T_c , it soon became clear that quasiparticles possess very unusual properties and may contribute in a significant way towards the heat flow. The controversy regarding which of the two entities, phonons or quasiparticles, dominates the heat transport in the superconducting state has not yet been fully settled. In the meantime, numerous experimental studies established common features in the thermal transport across different families of high- T_c perovskites, and probed the influence of the microstructure as the emphasis shifted from sintered samples towards single crystals. Availability of single crystals has led to studies of the anisotropy of the thermal transport and, in general, paved the way for more sophisticated investigations of heat transport. Among the most interesting ones are measurements of the thermal conductivity in a magnetic field. The presence of flux lines in the mixed phase of a superconductor represents an additional scattering for both the quasiparticles and phonons and the external magnetic field is a parameter which controls the intensity of scattering events. In this paper I review studies of the effect of the magnetic field on the thermal conductivity. Although the experimental findings are in a general agreement, the interpretation of the data is not without controversy. I will discuss the points of contention and offer suggestions for future work in this area.

J.8 4:20-4:40

"Thermoelectric Power: A Simple, Highly Instructive Probe of High- T_c Superconductors," **Jeffrey L. Tallon**, New Zealand Institute for Industrial Research, P. O. Box 31310, Lower Hutt, New Zealand

Although there is no consensus on the origins of the unusual transport properties of high- T_c superconductors (HTS) the temperature dependence of the thermoelectric power, $S(T)$, exhibits a universal behaviour as a function of hole concentration, p , for all of these materials. This, combined with the relative insensitivity of $S(T)$ to granular behaviour, leads to a simple and remarkably useful means to determine the doping state of any HTS material just from the room temperature thermoelectric power, $S(300)$. This is substantiated by a wide range of doping studies combined with neutron diffraction structural refinements. $S(T)$ shows a strong enhancement as the normal-state pseudogap opens at T_g and the p -dependence of T_g is identical to that of the pseudogap energy, $E_g(p)$, determined from heat capacity and NMR studies and, moreover, is distinct from the spin gap energy determined from inelastic neutron scattering. The doping dependence of $S(T)$ is shown to be inconsistent with the van Hove singularity scenario and in the case of $\text{YBa}_2\text{Cu}_3\text{O}_{7-d}$ indicates that the '60K' plateau is a doping effect and not caused primarily by oxygen ordering.

J.9 4:40-5

"High Pressure Study on Hg-Based Cuprates," **F. Chen**, X. D. Qiu, Y. Cao, L. Gao, Q. Xiong,* Y. Y. Xue and C. W. Chu, Department of Physics and Texas Center for Superconductivity at the University of Houston, Houston, TX 77204-5932; *Department of Physics, High Density Electronic Center, University of Arkansas, Fayetteville, AR 72701

The pressure effect on the superconducting transition temperature (T_c) (dT_c/dP) and the Seebeck coefficient (S) at 300 K of pure and doped $\text{HgBa}_2\text{Ca}_{n-1}\text{Cu}_n\text{O}_{2n+2+6}$

J.10 - K.3

have been systematically determined for $1 \leq n \leq 5$ and different δ up to 160 kbar. We have found: (1) dT_c/dP at low P is insensitive to δ for $\delta \leq \delta(\text{optimal})$, (2) dT_c/dP for $\delta(\text{optimal})$ is large, (3) the maximum P -induced T_c -enhancement is unusually large for pure, but less so for Hg-site doped, samples, (4) T_c - P is similar for compounds with $n = 1, 2$, and 3 at $\delta(\text{optimal})$, but becomes different for $n = 4$ and 5 , (5) $T_c(\text{max})$ in T_c - P varies slightly with δ , and (6) dS/dP (300 K) is positive. The observations suggest the importance of the factors other than carrier concentration to high temperature superconductivity. They will be compared with predictions by band calculations, universal T_c -carrier density relationship, and phenomenological theory on the pressure effect on T_c .

This work is supported in part by NSF, EPRI, the State of Texas through the Texas Center for Superconductivity at the University of Houston, and the T. L. L. Temple Foundation. This material was also prepared with the support of the U. S. Department of Energy, Grant No. DE-FC-48-95R810542. However, any opinions, findings, conclusions, or recommendations expressed herein are those of the authors and do not necessarily reflect the views of DoE.

J.10 5-5:20

"Structural Control of Transition Temperature and Flux Pinning in High- T_c Superconductors," **James D. Jorgensen**, Materials Science Division and Science and Technology Center for Superconductivity, Argonne National Laboratory, Argonne, IL 60439

Studies of a large number of compounds have provided a consistent picture of what structural features give rise to the highest T_c 's in copper-oxide superconductors. The highest T_c 's are observed for compounds (such as the Hg-Ba-Ca-Cu-O family) that have flat and square CuO_2 planes and long apical Cu-O bonds, with the 123 and 124 compounds, which contain copper in the blocking layer, being important exceptions that may teach us how to raise T_c further. In more recent work, attention has focused on how the structure can be modified, for example, by chemical substitution, to improve flux pinning properties. Two ideas are being investigated: (1) Increasing the coupling of pancake vortices to form vortex lines by shortening the blocking layer distance or "metallizing" the blocking layer; and (2) The formation of chemically-induced defects that can pin flux. Chemically substituted Hg-Ba-Ca-Cu-O compounds provide examples of such work.

This work is supported by the U. S. Department of Energy, Office of Basic Energy Sciences - Division of Materials Sciences, under contract No. W-31-109-ENG-38 and the National Science Foundation, Office of Science and Technology Centers, under grant No. DMR 91-20000.

J.11 5:20-5:40

"The Effect of Pressure on Superconducting Copper Mixed Oxides," **Massimo Marezio**, MASPEC-CNR, Via Chiavari 18/A, 43100 Parma, Italy

Pressure has been used either to synthesize new superconducting copper mixed oxides or to enhance in-situ the critical temperature of known materials. In both types of experiments important breakthroughs have been obtained. Two examples will be illustrated for the pressure-induced syntheses, namely that of $\text{C}_{1-y}\text{Cu}_y\text{Ba}_2\text{Ca}_n$.

Cu_nO_x which is a family of superconductors exhibiting T_c 's around 120K. The other example will be $\text{Hg}_2\text{Ba}_2\text{Ca}_{1-y}\text{Y}_y\text{Cu}_2\text{O}_x$ which is a solid solution for which T_c has not been optimized as yet.

CONCURRENT SESSIONS K & L

Saturday, March 16, 9:40 a.m. - 1 p.m.

SESSION K: Vortex, etc.

Chairs: **D. C. Larbalestier, M. B. Maple**
Granger B

K.1 9:40-10

"Thermodynamic Vortex-Lattice Phase Transitions in BSCCO," **Eli Zeldov**, Department of Condensed Matter Physics, Weizmann Institute of Science, Rehovot 71600, Israel

K.2 10-10:20

"Pancake Vortices in High-Temperature Superconducting Thin Films," **John R. Clem**, Maamar Benkraouda and Thomas Pe, Ames Laboratory* and Department of Physics and Astronomy, Iowa State University, Ames, IA 50011

A tilted stack of 2D pancake vortices in an infinite set of Josephson-decoupled superconducting layers has been found to be unstable when the angle of tilt is greater than 52 degrees. In this paper we consider the behavior of pancake vortices in a finite set of N superconducting layers. We present results for the magnetic-field and current density distributions generated throughout the multilayer structure by a single pancake vortex in an arbitrary layer. We apply these results to examine the stability of tilted stacks of pancake vortices, where the tilt is maintained by application of transport currents in the top and bottom superconducting layers.

*Operated for the U.S. Department of Energy by Iowa State University under contract no. W-7405-eng-82. This work was supported by the Director for Energy Research, Office of Basic Energy Sciences

K.3 10:20-10:40

"Correlation Lengths in the Flux Line Lattice of Type-II Superconductors," **Peter L. Gammel**, AT&T Bell Laboratories, Room ID-221, 600 Mountain Avenue, Murray Hill, NJ 07974

The flux line lattice (FLL), with its complex phase diagram, dominates the properties of the mixed state of type-II superconductors. Particularly important in high- T_c materials is the large regime of flux line liquid. While the liquid and other phases are described in terms of structural polytypes, there is a paucity of experiments which directly probe this structure. Generally, the phase diagram for the flux line lattice is inferred through analysis and scaling of transport data.

We describe three experiments which directly probe the structure of the FLL - non local transport, decoration and small angle neutron scattering (SANS). We have studied high- T_c (YBCO, BSCCO), layered (NbSe_2) and conventional (Nb) superconductors. Non local transport relies on the elastic properties of the flux lines

to determine their effective length along the magnetic field. Decoration examines the static, low field, correlation lengths perpendicular to the field at the sample surface. SANS is most sensitive to the correlation length parallel to the applied field, but is also influenced by the transverse correlation lengths. Taken together, these experiments form a detailed picture of the structural properties of the FLL.

K.4 10:40-11

"Magnetoresistivity of Thin Films of the Electron-Doped High T_c Superconductor $\text{Nd}_{1.85}\text{Ce}_{0.15}\text{CuO}_{4\pm\delta}$ " Jan Hermann, Marcio C. de Andrade, Carmen C. Almasen and **M. Brian Maple**, University of California at San Diego, IPAPS-0360, 9500 Gilman Drive, La Jolla, CA 92093-0360, and Wu Jiang, Sining N. Mao and Richard L. Greene, University of Maryland, Center for Superconductivity Research, College Park, MD 20742

We report measurements of the magnetoresistance of $\text{Nd}_{1.85}\text{Ce}_{0.15}\text{CuO}_{4\pm\delta}$ epitaxial thin films with varying oxygen content in magnetic fields H applied parallel ($H\parallel c$) and perpendicular ($H\perp c$) to the tetragonal c -axis. We observe critical scaling of the electrical resistivity that is consistent with a vortex-glass transition for a film with an optimum superconducting transition temperature T_c of ≈ 22 K and $H\parallel c$. The results allow us to trace the vortex-glass transition down to $T/T_c \sim 5 \times 10^{-3}$. The values of the Ginzburg-Landau zero temperature upper critical field $H_{c2}(0) = 80$ kOe and the in-plane zero temperature coherence length $\xi_{ab}(0) = 64$ Å were obtained from an analysis of the fluctuation conductivity. For an overoxygenated film with $T_c \approx 10$ K, an anomaly develops with increasing field for $H\parallel c$ and $T \leq 2$ K that is characterized by a minimum in the temperature dependence of the resistivity followed by a second resistive transition at lower temperature. The temperature where the second transition occurs is nearly independent of H ; the behavior closely resembles the one previously observed in $\text{Nd}_{2-x}\text{Ce}_x\text{CuO}_{4-\delta}$ single crystals and may be associated with the magnetic ordering of the Nd^{3+} ions.

K.5 11-11:20

"Comparative Study of Vortex Correlation in Twinned and Untwinned $\text{YBa}_2\text{Cu}_3\text{O}_{7-\delta}$ Single Crystals," Esteban Righi, **Francisco de la Cruz**, Daniel Lopez and Gladys Nieva, Comisión de Energía Atómica Bariloche and Instituto Balseiro, S. C. de Bariloche, RN, 8400, Argentina, and W. K. Kwok, J. A. Fendrich, G. W. Crabtree and L. Paulius, Materials Science Division, Argonne National Laboratory, Argonne, IL 60439

Vortex correlation in the c crystallographic direction in YBCO single crystals has been studied by means of transport measurements using uniform and non uniform electrical current injection. The solid-liquid phase transition in untwinned single crystals is followed by a discontinuous change from a vortex structure that is correlated in the c direction to a non correlated liquid in all directions. In this sense the first order phase transition is associated with a decoupling transition. This, together with previous results in BSCCO indicates that very small flux cutting energies characterize the intrinsic behavior of vortex liquids. In fact, correlated vortex liquids in the c direction are only possible when extended defects such as twin boundaries stabilize a finite temperature-dependent vortex correlation in that direction. In this case the liquid can be characterized by vortex lines with a diverging temperature dependent length in the field direction. We show that the electrical dissipation in the

ab and c directions in the liquid vortex state in YBCO is dominated by flux cutting processes.

K.6 11:20-11:40

"High-Pressure Raman Study of the Mercury-Based Superconductors and the Related Compounds," **In-Sang Yang** and Hye-Gyong Lee, Ewha Woman's University, Seoul, 120-750, Korea

We report pressure-induced effects on the Raman frequencies of the apical oxygen (O_A) in Hg- O_A -Cu bonds of mercury-based superconductors and some related compounds. The rate of increase in the force constant for O_A in Hg-1223 is the same as that of Hg-1201 below $P \approx 5$ GPa, beyond which the rate increased significantly for Hg-1223. For Hg-1212, the rate lies in between those of Hg-1201 and Hg-1223 without any abrupt change in the rate, below 10 GPa. Study on the Hg-1212 samples annealed in various conditions shows that the oxygen content at the $O-\delta$ site is not affecting the pressure dependence of the apical oxygen Raman mode. The major cause of the increase of the Raman frequency of the $O_A A_{1g}$ mode is attributed to the Hg- O_A bond strength and its change.

K.7 11:40-12

"Very High Trapped Fields: Cracking, Creep and Pinning Centers," **Roy Weinstein**, Department of Physics and Institute for Beam Particle Dynamics, University of Houston, Rm. 632 SR-1, Houston, TX 77204-5506, Charles C. Foster, Cyclotron Facilities, Indiana University, 2401 Milo B. Sampson Lane, Bloomington, IN 47405, and Victor Obot, Department of Mathematics, Texas Southern University, 3100 Cleburne, Nabrit Science Hall, Houston, TX 77004

The achievement of very high trapped fields, B_t , in HTS is limited by cracking under magnetic pressure, and by creep. Cracking is avoided by keeping the applied field, B_A , as low as possible during the field cooling (FC) activation process.

Reduction of B_A during FC induces voltages which generate quenches. The time interval in which $B_A \rightarrow 0$ is therefore increased, but this results in reduced B_t due to creep. This problem has been solved by use of additional cooling, during activation, to slow creep.

Using the above methods a trapped field of 10.1 Tesla at 42K has been achieved. The mini-magnet used was four disks of proton-irradiated, melt-textured Y123, each 2 cm diameter x 0.8 cm thick. To the best of our knowledge this is the highest trapped field ever achieved in an ingot of any material at any temperature.

A newer radiation process, which approximately doubles J_c compared to proton irradiation, has been used to introduce short homogeneous isotropic columnar pinning centers into Y123. In a mini-magnet of this material 3.1 Tesla was trapped at 77K. To the best of our knowledge this is a record field for an ingot of any material at 77K.

K.8 12-12:20

"Local Texture, Current Flow, and Superconductive Transport Properties of Tl1223 Deposits on Practical Substrates," **D. K. Christen**, Oak Ridge National Laboratory, P. O. Box 2008, M. S. 6061, Bldg. 3115, Oak Ridge, TN 37831-6061

K.9 - L.1

The $TlBa_2Ca_2Cu_3O_{8+x}$ (T11223) class of HTS materials have intrinsic properties that provide capabilities to operate at temperatures above 40 K in substantial magnetic fields. Here, we report on the microstructural and electrical transport properties of $TlBa_2Ca_2Cu_3O_{8+x}$ (T1123) deposits on practical, polycrystalline substrate materials, such as tapes of YSZ and silver. Short samples were formed by deposition of a Tl-free or Tl-poor precursor film, followed by thermal reaction in Tl_2O vapor. Analyses show that the deposits have *c*-axis-perpendicular texture, with local in-plane alignment, which gives rise to improved electrical transport properties that depend on sample dimensions. Measurements on different samples, on the same samples at different widths, and on samples with artificial, strong flux pinning defects lead to the conclusion that a relatively small fraction of the material comprises strongly-coupled current paths. Work on 3 - 10 μm thick deposits on silver indicate that these materials may be useful as a new class of HTS conductors.

Research co-sponsored by the DOE Division of Materials Sciences, and by the DOE Office of Advanced Utility Concepts, Superconductivity Program for Electric Energy Systems, both under Contract No. DE-AC05-96OR22464 with Lockheed Martin Energy Research Corporation.

K.9 12:20-12:40

"Muon Spin Rotation Studies of Magnetism in $La_{2-x}Sr_xCuO_4$ and $Y_{1-x}Ca_xBa_2Cu_3O_5$," Christof Niedermayer¹, **Joseph I. Budnick**² and Bernhard Christian¹, ¹Universität Konstanz, Fakultät für Physik, Postfach 5560, D 784434 Konstanz, Germany, ²Department of Physics, University of Connecticut, Storrs, CT 06268

We have studied the magnetic phase diagram for the bilayer compound $Y_{1-x}Ca_xBa_2Cu_3O_6$ in the regime of low doping (hole concentration within a CuO_2 plane, $p_{sh} < 0.1$). Hole doping is achieved by the substitution of Y^{3+} by Ca^{2+} . This provides a big advantage over the case of $YBa_2Cu_3O_{7-\delta}$ where the charge transfer from the CuO chains to the CuO_2 planes is rather complicated and makes the determination of p_{sh} difficult.

For $p_{sh} = 0.025$ we identify two distinct magnetic transitions at $T_N \sim 220$ K and $T_f \sim 25$ K. The latter transition is characterized by a sudden increase of the internal magnetic field at the muon site. Such a transition was recently reported from NQR and μSR studies on $La_{2-x}Sr_xCuO_4$ for $p_{sh} < 0.02$. It was interpreted in terms of freezing of the spin degrees of freedom of the doped holes into a spin glass like state which is superimposed on the Cu^{2+} antiferromagnetic background. A single spin glass like transition at a temperature T_g is observed for samples in the hole concentration range $0.05 < p_{sh} < 0.1$. While the threshold for superconductivity is almost the same ($p_{sh} > 0.06$) for the $Y_{1-x}Ca_xBa_2Cu_3O_6$ and the $La_{2-x}Sr_xCuO_4$ systems, the magnetic correlations coexisting with superconductivity are considerably stronger in the bilayer $Y_{1-x}Ca_xBa_2Cu_3O_6$ system as indicated by significantly increased transition temperature T_g .

K.10 12:40-1

"X-Ray Search for CDW in Single Crystal $YBa_2Cu_3O_{7-\delta}$," Peter Wochner, Brookhaven National Laboratory, Department of Physics, Bldg. 510B, Upton, NY 11973, E. Isaacs, AT&T Bell Labs, 3L-304, 600 Mountain Avenue, Murray Hill, NJ 07974, **Simon Moss**, University of Houston, Department of Physics, 4800 Calhoun, Houston, TX 77204-5506, Paul Zschack, Brookhaven National Laboratory, Bldg. 725, NSLS X14, Upton, NY 11973, and J. Giapintzakis and D. M. Ginsberg, University of Illinois, Department of Physics, 1110 West Green St., Urbana, IL 61801

Recently, H. L. Edwards et al (Phys. Rev. Lett **73**, 1154 (1994) observed, in STM experiments at 20K, modulations in the CuO chain layer of cold-cleaved single crystals of $YBa_2Cu_3O_{7-\delta}$ which they interpreted as a possible charge density wave (CDW). Since X-ray scattering is an ideal tool for the study of static or dynamic lattice displacements, we performed a synchrotron X-ray study at beamline X14 at the NSLS of BNL on a large high quality single crystal of $YBa_2Cu_3O_{7-\delta}$. The crystal was mainly single domain with a spatially well localized volume fraction of other twin orientations of roughly 10%. Appropriate scattering configurations have been chosen to enable observations of longitudinal or transverse CDWs with polarization either in the chain direction, $\parallel <010>$, or \perp to it in $<001>$. The X-ray energy of 16keV allowed us to reach large momentum transfers to increase the sensitivity to lattice displacements. In none of our scans which definitely covered the case of a 1-dimensional longitudinal CDW with propagation in the *b* direction as proposed by Edwards et al., did we find any additional intensity besides the main Bragg peak and the twin reflections. We therefore suspect that the STM finding is most likely a surface-induced phenomenon.

*Research at Houston sponsored by NSF (DMR-9208420) and the Texas Center for Superconductivity; at BNL on DOE (DE-AC-02-76CH000160).

SESSION L: Film & Properties

Chairs: **H. Weinstock, T. Claeson**
de Zavala

L.1 9:40-10

"HTS SQUIDS and Their Applications," **John Clarke**, University of California, Department of Physics, 366 LeConte Hall, Berkeley, CA 94720-7300

DC SQUIDS fabricated from thin films of $YBa_2Cu_3O_{7-x}$ (YBCO) and operated in liquid nitrogen at 77K now achieve magnetic flux noise levels of a few $\mu\Phi_0$ Hz^{-1/2} at frequencies down to a few hertz. Achieving this performance has required major reductions in the level of *1/f* noise generated by the thermally activated hopping of flux quanta and by fluctuations in the critical current of the junctions. To make sensitive magnetometers, one must enhance the effective area of the SQUID. The more simple magnetometers require only single layers of YBCO. More sophisticated devices involve multiple layers in which two YBCO films are separated by an insulating layer, usually $SrTiO_3$. To obtain high quality, low noise structures careful processing is required, for example, the use of a thin $SrTiO_3$ capping layer on the first YBCO film. Currently, the most sensitive magnetometers achieve a magnetic field noise below 10fT Hz^{-1/2}. Applications include geophysics, scanning SQUID microscopes and magnetocardiology.

This work was performed in collaboration with E. Dantsker, R. Kleiner, D. Koelle, F. Ludwig and A. H. Miklich, and supported by the U. S. Department of Energy under contract number DE-AC03-76SF00098.

L.2 10-10:20

"SQUID Imaging," **John R. Kirtley** and Chang C. Tsuei, IBM T. J. Watson Research Center, P. O. Box 218, Yorktown Heights, NY 10598, and Kathryn A. Moler, Princeton University, Department of Physics, Jadwin Hall, Washington Blvd., Princeton, NJ 08544

We have combined a novel low temperature positioning mechanism with a single-chip miniature SQUID magnetometer to form an extremely sensitive new magnetic microscope. This microscope is capable of imaging areas 1cm on a side, with a spatial resolution of a few microns and a magnetic field sensitivity of a few tenths of a microgauss in a one hertz bandwidth. Advanced integrated SQUID sensors provide excellent shielding of the pickup loop leads, and sensitivity to all three vector axes of the magnetic field. This microscope is a powerful tool for probing the microscopic properties of the high- T_c superconductors. We will present a review of such applications, including the first direct observation of the half-integer flux quantum effect, in 3-junction thin film rings of YBCO grown epitaxially on specially designed tricrystal substrates of strontium titanate; imaging of integer and half-integer Josephson vortices in grain boundaries and at a tricrystal meeting point, which provide the first direct measurement of the Josephson penetration depth; and scanning SQUID microscope tests of local time-reversal symmetry breaking in YBCO.

Work done in collaboration with: M. B. Ketchen, M. Rupp, J. Z. Sun, A. Gupta, B. A. Scott, and A. W. Ellis (IBM); M. Bhushan (SUNY Stony Brook)

L.3 10:20-10:40

"Imaging of Superconducting Vortices with a Magnetic Force Microscope," Alex de Lozanne, **Chun Che Chen**, Qinyou Lu and Caiwen Yuan, Department of Physics, University of Texas, Austin, TX 78712-1081, David A. Rudman, NIST Boulder, 325 Broadway, Boulder, CO 80303, James N. Eckstein, Varian Associates, Inc, E. L. Ginzton Research Center, Palo Alto, CA 94304-1025, and Marco Tortonesi, Park Scientific Instruments, 1171 Borregas Ave., Sunnyvale, CA 94089

We report the observation of flux lines in YBCO and BSSCO thin films with a home-made Magnetic Force Microscope. This technique measures the force between the superconducting film and an iron particle on a sharp tip, which is microfabricated at the end of a cantilever. In our case the measurement of the deflection of the microscopic cantilever is done by measuring the resistance of piezoresistors built into the cantilever. Typically we measure the film topography by scanning in contact with the surface while the vortex images are taken by oscillating the cantilever at a distance of 100-300 nm away from the surface. Samples are cooled down in a 10-100G magnetic field. Vortices are seen as round features with a diameter of about one micrometer. The vortex contrast decreases as the temperature approaches T_c . In most cases, vortices disappear from the field of view after topographic (contact) imaging, owing to the interaction between the magnetized tip and the vortex. In some cases we see correlation between the vortex positions and topographic features.

L.4 10:40-11

"Electronic Eyes Based on Dye/Superconductor Assemblies," **John T. McDevitt**, David C. Jurbergs, Steven M. Savoy, S. Eames and J. Zhao, Department of Chemistry and Biochemistry, The University of Texas at Austin, Austin, TX 78712

Recently, we have begun to explore methods that can be used to deposit molecular dye layers onto the surfaces of high- T_c superconductor thin film elements. These hybrid systems are found to be sensitive to the influence of light making them suitable for optical sensor applications. Here the dye structures serve as absorptive antenna layers which funnel efficiently and rapidly the light energy into the superconductor. This interaction leads to a temporal weakening of superconductivity which is easily sensed through electronic means. Since these hybrid structures respond most strongly to those wavelengths absorbed by the dye, a variety of optical sensors can be engineered from the molecular level to serve a number of different applications. These systems function as sensitive bolometric sensors which exhibit both high sensitivities and good wavelength selectivity. Importantly, the molecular antenna layer and superconductor sensor structures can be tailored independently, making these systems suitable for a variety of different applications. Color discrimination, machine vision and remote chemical sensing applications are plausible with these hybrid sensors. This paper will focus on the design, construction and optical response characteristics of these newly discovered dye/superconductor assemblies.

L.5 11-11:20

"The Search for Broken-Time-Reversal-Symmetry in High- T_c Superconductors: Status Report," **Aharon Kapitulnik**, Department of Applied Physics, Stanford University, Stanford, CA 94305

Some of the more interesting models proposed to explain high-temperature superconductivity in the cuprates involve the requirement that the ground state of the system possess incipient broken time reversal symmetry. The model that has attracted most of the attention is the so-called "anyon model" where the condensate is composed of new composite particles that obey fractional statistics. As charged particles, anyons will interact with light and thus expect to exhibit effects similar to magneto-optical effects in magnetic materials. While during the early days of high- T_c superconductivity there were several reports confirming the anyon scenario, later, more accurate measurements showed clearly that those previous results were most likely a consequence of interacting with the strong linear birefringence of the material with no evidence for broken time reversal symmetry. In fact, Sagnac interferometer measurements with high accuracy had put a tight limit on the level of broken time reversal symmetry allowed. In this paper we review those early results and add new results that put new bounds to the allowed level of broken time reversal symmetry in the cuprates.

L.6 11:20-11:40

"Pressure Effect on the Superconducting and Normal-State Properties for the YBCO/PBCO Superlattice," **J. G. Lin**¹, M. L. Lin¹, H. C. Yang¹, Z. J. Huang² and C. Y. Huang^{1,3}, ¹Department of Physics, National Taiwan University, Taipei, Taiwan, R. O. C., ²Texas Center for Superconductivity at the University of Houston, Houston, TX 77204-5932, ³Center for Condensed Matter Sciences, National Taiwan University, Taipei, Taiwan, R. O. C.

L.7 - L.10

The pressure on the resistivity ρ , superconducting transition temperature T_c for two $(YBCO)_n/(PBCO)_m$ superlattices have been investigated, and the results have been compared with those for pure YBCO. For pure YBCO, T_c increases linearly with increasing pressure; while the superlattices with $n/m = 120/120$ and $48/60$, the temperature dependence of ρ shows a metal-to-semiconducting transition at 7 kbar. Based on our analysis, the observed unusual transition may be due to the pressure-enhanced scattering effect on the interfaces between the YBCO- and the PBCO-layer.

* This work is supported in part by the National Science Council of the R. O. C. under grant No. NSC-85-2112-M-002-022.

L.7 11:40-12

"Magnetocardiography in a Magnetically Noisy Environment Using High- T_c SQUIDS,"

John H. Miller, Jr., Nilesh Tralshawala, James Claycomb and Ji-Hai Xu, Texas Center for Superconductivity at the University of Houston, Houston, TX 77204-5932

The ability to operate high- T_c SQUID sensors in a clinical environment, without requiring a magnetically shielded room, is an important prerequisite for attaining widespread acceptance, by physicians, hospitals, clinics, and insurance companies, of diagnostic applications of biomagnetic measurements, such as magnetocardiography (MCG). Ambient magnetic field noise results from a variety of sources, including microphonics in the earth's field, power line noise at 60 Hz and its harmonics, and digital noise from nearby equipment. This noise must be reduced by several orders of magnitude to enable operation in the frequency range of interest – typically ranging from 0.3 to 400 Hz.

We are combining several approaches towards the goal of achieving such noise reduction, including localized high- T_c superconducting (HTS) magnetic shielding, electronic subtraction of sensor and reference signals, active feedback and noise compensation, and digital signal processing. Thus far we have successfully measured the QRS complex and T-wave of a magnetocardiogram in a magnetically noisy environment, such as that encountered in the Catheterization Laboratory at Texas Children's Hospital.

L.8 12-12:20

"Pinning and Anisotropy Properties of High- T_c Microcrystals by Miniaturized Torquemeter," **C. Rossel**¹, P. Bauer¹, D. Zech², J. Hofer² and H. Keller², ¹IBM Research Division, Zürich Research Lab., CH-8803 Rüschlikon and ²Physik-Institut der Universität Zürich, CH-8057 Zürich, Switzerland

Field and angular-dependent torque measurements can provide valuable information on the pinning and anisotropy properties of the flux line lattice, and on the role of thermal fluctuations in high- T_c superconductors. Quantities such as the effective mass anisotropy ratio γ , the in-plane coherence length ξ_{ab} and the penetration depth λ_{ab} have been derived in microcrystals of the $YBa_2Cu_4O_8$, $Hg_1Ba_2Ca_3Cu_4O_{10}$ and $Bi_2Sr_2Ca_1Cu_2O_8$ phases. For this purpose, a new, miniaturized and highly-sensitive torque magnetometer based on Si piezoresistive cantilevers has been developed. This device allows us to measure the magnetic moment m of tiny crystals ($< 1 \mu\text{g}$) mounted on the lever, via the torque $\vec{\tau} = \vec{m} \times \vec{B}$ generated in a homogenous field B . The deflection of the lever is sensed by changes in the piezoresistance with a resolution of better than 0.1 \AA . This corresponds to a torque

sensitivity of $\Delta\tau \leq 10^{-14} \text{ Nm}$, or to a magnetic moment as small as $m \leq 10^{-14} \text{ Am}^2$ measured at 1 Tesla, a value three orders of magnitude smaller than that achieved in commercial SQUID magnetometers.

L.9 12:20-12:40

"HTS Materials for High Power rf and Microwave Applications*," **Dean W. Face**, Charles Wilker, Zhi-Yaun Shen and Philip S. W. Pang, DuPont Superconductivity, Experimental Station E304/C118, Wilmington, DE 19880-0304

Many of the most promising applications of HTS materials require films with low surface resistance at high rf power levels. This talk will review recent work at DuPont to develop $YBa_2Cu_3O_7$ and $Tl_2Ba_2CaCu_2O_8$ films and devices for high power rf and microwave applications. The high power performance of unpatterned 2 and 3 inch diameter films has been characterized using a 5.56 GHz HTS-sapphire resonator. For YBCO at 70 K, the surface resistance remains below $200 \mu\Omega$ (scaled to 10 GHz) for microwave surface current densities up to $4 \times 10^6 \text{ A/cm}^2$. Similar measurements have been made for $Tl_2Ba_2CaCu_2O_8$ films. Coplanar transmission lines patterned from both $YBa_2Cu_3O_7$ and $Tl_2Ba_2CaCu_2O_8$ films show low levels of harmonic generation up to average rf current densities greater than $2 \times 10^6 \text{ A/cm}^2$. Recent work to develop planar high power filters with good performance up to and exceeding 20 watts will be discussed.

*This work was partially supported by the Technology Reinvestment Program NASA Cooperative Agreement NCC 3-344

L.10 12:40-1

"High-Accuracy Specific-Heat Study on $YBa_2Cu_3O_7$ and $Bi_2Sr_2CaCu_2O_8$ Around T_c in External Magnetic Fields," **Andreas Schilling**, Oliver Jeandupeux, Cristoph Wälti, Anne van Otterlo and Hans-Rudolf Ott, ETH Zürich, Laboratorium für Festkörperphysik, ETH Hönggerberg, 8093 Zürich, Switzerland

We have developed a high-resolution calorimeter that enables us to investigate phase transitions in high- T_c materials below room temperature with a very high accuracy. The resolution is sufficient to deduce an upper limit for a possible latent heat $L < 0.05 \text{ k}_B T$ per vortex per layer at the irreversibility line of our investigated $YBa_2Cu_3O_7$ single crystals in an external magnetic field $\mu_0 H = 7 \text{ T}$ parallel to the c axis (Phys. Rev. B **52** (1995) 9714). The high resolution in the specific-heat $C_p(T)$ data ($\delta C_p / C_p < 4 \times 10^{-3} / [\text{sample mass in mg}]$, with a negligibly small instrumental broadening on the temperature scale), makes it also possible to analyse the second-order specific-heat discontinuities $\Delta C_p(H, T)$ of $YBa_2Cu_3O_7$ and $Bi_2Sr_2CaCu_2O_8$ at T_c in detail. Combining these results with corresponding magnetization $M(H, T)$ data that we collected on the same specimens, we may conclude that the 3D-XY model for describing the phase transition to superconductivity at T_c does not reproduce in a satisfactory way the experimental thermodynamic data from $YBa_2Cu_3O_7$ for external magnetic fields exceeding $\mu_0 H = 1 \text{ T}$.

POSTER SESSIONS

TUESDAY, MARCH 12

4-6 p.m., Granger A & B

**Poster Sessions 1A & 1B: HTS Theory,
Experiment, Material, & Properties**

POSTER SESSION 1A

P1A.1

"Anomalous Charge-Excitation Spectra in t-J and Hubbard Models," **T. K. Lee**, Dept. of Physics, Virginia Tech, Blacksburg, VA 24061, Y. C. Chen, Tung-Hai University, Taichung, Taiwan, R. Eder, Dept. of Applied and Solid State Physics, University of Groningen, The Netherlands, H. Q. Lin, Chinese University of Hong Kong, Hong Kong, Y. Ohta, Dept. of Physics, Chiba University, Chiba, Japan, and C. T. Shih, National Tsing Hua University, Hsinchu, Taiwan

Strong correlations in the t-J and Hubbard models are shown to lead to anomalous charge and spin excitation spectra. Results of applying exact diagonalization method to both models with 10 electrons in 16 sites are presented for different J/t and U/t . While the lowest spin excitation occur at wave vector $2k_F$, the lowest charge excitation is at wave vector $\mathbf{Q} = (\pi, 0)$ in the strong coupling models. This state is more suitably described as a collective excitation instead of an excited particle-hole-pair state at $2k_F$. Similar results were observed in the one-dimensional Luttinger liquid. Excitations obtained for 26 electrons in 36 sites by using Power-Lanczos method¹ are consistent with this anomalous behavior observed for 16 sites.

¹Y. C. Chen and T. K. Lee, Phys. Rev. B **51**, 11548 (1993).

P1A.2

"Exact Diagonalization Study of the Single Hole t-J Model on a 32-Site Lattice," **P. W. Leung**, Department of Physics, Hong Kong University of Science & Technology, Clear Water Bay, Hong Kong, and Robert J. Gooding, Department of Physics, Queen's University, Kingston, Ontario, Canada

Using exact diagonalization techniques, we solve the single-hole t-J model on a 32-site square lattice. This square cluster is by far the largest one can deal with using this approach. Compared to other smaller square clusters, it has allowed reciprocal lattice vectors along high symmetry directions in the first Brillouin zone. This makes it possible to compare the calculated results with experiments. The spectral function, quasiparticle dispersion relation, bandwidth, and various spin correlation functions are calculated exactly on this cluster. These calculations involve finding the lowest eigenstates of the Hamiltonian matrix in a Hilbert space with more than 300 million basis states. They also serve as an acid test of analytical theories of the t-J model. Our measured quasiparticle dispersion relation and spin correlations agree well with that determined using the self-consistent Born approximation. The effect

of the next nearest neighbor hopping term (t') will also be discussed. We then make a quantitative comparison of our spectral functions to recent ARPES data for a single hole propagating in the antiferromagnetic insulator $\text{Sr}_2\text{CuO}_2\text{Cl}_2$.

P1A.3

"Electronic Properties of the Layered Cuprates," **Nejat Bulut**, University of California at Santa Barbara, Department of Physics, Santa Barbara, CA 93106

Photoemission, NMR and neutron scattering experiments have produced valuable information on the electronic structure of the layered cuprates. Here, the results of these experiments are compared with the results of the numerical calculations on the strongly correlated models such as the Hubbard or the t-J models. In addition, the data on the superconducting state of the cuprates is discussed within a d-wave superconducting model.

P1A.4

"Electron-Spin Diffusion Constant as Diagnostics for Spin-Charge Separation in the Metallic Cuprates," **Qimiao Si**, Rice University, Department of Physics, P. O. Box 1892, Houston, TX 77251

We calculate and study the relationship between the electron-spin resistivity and electrical resistivity in models of relevance to the normal state of the high T_c cuprates. These models describe metallic states with or without spin-charge separation. We found that, given a linear temperature dependence of the electrical resistivity, the electron-spin resistivity should also be linear in temperature in the absence of spin-charge separation. In the presence of spin-charge separation, however, the electron-spin resistivity will in general have a different temperature dependence. Based on these results, we propose to use the temperature dependence of the electron-spin diffusion constant to test spin-charge separation in the cuprates.

P1A.5

"Magnetic Frustration and Spin-Charge Separation in 2D Strongly Correlated Electron Systems," **William Putikka**, Department of Physics, University of Cincinnati, ML-0011, Cincinnati, OH 45221-0011

High temperature expansions for the spin and charge correlation functions, $S(\mathbf{q})$ and $N(\mathbf{q})$, of the 2D t-J model show different characteristic wave vectors, indicating different momentum distributions in the Brillouin zone for the spin and charge degrees of freedom and strongly suggesting a form of spin-charge separation in the 2D t-J model. The existence of spin-charge separation raises the deeper question of what causes this behavior. Low density expansions for the Hubbard model and renormalization group studies of 2D interacting electrons starting from weak coupling give no indication of spin-charge separation in 2D. Thus, unlike 1D, dimensionality alone does not seem to be sufficient to produce spin-charge separation in an interacting 2D model. Also, the characteristic wavevectors found with $S(\mathbf{q})$ and $N(\mathbf{q})$ are themselves 2D and in general incommensurate, suggesting the possibility of a

P1A.6 - P1A.11

distinct 2D mechanism for spin-charge separation. I propose that magnetic frustration provides this mechanism, where the frustration arises between AF and FM fluctuations. This frustrated state is unique to 2D in that only for 2D are T_C and T_N rigorously degenerate by symmetry and dimensionality ($T_C = T_N = 0$ by the Hohenberg-Mermin-Wagner theorem). From the calculated phase diagram of the 2D t - J model the frustration should be most pronounced for small J/t and 15%-20% doping. The existence of a frustrated state is supported by the low temperature entropy which is considerably larger for the 2D t - J model than for the non-interacting tight binding model in this parameter range. The behaviors of the AF and FM magnetic correlation lengths also support a picture of strong competition between AF and FM correlations. The behavior I propose for the 2D t - J model requires all of the characteristic features found in the normal state of high temperature superconductors: two dimensionality, a bipartite lattice, strong repulsive correlations and doping near half filling.

P1A.6

"Magnetic Excitation in High- T_c Cuprates," **Hiroshi Kohno**¹, Bruce Normand² and Hidetoshi Fukuyama¹, ¹Department of Physics, University of Tokyo, 7-3-1 Hongo, Bunkyo-ku, Tokyo 113 Japan, ²Theoretische Physik, ETH-Hönggerberg, CH-8093 Zürich, Switzerland

Several aspects of magnetic excitation in high- T_c cuprates, revealed by NMR, inelastic neutron scattering and phonon anomalies, will be discussed based on the results of the slave-boson mean-field approximation to the t - J model. We first review the results including material dependence through Fermi surface shape, spin gap behaviours above T_c due to singlet formation, and phonon anomalies. In a closer look for YBCO, however, a disagreement is seen in the relative location of the resonance-like excitation found experimentally at energy $\omega = 41\text{meV}$. This '41meV problem' is pursued, according to the recently-proposed scenario, by taking account of η -pair process, a finite-momentum excitation in the particle-particle channel. The result shows slightly increased weight around '41meV', but is not enough to form a resonance-like peak.

P1A.7

"Thermodynamics of d-Wave Pairing in Cuprate Superconductors," **S. P. Kruchinin**, Bogolyubov Institute for Theoretical Physics, 252143, Kiev, Metrologicheskaya 14-b, Ukraine

The mechanism of d-pairing introduced by D. Pines is considered. The thermodynamical potential of the system is calculated. The thermal capacity is studied. It has been shown that the temperature dependence of thermal capacity corresponds to d-pairing.

P1A.8

"Coupled States in Electron-Phonon System of HTSC Crystals," **S. P. Kruchinin** and A. M. Yaremko, Bogolyubov Institute for Theoretical Physics, Kiev, 252143, Ukraine, Institute of Semiconductors, Kiev-28, 252659, Ukraine

A new approach to the SC problem is proposed taking into account complex multi band structure of HTSC superconductors. Namely, we study the conditions when the coupled states in the electron system can appear taking into account only

interactions between quasiparticles of electron-phonon system. Our calculations have shown that hypothesis of electron pairing postulated in BSC is only approximate. That is the case of both momenta ($k+k' \neq 0$) and so spins ($s+s' \neq 0$).

P1A.9

"Neutron Scattering: A Signature of the Gap Symmetry in High- T_c Superconductors," **Andreas Bill**, Lawrence Berkeley Laboratory, 1 Cyclotron Road, MS 62-203, Berkeley, CA 94720, Vladimir Hizhnyakov, Tartu University and Estonian Academy of Sciences, Physics Department, Riia 142, EE2400 Tartu, Estonia, and Ernst Sigmund, University of Cottbus, Institute für Theoretische Physik, P. O. Box 101344, 03013 Cottbus, Germany

The influence of different type of gap anisotropies Δ_k on the phonon dispersion below T_c is studied in systems with tetragonal and orthorhombic point groups. It is shown that along specific directions of the Brillouin zone the shift and lifetime of phonons strongly depend on the symmetry of Δ_k . The study includes s -, d - as well as $(s + d)$ -wave symmetries of the gap. Numerical calculations are performed for the Raman observed phonons of $\text{YBa}_2\text{Cu}_3\text{O}_7$ along [100] and [110].

The theoretical predictions suggest a way to determine the symmetry of the superconducting order parameter in high- T_c materials using q -dependent neutron scattering experiments.

Finally, we study the phonon renormalization for the gap resulting from non-totally screened long range electron-phonon coupling. This interaction has been shown to give a contribution to the gap of the type observed in recent experiments.

P1A.10

"Anisotropy of the Gap Induced by Unscreened Long Range Interactions," Vladimir Hizhnyakov, Tartu University and Estonian Academy of Sciences, Physics Department, Riia 142, EE2400 Tartu, Estonia, **Andreas Bill**, Lawrence Berkeley Laboratory, 1 Cyclotron Road, MS 62-203, Berkeley, CA 94720, and Ernst Sigmund, University of Cottbus, Institute für Theoretische Physik, P. O. Box 101344, 03013 Cottbus, Germany

The anisotropy of the superconducting order parameter in the ab -plane is explained by unscreened interaction of charge carriers with long-wave optical phonons. The screening is absent due to the low frequency of long-wave plasmons in layered structures. Solutions of the gap equation for different screening and filling factors are presented.

P1A.11

"Boundary Effects and the Order Parameter Symmetry of HTC Superconductors," **Safi R. Bahcall**, Department of Physics, U.C. Berkeley, Berkeley, CA 94720

Apparently conflicting phase-sensitive measurements of the order parameter symmetry in high- T_c superconductors may be explained by the appearance of regions near boundaries in which the order parameter has a symmetry different than that of the bulk superconductor. Such states can lead to interesting and testable effects.

PIA.12

"The Ginzburg-Landau Equations for d-Wave Superconductors with Nonmagnetic Impurities," C. S. Ting, **W. Xu** and Y. Ren, Texas Center for Superconductivity at the University of Houston, Houston, TX 77204-5932

The Ginzburg-Landau equations for a d-wave superconductor with nonmagnetic impurities are derived in the framework of the Gorkov's weak-coupling theory of superconductivity. The weak scattering in the Born limit as well as the strong scattering in the unitary limit of the impurities are both considered in the calculation. The effect of impurities on the magnetic field penetrating depth and the induced s-wave order parameter are also studied.

PIA.13

"Inter-Band Pairing: Resolution of Observed d-Wave and s-Wave Tunneling with Isotropic s-Wave Pairing," **Jamil Tahir-Kheli**, Beckman Institute, Caltech 139-74, Pasadena, CA 91125

A fundamentally different, yet conceptually and computationally simple theory is presented for high temperature superconductivity. We assume the existence of two bands, one with predominantly planar $d_{x^2-y^2}$ character on the copper sites and the other with predominantly p_z character with lobes pointing normal to the CuO planes on the oxygen sites. An attractive phonon coupling *across* the bands is assumed with a purely isotropic (s-wave) attraction. Thus, a Cooper pair consists of a $k \uparrow$ electron from one band and a $-k \downarrow$ electron from the other band. Due to the different masses of the two bands, Cooper pairs can carry current, or equivalently, are not invariant under time-reversal. This leads to a dramatic change in the standard picture of Josephson tunneling. It is shown that the d-wave tunneling results of Tsuei et al. on YBCO tricrystals and Wollman et al. on YBCO-Pb corner junctions and the s-wave result of Chaudhari on hexagonal YBCO junctions are **all** a natural consequence of inter-band pairing. Inter-band pairing makes the orbital nature of the bands contribute to the tunneling current. Finally the temperature dependence of the Knight shifts in YBCO7 and YBCO6.63 and the various spin relaxation rates are qualitatively explained in the normal and superconducting phases.

PIA.14

"Effects of Impurity Vertex Correction on NMR Coherence Peak of Conventional Superconductors," **Han-Yong Choi**, Department of Physics, Sung Kyun Kwan University, Suwon, 440-746, Korea

We study the effects of nonmagnetic impurity vertex correction on nuclear spin-lattice relaxation rate $1/T_1$ of conventional superconductors within the Eliashberg formalism. We obtain, with a self-consistent t-matrix, treatment of impurity scatterings, the expressions for impurity vertex function and nuclear spin-lattice relaxation rate. The $1/T_1$ is evaluated with a simple approximation on angular average, and found to agree in the clean limit with the previous result that $1/(T_1 T)$ remains unrenormalized under the impurity vertex correction. As dirtiness is increased, on the other hand, the coherence peak in $1/(T_1 T)$ is found to increase due to the impurity vertex correction. The coherence peak increases by about a factor of 2, as one goes from the clean to dirty limit, which is in good agreement with the NMR measurements on Al- and In-based superconductors. This observation raises an

interesting possibility that the experimental observation of the NMR coherence peak increase may be understood in terms of impurity vertex correction rather than the gap anisotropy smearing by impurities.

PIA.15

"Comparison of Three-Band and t-t'-J Model Calculations of the One-Hole Spectral Function in an Antiferromagnet with Photoemission Experiments," **George Reiter**, Department of Physics, University of Houston, 4800 Calhoun, Houston, TX 77204-5506, and Oleg A. Starykh, Department of Physics, University of California at Davis, Davis, CA 95616

Using the self-consistent Born Approximation in both cases, we give a comparison of the best fitting dispersion relations for the t-t'-J model and the three band model including direct oxygen-oxygen hopping with photoemission measurements of Wells et al. for a single hole in an antiferromagnet. A three-band calculation using the parameters of Hybertsen et al. determined by fits to local density functional calculations is also presented.

PIA.16

"c-Axis Electronic Structure and Transport in Copper-Oxides," **Joseph M. Wheatley** and J. R. Cooper, Interdisciplinary Research Centre in Superconductivity, Cambridge, CB3 0HE, United Kingdom

The mechanism of charge transport along the c-axis in Copper-Oxides is reviewed. The three-dimensional electronic structure of Copper-Oxides can be interpreted in terms of a four band model including the Cu 4s orbital [1]. Projection to a 3D extended t-J model is carried out using an intercell perturbation method, for monolayer and bilayer systems. This results in an anisotropic renormalization of hopping matrix elements; the ratio $\frac{t_c}{t_{ab}}$ is reduced. Taking this effect into account, we suggest that the observed resistivity anisotropies are not anomalously large.

Semi-classical Bloch-Boltzmann theory for c-axis magneto-transport in quasi-two dimensional systems in arbitrary magnetic field strengths is described. It is shown, for example, how this theory can be used to determine the momentum dependence of in-plane scattering rates over the quasi-2D Fermi surface. The inferred lifetime variation on the Fermi Surface in overdoped $Tl_2Ba_2CuO_6$ [2] is at most 40%. This weak effect is too small to account for the temperature dependence of the Hall coefficient in this material. Despite notable successes, the validity of the Bloch-Boltzmann approach to c-axis transport in Copper-Oxides must be questioned in the light of the small ratio of c-axis mean free path to c-axis lattice parameter.

[1] O. K. Andersen et al, Physical Review B, 49, 4145 (1994).

[2] N. Hussey et al, Physical Review Letters, 76, 122 (1996)

PIA.17

"Paramagnetic Meissner Effect and Time Reversal Non-Invariance from Spin Polarization," **Alpo Kallio**, Viktor Sverdlöve and Martti Rytivaara, Theoretical Physics, Department of Physical Sciences, University of Oulu, Linnanmaa, FIN-90570 Oulu, Finland

P1A.18 - P1A.21

We propose that recent experiments for paramagnetic Meissner effect in single crystals by Lucht *et al.* can be understood in terms of pairing fermion (quasiparticle) spin polarization. The polarization comes from the fact that for Coulomb Fermi systems the polarized state has lower energy than the unpolarized state due to the Coulomb interactions when the pairing fermion density gets small below T_c . With suitable surface topology the polarized spins cannot be screened by supercurrents inside a surface layer.

The same theory explains also the double transition in UPt_3 and the observed breakdown of time reversal invariance associated with polarized spins below the lower peak at T_c . The breakdown therefore need not to be associated with the superfluid order parameter. The low temperature Schottky effects seen in high- T_c cases are also proposed to be caused by the polarization and therefore is an intrinsic effect.

The Schottky effect and the linear specific heat term follow naturally from the existence of a light spectator fermion band which is needed also to obtain the binding mechanism for bosons out of the heavier band of pairing fermions by applying accurate many-body formalism for mixtures.

P1A.18

"Hall-Effect Scaling and Chemical Equilibrium in Normal States of High- T_c Superconductors," **Alpo Kallio**, Viktor Sverdlove and Carolina Honkala, Theoretical Physics, Department of Physical Sciences, University of Oulu, Linnanmaa, FIN-90570 Oulu, Finland

We give a simple treatment of boson fermion chemical equilibrium reaction $B^{2+} \leftrightarrow 2b^+$ suitable for understanding the normal states of superconductors such as 123 where the bosons may continue to exist in the form of preformed pairs for $T > T_c$ and gradually decay into pairing holes. The densities of bosons and fermions, given by a function $f(T)$, are temperature dependent. A proper treatment in analogy with ionization using the grand potential $\Omega(T, V, \mu)$ leads to reduction of free boson contribution to entropy and specific heat near T_c . Large free boson contribution immediately above T_c , not seen in experiments, has been the main argument against boson models. The treatment explains in a simple fashion also the Hall coefficient scaling law observed experimentally by Hwang *et al.* in *LSCO*. We propose a "rational" principle how to manufacture superconductors with maximal T_c , based on the fact that bosons remain localized down to a temperature T_{BL} slightly above T_c in 123 but close to the coherence temperature in heavy fermions. For this reason the bosons remain strongly correlated also below T_c . The minimum of Hall density $n_{ab}(T)$ at T_{BL} is produced by the contribution from the delocalized bosons.

P1A.19

"Spin-Susceptibility of Strong Correlated Bands in Fast Fluctuating Regime," **Mikhail Eremin**, Kazan State University, Department of Quantum Electronics and Radiospectroscopy, Lenina str., 18, Kazan, 420008, Russia

We have deduced new expressions for spin-susceptibility using Hubbard-like theory for HTSC. When the chemical potential is disposed at the upper Hubbard-like band the spin-susceptibility can be written as:

$$\chi_1(\theta, \delta) = (1 + \delta)^2 \chi_p(\theta) / [16 \langle X^{2,2} \rangle + 4\lambda_1(\theta, \delta) - \chi_1^*(\theta, \delta)]$$

Here $1 + \delta$ is a number of holes per one copper site, $\langle X^{2,2} \rangle$ is number of Zhang-Rice singlets, $\chi_p(\theta)$ is a typical expression for Pauli-like susceptibility. $\lambda_1(\theta, \delta)$ and $\chi_1^*(\theta, \delta)$ are the functions of temperature θ and doping level δ . An interesting feature of the function $\chi^*(\theta, \delta)$ is that its sign can change upon doping. Numerical calculations are reported in comparison with the experimental data for the temperature and doping dependence of $Cu(2)$ Knight shifts in layered cuprates.

If the chemical potential is disposed at the low Hubbard-like band the expression for susceptibility can be written as follows:

$$\chi_2(\theta, \delta) = (1 - \delta)^2 \chi_p(\theta) / [8 \langle X^{0,0} \rangle - \delta - 4\lambda_2(\theta, \delta) - \chi_2^*(\theta, \delta)]$$

where $\langle X^{0,0} \rangle$ is a so-called vacuum average or number of Cu^+ ions per one copper site. We are using this expression for the analysis of the temperature and doping dependence of $Cu(1)$ Knight shifts in chains of the Y-Ba-Cu compounds. We point that expressions deduced for spin-susceptibility are not sensitive to Green's functions decouple scheme. The fast spin fluctuating regime is only essential for that.

P1A.20

"Pairing Instability and Anomalous Response in an Interacting Fermi Gas," **Y. M. Malozovsky** and J. D. Fan, Department of Physics, Southern University and A & M College, Baton Rouge, Louisiana

The Pairing instability induced by either a given attractive interaction or particle-hole excitations is examined by using the perturbation diagram approach. A graphical derivative method based on Ward's identity is developed to represent the contributions to the interparticle interactions from different channels. It is shown that the pairing instability can be induced by the particle-hole excitations when the "original" interaction is repulsive, in contrast to the conventional Cooper instability caused by the given attractive interaction.

The effect of vertex corrections on the charge and spin responses of the Fermi gas is also considered. It is shown that the interaction in the particle-hole channel induces multipair excitations ("Cooper pair" -like) in both the charge and spin channels. It leads to the appearance of the anomalous term $Im\chi \sim \omega/T$ in both the charge and spin responses of the Fermi gas in addition to the normal response $\sim \omega/v_F k$.

-Supported by DOE under grant No. DE-FG05-94ER25229 through the Science and Engineering Alliance, Inc.

P1A.21

"The Connections of the Experimental Results of Universal Stress Experiments and of Thermal Expansion Measurements and the Mechanisms of Microscopic Dynamics Process on CuO_2 Planes," **Dawei Zhou**, R & D Department, General Superconductor, Inc., 1663 Technology Avenue, Alachua, FL 32615

The experimental results of universal stress on the superconducting transition in YBCO by U. Welp *et al.* (Phys.Rev.Lett. 69, 2130, 1992) indicates that T_c is linear in p_i with slopes $dT_c/dp_a = -2.0$ K/Gpa, $dT_c/dp_b = +1.9$ K/GPa, and $dT_c/dp_c = -0.3$ K/GPa. These results confirmed that the small hydrostatic pressure dependence of T_c in YBCO is due to a cancellation of large and opposite effective effect in the a-b plane. This indicated that the pressure dependence of T_c and the relative sign change for the

a- and b- axis compression may reflect the symmetry of 4-particle (electrons or electrons with hole) or higher order quantum tunneling cyclic loops (QTCLs) on the CuO_2 plane in high T_c superconductor. Because of the existence of mixed valences on the CuO_2 plane, the electron/holes in high T_c superconductor are weakly localized and strongly correlated thus able to form QTCL. The QTCLs have $k=0$ in the center of the mass frame, and a non-zero angular momentum. Each QTCL has total spin $S=0$. Each QTCL can contain two or more Cooper pairs in real space and in k -space. This dynamics is consistent with observations of very short coherence length on the CuO_2 plane. This is consistent with the thermal expansion measurement results (C. Meinelgast et. al Phys. Rev. Lett. 67, 1634, 1991) that indicates that superconductivity favors asymmetric ($b=a$) CuO_2 plane.

P1A.22

"Phenomenology: What the Data Say*," **John D. Dow**, 6031 East Cholla Lane, Scottsdale, Arizona 85253, and Howard A. Blackstead, Department of Physics, University of Notre Dame, Notre Dame, IN 46556

A study of local magnetic exchange scattering (the difference between Ni and Zn) and its effects on T_c should reveal that (i) Ni is a stronger pair-breaker than Zn if the correct theory is either cuprate-plane or charge-reservoir BCS-like – observed only for $\text{Nd}_{2-x}\text{Ce}_x\text{CuO}_4$, whose cuprate-planes are adjacent to its charge-reservoirs, (ii) Ni is a weaker pair-breaker than Zn if the correct theory is a spin-fluctuation pairing cuprate-plane model – not observed, but thought to have been observed *only* in $\text{YBa}_2\text{Cu}_3\text{O}_7$, or (iii) Ni breaks pairs the same as Zn if the cuprate-plane impurity-site lies outside the superconducting condensate (*i.e.*, if the superconductivity originates in the charge-reservoirs instead of in the cuprate-planes) – *observed for all other high-temperature superconductors*. This test locally probes the Cooper-pair binding and is definitive, as contrasted with measurements of $\Delta(k_x, k_y)$. Furthermore, the pair-breaking matrix-element extracted from the data decays exponentially with d , the distance between the impurity site in a cuprate-plane and the nearest oxygen site in a charge-reservoir. Hence the data themselves say very clearly that the superconductivity originates in the charge-reservoirs, not in the cuprate planes, with polarization-pairing. They also say that cuprate-planes are mechanically good but electronically bad for superconductivity.

*H. A. Blackstead and J. D. Dow, Philos. Mag. 73, 223 (1996).

P1A.23

"Current Instabilities in Reentrant Superconductors," **David Frenkel** and Jeffrey Clayhold, Texas Center for Superconductivity

The resistivity curve of a reentrant superconductor has a region in which the resistance rapidly drops with *increasing* temperature. This is a potential source of thermal instabilities, since local ohmic heating decreases local resistance, leading to a further increase of the local heating rate.

We consider a model in which a film of a reentrant superconductor is on an electrically insulating substrate, which acts as a heat conductor. The bottom of the substrate is kept in a bath at a fixed temperature.

We have conducted a theoretical study of the resulting time-dependent heat diffusion equation in the substrate, with a *nonlinear* temperature-dependent heat

source term on the boundary, due to a locally temperature dependent resistivity of the film. For a fixed current source the boundary term is also *nonlocal*, due to the current conservation constraint.

We have found that for a fixed voltage source, there is a run-away thermal instability at larger biases. More interesting is the case of a fixed *current* source. Linear stability analysis shows that above a certain current level, the uniform current-carrying state develops an instability towards a spatially inhomogeneous state. Numerical calculations show that the nonuniform current distribution has a "hot channel," whereby there is a narrow strip where most of the current is concentrated. This strip is ohmically heated to be warmer than the surrounding areas, thus allowing locally the lower resistivity needed by the current channel.

We have further found that for a sufficiently wide substrate the nonuniform current state has a hysteretic character over a range of total current values. This allows for bistability, when both the uniform and nonuniform current carrying states are locally stable. For narrower samples, the bistability disappears.

By examining the Frobenius integrability condition for the flows in the space of temperature distributions, we have found a special model for which a global variational principle exists, allowing analytical corroboration of the numerical results.

The I-V characteristics shows a regime of negative differential conductance, raising the possibility of applications for high-resolution phase-sensitive bolometry at nonzero frequencies.

*This work has been supported by the Texas Center for Superconductivity.

P1A.24

"Time-Window Extension for Magnetic Relaxation from Magnetic-Hysteresis-Loop Measurements," Qianghua Wang^{1,2}, Xixian Yao², Z. D. Wang¹ and **Jian-Xin Zhu**¹, ¹Department of Physics, University of Hong Kong, Pokfulam, Hong Kong, ²Physics Department and National Laboratory of Solid State Microstructure, Nanjing University, Nanjing 210093, China

A one to one map is established between the time t in a relaxation measurement and the field sweeping rate \dot{H} in a magnetic-hysteresis-loop (MHL) measurement. Utilizing this map, we are able to extend the time-window of the relaxation curve from the MHL measurements. The advantage over previous extension schemes lies in the fact that in the present scheme no microscopic uncertainties are involved. The present scheme can be applied conveniently to extend the time window of relaxation, to connect multiple relaxation measurements (e.g., starting from different stages of magnetization) performed under the same external conditions, and thereby to investigate the activation energy for pinned flux motion in a wider range of currents. The present algorithm is applied to reported experiments.

P1A.25

"Numerical Study of Washboard Effect in High- T_c Superconductors," **Z. D. Wang** and K. M. Ho, Department of Physics, University of Hong Kong, Pokfulam Road, Hong Kong

Using a simple model of the moving vortex lattice, the washboard effect in the mixed state of high- T_c superconductors, which is due to the interference between the intrinsic oscillation of the vortex lattice and the applied ac driving current, is

P1A.26 - P1B.2

investigated by numerical simulation. We observe that interference peaks appear in the dV/dI -V curve whenever the intrinsic and external frequencies are harmonically or sub-harmonically related. The obtained numerical results are in good agreement with recent experimental measurements on *YBCO* crystal. We also study the case when the ac driving current consists of two frequencies, and observe that the corresponding washboard effect is related not only to the two basic frequencies of the ac current but also to their combination terms.

P1A.26

"Vortex Vacancy Motion as the Origin of the Hall Anomaly," **Ping Ao**, Department of Physics, University of Washington, P. O. Box 351560, Seattle, WA 98195

General theoretical reasonings have shown that the Magnus force is an intrinsic property of vortex dynamics in superconductors. But its straightforward application cannot explain the sign anomaly of the Hall effect in the mixed state of many superconductors. We show that a proper consideration of the competition between the many-body collective effect and pinning leads to the resolution of this long standing puzzle. Specifically, we argue that the Hall anomaly is a property of a vortex lattice rather than that of an individual vortex, and demonstrate that the anomaly is due to the motion of vortex vacancies. We obtain the relevant energy scale in the problem: the vacancy formation energy, and at low temperatures we find a scaling relation between the Hall and longitudinal resistivities: $\rho_{yx} = A\rho_{xx}^v$, with v varying between 1 and 2 depending on sample details. Near T_{c0} and at low magnetic fields we find the Hall conductivity as $\sigma_{xy} = \alpha_1 (1-T/T_{c0})^2/B$. All of them are consistent with experiments.

P1A.27

"Vortex Dynamics in Superfluids: Cyclotron Motion," **Ertugrul Demircan**¹, Ping Ao² and Niu Qian¹, ¹Department of Physics, University of Texas at Austin, RLM 5.208, Austin, TX 78741, ²Department of Theoretical Physics, Umea University, S-901 Umea, Sweden

Vortex dynamics in superfluids is investigated in the framework of the nonlinear Schrödinger equation. We have identified a new length scale (adiabatic length), $r_c = (\hbar/m\omega_0)^{1/2}$, within which the condensate can adiabatically follow the vortex motion but not so at distances beyond it, where m is the mass of the superfluid particles and ω_0 is the frequency scale of the vortex motion. The natural motion of the vortex is of cyclotron type, whose frequency is found to be on the order of phonon velocity divided by the coherence length, and may be heavily damped due to phonon radiation. Trapping foreign particles into the vortex core can reduce the cyclotron frequency and make the cyclotron motion underdamped. A further downward renormalization of the cyclotron frequency occurs due to the adiabatic following of the condensate within r_c which is larger than the coherent length due to the slower motion of the vortex. We have also discussed applications on the dynamics of vortices in superconducting films.

P1A.28

"Zero-Bias (Tunneling-)Conductance Peak (ZBCP) as a Result of Midgap Interface States (MISs) – Model Calculations," **Chia-Ren Hu**, Texas A&M University

Previously we have shown: (1) On any non-{100} surface of a *d*-wave superconductor (DWSC), there is a sizable area density of midgap *surface* states (MSSs), which can have many observable consequences, including the potential of explaining the ubiquitously observed ZBCP in tunneling measurements made on various high- T_c (HT)SCs;¹ (2) The idea can be extended to practically any flat *interface* between two DWSCs of different gap-nodes orientations, which would correspond to a *grain boundary* between two grains of HTSCs with different *a, b*-axes orientations, *if* they have *d*-wave pairing. We then proposed that these MISs are much more likely responsible for the observed ZBCP, than the MSSs, due to the unlikelihood of non-{100} surfaces.² Here we report model calculations of (*c*-axis) tunneling characteristics into a system containing two *d*-wave strip-shaped grains with total width = $30\xi_{ab}$, obeying periodic boundary conditions (for simplicity) to contain two interfaces. The gap-nodes orientations on the two sides differ by 45° . A ZBCP is clearly obtained in these calculations, which disappears as the temperature is raised. Replacing the (normal) tunneling probe by a low- T_c superconductor, a dip in the middle of the broadened ZBCP is obtained, all in agreement with many existing observations!

¹C.-R. Hu, PRL **72**, 1526; J. Yang and C.-R. Hu, PRB **50**, 16766 (1994).

²C.-R. Hu, Bull. Amer. Phys. Soc. **40**, 789 (1995).

POSTER SESSION 1B

P1B.1

"Low Temperature Scanning Tunneling Microscopy and Spectroscopy of the CuO Chains in *YBa₂Cu₃O_{7-x}*," **David J. Derro**, Tamotsu Koyano, Alex Barr, John T. Markert and Alex L. de Lozanne, Department of Physics, University of Texas, Austin, TX 78712-1081

Over the last few years we have developed a technique for cleaving single crystals of *YBa₂Cu₃O_{7-x}* at low temperature. The clean (001) surface is then studied in-situ with a scanning tunneling microscope. The most interesting layer shows the CuO chains on the surface, with a few oxygen vacancies. An energy gap (about 25mV) is clearly observed on this surface except near the oxygen vacancies. The chains show strong modulations along their length which can be due to either a charge density wave or to Friedel oscillations. These modulations have been observed recently by neutron diffraction [Mook et al.], which confirms their existence in the bulk. We have also used Current Imaging Tunneling Spectroscopy (CITS) to obtain a spatial map of the gap. We are now repeating these measurements with an applied magnetic field, which should yield images of vortices and spectroscopy of their cores.

P1B.2

"Momentum Dependence of the Superconducting Gap of *Bi₂Sr₂CaCu₂O₈*," J. C. Campuzano and **Hong Ding**, University of Illinois at Chicago, Department of Physics, 845 W. Taylor St., Chicago, IL 60607, M. R. Norman, M. Randeria and A. F. Bellman, Argonne National Laboratory, D. Ginsberg, University of Illinois-Urbana, T. Yokoya, T. Takahashi and H. Katayama-Yoshida, Tohoku University, Japan, and T. Mochiku and K. Kadowaki, National Research Institute for Metals, Japan

We show detailed measurement of the superconducting gap along the Fermi surface of $\text{Bi}_2\text{Sr}_2\text{CaCu}_2\text{O}_8$ by high resolution angle-resolved photoemission spectroscopy (ARPES). It is found that umklapp bands due to the incommensurate superlattice in this material may obscure the intrinsic momentum dependence of the gap. By taking these into consideration, we find a d-wave-like gap function. We also show some results on the controlled introduction of point scattering centers on the gap function and the spectral function.

P1B.3

"Use of Tricrystal Microbridges to Probe the Pairing State Symmetries of Cuprate Superconductors," John H. Miller, Jr., **Jiangtao Lin** and Zhongji Zou, Texas Center for Superconductivity, University of Houston, Houston, Texas 77204-5932, and Quan Xiong, University of Arkansas, Physics Department, Fayetteville, AR 72701

We have measured the field-modulated critical currents of cuprate thin film microbridges on tricrystal substrates. Such measurements are capable of detecting either a complex or a real mixture of *s*- and *d*-wave components of the order parameter. Two central peaks, of approximately equal height, are observed in the field-modulated critical currents of frustrated YBCO tricrystal microbridges operating in the short junction limit, consistent with predominantly $d_{x^2-y^2}$ pairing symmetry with little or no imaginary *s*-wave component. However, the critical current is nonvanishing at zero field, consistent with the existence of a *real* mixture of large *d*-wave and small *s*-wave components. Such a *d* + $c\phi$ symmetric pairing state is equivalent to an orthorhombic *d*-wave order parameter, which exhibits a sign change but has different magnitudes along the two principal symmetry directions. We observe only a single central peak in the field-modulated critical current of an unfrustrated tricrystal device, thus allowing us to rule out artifacts unrelated to pairing state symmetry.

We have also carried out tricrystal microbridge experiments on cuprate superconductors with a wide range of critical temperatures, including doped and ion-irradiated YBCO, and Tl-based cuprates. The results suggest that the size of any apparent *s*-wave component is reduced as the orthorhombicity is reduced and the material becomes more tetragonal.

P1B.4

"Ground State of Superconducting LaSrCuO in 61-Tesla Magnetic Fields," **Gregory S. Boebinger**, Yoichi Ando and Albert Passner, AT&T Bell Laboratories, 600 Mountain Avenue, 1D-208, Murray Hill, NJ 07974, Masayuki Okuya, Tsuyoshi Kimura, Jun-ichi Shimoyama and Kohji Kishio, University of Tokyo, Department of Applied Chemistry, Hongo 7-3-1, Bunkyo-ku, Tokyo 113, Japan, Kenji Tamasaku, Noriya Ichikawa and Shin-ichi Uchida, University of Tokyo, Superconductivity Research Course, Yayoi 2-11-16, Bunkyo-ku, Tokyo 113, Japan, and Igor E. Tروفимov, Fedor F. Balakirev and P. Lindenfeld, Rutgers University, Department of Physics and Astronomy, P. O. Box 849, Picataway, NJ 08855

Using the pulsed magnet at AT&T Bell Laboratories, we measure the normal-state dc resistivity and Hall effect of superconducting $\text{La}_{2-x}\text{Sr}_x\text{CuO}_4$ down to ^3He temperatures. We have previously reported that underdoped $\text{La}_{2-x}\text{Sr}_x\text{CuO}_4$ samples exhibit an unusual insulating behavior in which both ρ_{ab} and ρ_c diverge as $\ln(1/T)$ over a wide range of temperatures below T_c [1]. As the carrier concentration is increased in the under-doped regime, the divergence becomes weaker. Upon further increasing

the carrier concentration into the over-doped regime, we find evidence of an insulator-to-metal (I-M) transition occurring very near optimal doping. The magnitude of the sheet resistance per CuO_2 layer is well below $h/4e^2$ at the I-M transition.

[1] Y. Ando invited talk this conference, and Y. Ando, G. S. Boebinger, A. Passner, T. Kimura, and K. Kishio, Phys. Rev. Lett. 75, 4662 (1995).

P1B.5

"Behavior of ScN and ScS Contacts Under Microwave Irradiation," **Alexei B. Agafonov**, Dimitriy A. Dikin, Andrei L. Solovjov and Vitaly M. Dmitriev, Department of Superconductivity, B. Verkin Institute for Low Temperature Physics and Engineering, 47, Lenin Ave., Kharkov, 310164, Ukraine

Measurements of the I-V characteristics and their derivatives of ScN and ScS metallic weak links prepared by point contact and break-junction technique and made of Y(123), Bi(2212), Tl(2212) have been performed in the temperature range from 4.2 K to 100 K. Contacts were irradiated by microwave field of wide frequency range $10^5 \div 2 \cdot 10^{10}$ Hz. Temperature dependences and behaviour under irradiation of the critical and excess currents are reported. Observed effects point to the presence of Cooper-pair as well as quasiparticles photon assisted charge transport. We revealed the clear evidence of existence in these structures of nonlinear and nonequilibrium phenomena typical for conventional weakly coupled structures, such as planar microbridges or bridges of variable thickness. But high- T_c samples indicate much more complicated picture of the quasiparticles dynamics. That is the subject of our discussion.

P1B.6

"Electronic Raman Scattering in $\text{YBa}_2\text{Cu}_4\text{O}_8$ at High Pressure," **Tao Zhou**, Karl Syassen and Manuel Cardona, Max-Planck-Institut für Festkörperphysik, Heisenberg strasse 1, 70569 Stuttgart, Germany

We report on the electronic Raman scattering in $\text{YBa}_2\text{Cu}_4\text{O}_8$ under hydrostatic pressure up to 9 GPa. We find that at pressure below 1.5 GPa, consistent with the early report of Donovan *et al*, the continuum in the normal state is strongly temperature dependent in all polarizations. This temperature dependence follows a Bose-Einstein form. With increasing pressure, the temperature dependence implied by the Bose-Einstein factor gradually decreases and, above 6 GPa, the electronic continuum of the normal state is very weakly temperature dependent in all polarizations, an effect which is also observed in $\text{YBa}_2\text{Cu}_3\text{O}_7$ even at ambient pressure. In $\text{YBa}_2\text{Cu}_4\text{O}_8$, T_c firstly increases drastically with pressure at a rate of 5.5 K/GPa, and gradually saturates above 6 GPa. This pressure induced T_c change is generally believed to be related to the increase of the hole carrier concentration within the copper-oxygen planes, namely with increasing pressure the sample is tuned from underdoped to optimally doped. Given this scenario, we can explain our results naturally by a model recently proposed by Varma, which suggests that the so-called marginal-Fermi-liquid behavior only occurs in a narrow range around the optimally doped condition. Additionally, we report on the pressure dependent rearrangement of the continuum which occurs below T_c .

P1B.7 - P1B.11

P1B.7

"Raman Scattering on $HgBa_2Ca_{n-1}Cu_nO_{2n+2+\delta}$ ($n=1,2,3,4,5$) Superconductors," **Xingjiang Zhou** and Manuel Cardona, MPI für Festkörperforschung, Heisenbergstraße 1, 70569, Stuttgart, Germany, and C. W. Chu and Q. M. Lin, Texas Center for Superconductivity, University of Houston, Houston, TX 77204-5932

Polarized micro-Raman scattering measurements have been performed systematically on the five members of $HgBa_2Ca_{n-1}Cu_nO_{2n+2+\delta}$ ($n=1,2,3,4,5$) superconductors. The evolution of the spectrum, which mainly involves phonons around 590, 570, 540 and 470 cm^{-1} , with the increasing number of CuO_2 layers, n , has been observed. With increasing n , the 590 cm^{-1} phonon decreases in intensity and then disappears, while the 540 and 470 cm^{-1} phonons begin to appear with increasing intensities. High power laser radiation leads to an intensity decrease of the 540 and 470 cm^{-1} phonons, which indicates that these two phonons are related to the extra oxygen on HgO_δ planes. The spectrum of these two phonons also changes with different laser excitations. The phonon assignment, the spectrum evolution with increasing n , and its variation with laser excitation frequency will be discussed.

P1B.8

"Anisotropy of Thermal Conductivity of YBCO and Selectively Doped YBCO Single Crystals," **Partick F. Henning**¹, Jack E. Crow² and Gang Cao³, ¹Department of Physics, Florida State University, Keen Building, and ²Director's Office and ³Department of Science, NHFML, 1800 E. Dirac Drive, Tallahassee, FL 32306

The anisotropy of the thermal conductivity of single crystals of YBCO has been studied. Along the a - b plane, the thermal conductivity has the expected $1/T$ behavior at high temperatures followed by a sharp upturn at T_c and a peak near $T_c/2$. Along the c axis the thermal conductivity shows a $1/T$ behavior at high temperatures. However, the thermal conductivity shows no break in slope at T_c and a peak near 20 K. This behavior is compared to the behavior of heavily doped $Y_{1-x}Pr_xBa_2Cu_3O_{7-\delta}$, $YBa_2(Cu_{1-x}Zn_x)_3O_{7-\delta}$, and $YBa_2(Cu_{1-x}Al_x)_3O_{7-\delta}$ single crystals. At particular levels of doping, these classes of crystals have thermal conductivities along the a - b plane showing no break at T_c and a peak at 20 K. The similarity of this behavior to the thermal conductivity along the c -axis in the pristine material will be discussed.

P1B.9

"Thermal Conductivity of High- T_c Superconductors," **Michel Houssa** and Marcel Ausloos, S.U.P.R.A.S, Institute de Physique B5, Universite de Liège, Department of Solid State Physics, B-4000 Liège, Belgium

The electronic contribution κ_e to the thermal conductivity of high- T_c superconductors was calculated using a variational method. We took into account the scattering of heat carrying electrons by point defects as well as by acoustic phonons. We considered both isotropic s -wave and anisotropic $d_{x^2-y^2}$ -wave gap parameter symmetries. The electronic density of states was chosen to be relevant for 2D and 3D systems and a Van Hove singularity was included if necessary. The peak structure observed in single crystals of $YBa_2Cu_3O_{7-\delta}$ and $Bi_2Sr_2CaCu_2O_8$ could be well reproduced with very reasonable values of the physical parameters. The values found for the transport electron-acoustic phonon coupling constant λ_{tr} laid in the weak coupling limit, in agreement with the analysis of electrical resistivity data on similar

samples. However, the very low temperature behavior of κ in these materials was found to be incompatible with an s -wave gap parameter but could only be explained by considering gap parameter of $d_{x^2-y^2}$ -wave type.

P1B.10

"Dielectric Anomaly of $La_{2-x}Sr_xCuO_4$ Film at $x=1/4^n$," **Masanori Sugahara**, Yokohama National University, Faculty of Engineering, 156 Tokiwadai, Hodogaya, Yokohama, 240, Japan

The resistivity of bulk $La_{2-x}Sr_xCuO_4$ materials drops sharply at $x \approx 4^{-n}$ from low up to room temperature with some appurtenant anomaly at $x \approx 2 \times 4^{-n}$.¹

Anomalous dielectric response of $La_{2-x}Sr_xCuO_4$ thin film at $x \approx 1/4$ and $1/16$ is found when charge moves long c axis. The capacitance C_t of multi-layer structure Pd/ $La_{2-x}Sr_xCuO_4$ /SrTiO₃/Pd increases sharply exceeding the capacitance C_{STO} of Pd/SrTiO₃/Pd structure from low to room temperature,^{2,3} where effective dielectric constant of the conductive normal state is considered to be negative. Some anomaly is found also at $x \approx 2 \times 4^{-n}$. The C-V measurement reveals the existence of "critical voltage" in the anomalous dielectric property.

Theoretical study² suggests that the dielectric anomaly in the conductive normal state is based on 2D Wigner crystallization of carrier (hole-pair) system in CuO_2 layer analogous to the carrier state in the integral quantum Hall effect. The motion of 2D-crystallization pair charge along c axis is dual to the 3D motion of BCS pair charge "crystallized" in the momentum space. Experimental study is made on the MQE dual to Josephson effect which is expected from the theory.

- 1) M. Sugahara, Jpn. J. Appl. Phys. **31** (1992) 324; M. Sugahara and J.-F. Jinag, Appl. Phys. Lett. **63** (1993) 255; Physica B, **194-196** (1994) 2166.
- 2) to be published in the Bulletin of the Faculty of Engineering, Yokohama National University, Vol. 45, March 1996.
- 3) to be published in Jpn. J. Appl. Phys. March 1996

P1B.11

"Angular Dependence of the c -Axis Normal State Magnetoresistance in Single Crystal $Tl_2Ba_2CuO_6$," **Nigel E. Hussey**, John R. Cooper and Joe M. Wheatley, University of Cambridge, IRC in Superconductivity, Madingley Road, Cambridge, CB3 0HE, United Kingdom

We report measurements of the normal-state magnetoresistance (MR) from 30K - 340K in fields B up to 13T for single crystals of overdoped $Tl_2Ba_2CuO_6$ ($T_c \approx 25K$). For out-of-plane current flow, the transverse MR $\Delta\rho_c/\rho_c$ is large and positive. On rotating B within the ab -plane, $\Delta\rho_c/\rho_c$ exhibits a striking anisotropy with four-fold symmetry. The amplitude of this effect increases as B^4 and the maximum MR occurs for B along the $[110]$ crystallographic directions, i.e. at 45° to the $Cu-O-Cu$ bonds. This is the first direct evidence for anisotropy of the in-plane mean free path in the cuprates. We show that several, but not all, of the observations are consistent with Boltzmann transport theory and a nearly two dimensional Fermi surface, and briefly discuss an alternative model involving two relaxation times.

P1B.12

"Hall Effect and Magnetoresistance in Normal State in LaSrCuO," **Fedor E. Balakirev**, Sabyasachi Guha, Igor E. Trofimov and Peter Lindendorf, Department of Physics and Astronomy, Rutgers University, P. O. Box 849, Piscataway, NJ 08855

We report the measurements of the magnetoresistance and Hall effect of thin films of $La_{2-x}Sr_xCuO_4$ with different compositions between T_c and 350 K. The specimens were grown on $LaSrAlO_4$ substrates by laser ablation, and are single-crystal films with their *c*-axis perpendicular to the film plane, as shown by x-ray diffraction. The magnetoresistance, with the current in the film plane, was measured with the field both in the transverse direction (parallel to the *c*-axis) and in the longitudinal direction (parallel to the film plane). Starting from 10 K above T_c the magnetoresistance is proportional to B^2 up to our highest field (10 T), while at lower T it has the form characteristic for superconducting fluctuations. At high temperatures the orbital part of the magnetoresistance is found to be proportional to the square of the tangent of the Hall angle, but there are large deviations at temperatures that are lower although not yet in the fluctuation regime. Measurements of compounds with Nd substituted for some of the Sr show the same characteristic T-dependence of the magnetoresistance, while the behavior of the Hall angle is quite different.

P1B.13

"The Effect of Sr Impurity Disorder on the Magnetic and Transport Properties of $La_{2-x}Sr_xCuO_4$, $0.02 \leq x \leq 0.05$," **Robert J. Gooding**¹, Robert J. Birgeneau² and Noha M. Salem¹, ¹Department of Physics, Queen's University, Kingston, Ontario, Canada, ²Department of Physics, MIT, Cambridge, MA 02139

We consider the spin-glass regime of the $LaSrCuO$ high T_c compound, and describe the effect of the disordered pinning potential introduced by the Sr impurities. The spin texture that results from these impurities corresponds to domains of antiferromagnetically ordered Cu spins, the domains being separated by strongly disordered domain walls. These domain walls are highly conducting, and thus holes can easily hop from one Sr impurity region to another. This result explains the following experimental data: (i) The cutoff length $\xi(x,0)$ found in the neutron scattering result of B. Keimer *et al.* for the spin correlation length, viz. $\xi^{-1}(x,T) = \xi^{-1}(x,0) + \xi^{-1}(0,T)$, arises from the geometry of these domains. (ii) The absence of any incommensurability in the magnetic response for $x < 0.05$ follows from the expulsion of the holes from these magnetic domains into the highly conducting, magnetically disordered domain walls. (iii) The anomalously small Curie constant observed above the spin-glass phase transition temperature may be attributed to the behaviour of each domain acting as an effectively isolated low-spin magnetic unit.

P1B.14

"Mössbauer Studies of $Re_{1.85}Sr_{0.15}CuO_4$ T' Phase," Ada Lopez, Elisa Baggio-Saitovitch, Mauricio A. C. de Melo, **Dalber Sánchez**, and Izabel A. Souza, Centro Brasileiro de Pesquisas Físicas, Depto. Mat. Condensada e Espectroscopia, Rua Xavier Sigaud, 150, 22290-180, Rio de Janeiro, Brasil, and Jochen Litterst, TU-Braunschweig, Inst. für Metallphys. und Nukl. Fest., Mendelssohnstr. 3, Braunschweig, Germany

Many studies of high T_c superconductors have focused on the modification of magnetic properties as the number of carrier is varied, converting the materials from

antiferromagnetic insulators to metals that eventually exhibit superconductivity. Among all of the cuprate superconductor, the $(La_{1-x}Gd_x)_{1.85}Sr_{0.15}CuO_4$ system change from a superconducting, to a paramagnetic and finally to an antiferromagnetic material with increasing Gd concentration, the local Cu-O unit being an octahedron (T' phase), a pyramid (T* phase), and a square (T'' phase), respectively. Local information from a microscopic technique as ^{57}Fe , ^{119}Sn and ^{151}Eu Mössbauer spectroscopy is particularly valuable in this system, since iron and tin substitute copper in the Cu layers while europium can be substitute lanthanum between the Cu layers. We will discuss our Mössbauer results in the T' phase using ^{57}Fe , ^{119}Sn and ^{151}Eu isotopes in the $RE_{1.85}Sr_{0.15}CuO_4$ where RE are some rare-earth (Gd, Eu, Pr and Nd). We will focus mainly the magnetism and the spin dynamics in the T' phase.

P1B.15

"Observation of a Pair-Breaking Field in $RENi_2B_2C$ Compounds," **Dalber R. Sánchez**¹, Elisa Baggio-Saitovitch¹, Hans Mickitz², Magda B. Fontes¹ and Sergey L. Bud'ko¹, ¹Centro Brasileiro de Pesquisas Físicas, DME, Rua Xavier Sigaud 150, CEP 22290-180, Urca, Rio de Janeiro, Brazil, ²II. Physikalisches Institut, Universität zu Köln, D-50937 Köln, Germany

The rare earth (RE) nickel borocarbide layered compounds offer a possibility to study the interplay between superconductivity and magnetism. We have measured the ^{57}Fe Mössbauer spectra of $RENi_2B_2C$ (RE = Tb, Dy, Ho, Er) doped with 1 at % ^{57}Fe for $300K > T > 3K$.

The room temperature spectra essentially show one quadrupole doublet for all the samples, however at low temperatures a magnetic hyperfine field (B_{hf}) is observed at the ^{57}Fe nucleus in two compounds: $TbNi_2B_2C$ for $T < 15K$ and $HoNi_2B_2C$ for temperature region $5.5K > T > 4.2K$. In the case of $TbNi_2B_2C$ a weak ferromagnetic behavior was already observed for $T < 8K$, this phase transition is also detected by our Mössbauer measurements as a slope change in the plot of $B_{hf} - T$ near 8K. No magnetic hf field is observed in the superconducting compounds $DyNi_2B_2C$ and $ErNi_2B_2C$ down to 4.2K. Since $TbNi_2B_2C$ is not superconducting at all and superconductivity disappears in $HoNi_2B_2C$ in the temperature region $6K > T > 4.7K$ (reentrance behavior) we conclude that the transferred magnetic hf field at the ^{57}Fe nucleus in these two compounds, resulting from the non collinear antiferromagnetic spin structure of the RE moments, acts as a pair-breaking field at the Ni planes.

P1B.16

"Pressure Effects on T_c of $HgBa_2Ca_{n-1}Cu_nO_{2n+2+\delta}$ with $n \geq 4$," **Y. Cao**, X. D. Qiu, Q. M. Lin, Y. Y. Xue and C. W. Chu, Texas Center for Superconductivity and Department of Physics at the University of Houston, Houston, TX 77204-5932

The hydrostatic pressure effect (dT_c/dP) on T_c in $HgBa_2Ca_{n-1}Cu_nO_{2n+2+\delta}$ was measured and compared for $1 \leq n \leq 6$ up to 16 kbar. For $n \geq 4$, dT_c/dP is insensitive to δ over a fairly broad δ -range near the optimum doping level. There is a step-like drop of dT_c/dP with n near 4. The dT_c/dP is ~ 2 K/GPa for $n = 1, 2$, and 3, while the dT_c/dP is ~ 1 K/GPa for $n \geq 4$. Combining these results with the quasi-hydrostatic pressure results up to 30 GPa, which show a universal enhancement of ~ 30 K for $n \leq 3$ and a much smaller one for $n = 4$ and $n = 5$, we suggest that the number of CuO_2 -layers affects the dT_c/dP in a rather complicated way.

P1B.17 - P1B.20

This work is supported in part by NSF, EPRI, the State of Texas through the Texas Center for Superconductivity at the University of Houston, and the T. L. L. Temple Foundation. This material was also prepared with the support of the U. S. Department of Energy, Grant No. DE-FG-48-95R810542. However, any opinions, findings, conclusions, or recommendations expressed herein are those of the authors and do not necessarily reflect the views of DoE.

P1B.17

"Effect of High Pressure on the Normal State Resistivity of Yttrium Doped Bi-2212 System," S. Natarajan and S. Ravikumar, Department of Physics, Anna University, Madras, Tamil Nadu, India

The Bi-2212 system has gained much importance in recent years because it exhibits Metal Insulator Transition (MIT) when a rare earth ion is doped at the calcium site. Almost all rare earth doped Bi-2212 systems show a rise in T_c for small rare earth concentrations. In the normal state the systems approach the MIT for higher rare earth concentrations. In this paper we report the synthesis of Y doped Bi-2212 samples and the effect of high pressure on the normal state resistivity. Samples of nominal composition $Bi_2Sr_2Ca_{1-x}Y_xCu_2O_{8+\delta}$ ($x = 0, 0.2, 0.3$ and 0.4) were synthesised through solid state reaction. The high pressure resistivity measurements were performed using Opposed Anvil High Pressure Device (OAHPD) on the samples with composition $Bi_2Sr_2Ca_{0.7}Y_{0.3}Cu_2O_{8+\delta}$ having the highest T_c (91K). The measurements show increase in the relative resistivity up to 20 kbar followed by a steady fall, reaching saturation at 45 kbar. The above result suggests that pressure may induce MIT in this system. Further studies on the samples having chemical composition near MIT regime are under progress. The results will be discussed in detail with reference to other high T_c systems investigated earlier.

P1B.18

"Strong Overdoping, Similar Depression of T_c by Zn and Ni Substitution and Departure from the Universal Thermopower Behaviour in (Ca, La)-1:2:3," Dan Goldschmidt and Yakov Eckstein, Department of Physics, Technion, Haifa 3200, Israel

In the new tetragonal 1:2:3 (Ca,La)(Ba,La)₂Cu₃O_y (CLBCO) family, electron concentration become constant by cosubstitution, in equal amounts, of charge-compensating Ca²⁺ and La³⁺ ions and by keeping the oxygen content constant. Nevertheless, T_c and transport properties change substantially indicating that doping (band filling) occurs. In the underdoped regime all doping effects due to cations and oxygen can be cast into a single parameter $y - y_{M-I}$ independent of Ca and La concentration (where $y - y_{M-I}$ is the oxygen content y measured relative to the metal-insulator transition), suggesting that these materials have essentially the same band structure. Our results are interpreted within the simple band picture modified to consider the existence of low-mobility states near E_F , besides the CuO₂ band.

We have further substituted Zn and Ni impurities in CLBCO and by tuning y found T_c^{max} . Zn and Ni cause almost equal depression of T_c^{max} with impurity concentration, that is, the difference in effectiveness of T_c depression caused by both impurities in an order of magnitude smaller in CLBCO than it is in YBCO. The resistivity almost does not change. We also observed big departure from the universal thermopower (TEP) behaviour. In many cuprates the universal TEP plot determines the state of doping of a given material. In these materials the CuO₂ planes seem to

remain intact. In CaLaBaCuO, the departure from the TEP plot apparently occurs due to impurities that enter on the planar Cu site. Moreover, the strong depression of T_c occurs at constant band filling indicative of pair breaking or interaction weakening rather than lowering of the DOS. Our results suggest that pair breaking does not depend on the magnetic nature of the impurity even when substitution occurs within the CuO₂ planes.

Recently we also found that these materials are stable under high oxygen pressure and become strongly overdoped ($T_c \rightarrow 0$ K on the overdoped side in the Ni-substituted materials). Transport and superconducting properties show the behaviour typical of other overdoped systems. We believe that CLBCO is a model system for investigating the inherent properties of cuprates allowing one to separate effects due to impurities and to doping, as well as to investigate the interesting regime of overdoping.

P1B.19

"Nonlinear Dynamics in the Mixed State of High Temperature Superconductors," Mark W. Coffey, Regis University, Department of Chemistry, 3333 Regis Blvd., Denver, CO 80221

A new formulation of the (1+1)-dimensional coupled nonlinear electrostatics of high-temperature superconductors in the mixed state is presented. Special coordinates are used to combine the governing Maxwell and London partial differential equations. A novel nonlinear wave equation for the specific area A is derived for a type-II superconductor, including dissipation. The effects of nonlocal vortex interaction and vortex inertia are also included. In the ultraclean regime this system has special integrability properties and shows solitonic behavior. Soliton propagation could be used to study the vortex mass and other dynamical parameters. The dispersion relation of the linearized problem can be studied in various limits. The full coupled problem shows a rich variety of phenomena even for weak nonlinearity but with varying degrees of dispersion.

P1B.20

"The Drude Model of Transport Properties in Pure, Pr- and Ca-Doped RBa₂Cu₃O_{7-δ} Systems," W. Y. Guan, Department of Physics, Tamkang University, Tamsui, Taiwan, R.O.C.

We report detailed studies of the normal state resistivity and Hall-effect in pure, Pr- and Ca-doped RBa₂Cu₃O_{7-δ} systems. We find a linear temperature dependence of the normal state resistivity ρ_n ($\rho_n \propto T$) and the Hall number n_H ($n_H \propto T$) above T_c . This fact seems to be the most puzzling in the normal state transport properties of the high- T_c cuprates: *The higher the carrier density, the smaller the conductivity!* At a constant temperature both ρ_n and n_H are dependent on ionic radius of rare earth $r_{R^{3+}}$, viz. the larger R^{3+} ionic radius, the larger ρ_n ($\rho_n \propto r_{R^{3+}}$), but the lower n_H ($n_H \propto 1/r_{R^{3+}}$). For a fixed temperature the relation of $\rho \propto 1/n_H$ in the simple Drude model is well confirmed for pure, Pr- and Ca-doped RBa₂Cu₃O_{7-δ} systems with different R ion. *The higher the carrier density, the higher the conductivity.*

*Supported by the National Science Council, R.O.C. Grant No. NSC90208M00795.

P1B.21

"Anomalous Pr Ordering and Filamentary Superconductivity for the Pr₂12 Cuprates*," **Huan-Chiu Ku**, Y. Y. Hsu, S. R. Lin, D. Y. Hsu, J. F. Lin, Y. M. Wan and Y. B. You, Department of Physics, National Tsing Hua University, Hsinchu, Taiwan 300, Republic of China

The anomalous Pr antiferromagnetic ordering temperature $T_N(\text{Pr})$ for the Pr₂12 cuprate system $M_2A_2\text{PrCu}_2\text{O}_7$ ($M = \text{Cu, Tl, Bi, Pb}$; $A = \text{Ba, Sr}$) was studied through the synthesis of all Pr₂12 compounds: Tl-2212, (Bi,Pb)-2212, (Pb,Cu)-2212 and Cu-2212C, Cu-2212C/1212C. Contrary to the normal (no $T_N(\text{Pr})$ observed down to 1.6 K) orthorhombic Bi-2212 $\text{Bi}_2\text{Sr}_2\text{PrCu}_2\text{O}_8$, a new tetragonal (Pb,Cu)-2212 $(\text{Pb}_{0.5}\text{Cu}_{0.5})_2(\text{Ba}_{0.5}\text{Sr}_{0.5})_2\text{PrCu}_2\text{O}_8$ compound with high $T_N(\text{Pr})$ of 9 K was observed [1]. The phase stability of the Pr₂12 compounds, the systematic variation of $T_N(\text{Pr})$ for these Pr₂12 compounds due to the variation of superexchange coupling strength, and the occurrence of filamentary superconductivity due to the metal-insulator transition will be discussed in detail.

[1] C. L. Yang, J. H. Shieh, Y. Y. Hsu, H. C. Ku and J. C. Ho, Phys. Rev. B 52, 10452 (1995).

*Supported by NSC of ROC under contract NSC85-2112-M007-043 and -044PH.

P1B.22

"Superconductivity and Structural Aspects of $\text{Y}_{1-x}\text{Ca}_x\text{Ba}_2\text{Cu}_3\text{O}_{7-\delta}$ with Variable Oxygen Content," V. P. S. Awana¹, **J. Albino Aguiar**¹, S. K. Malik^{1,2}, W. B. Yelon^{1,3} and A. V. Narlikar⁴, ¹Departamento de Física, UFPE, 50670-901, Recife-PE, Brasil, ²Tata Institute of Fundamental Research, Bombay 400005, India, ³University of Missouri Research Reactor, Columbia, MO 65211, ⁴Department of Physics, National Physical Laboratory, New Delhi, 110012, India

We have mapped nearly full phase diagram of $\text{Y}^{3+}/\text{Ca}^{2+}$ doping with variable oxygen stoichiometry till the solubility limit of Ca at Y-site in Y₁₂₃ system. $\text{Y}_{1-x}\text{Ca}_x\text{Ba}_2\text{Cu}_3\text{O}_{7-\delta}$ samples with $0.0 \leq x \leq 0.30$ were synthesized through conventional solid state reaction route. X-ray diffraction studies reveal that on Ca doping, the c-parameter of the system remains unchanged in oxygen annealed compounds, while it increases for the Ar annealed (Ca doped) compounds. The oxygen content decreases for oxygen annealed compounds but remains nearly unchanged in the Ar annealed compounds. Our neutron diffraction measurements show that Cu(2)-O(2) distances increase with Ca doping at Y-site in $\text{YBa}_2\text{Cu}_3\text{O}_{7-\delta}$ compound with $\delta \cong 0$, which suggests that overdoping (increase in carriers beyond optimum) is unlikely to be cause for the decrease in T_c of Ca-doped oxygen annealed compounds. Increased Cu(2)-O(2) distances and the flat Cu-O planes may be responsible for the decrease in T_c of $\delta \cong 0$ compounds. On the other hand, in the case of oxygen deficient compounds, the Ca^{2+} substitution at Y^{3+} site does induce mobile holes, by decreasing the Cu(2)-O(2) distances in the adjacent Cu-O planes and hence increases or even brings the bulk superconductivity at 43K in the tetragonal $\text{Y}_{0.7}\text{Ca}_{0.3}\text{Ba}_2\text{Cu}_3\text{O}_{7-\delta}$ system with $\delta \cong 0$.

P1B.23

"Superconducting Properties of Nb Thin Films," Ana Luzia V. S. Rolim, J. C. de Albuquerque, E. F. da Silva, Jr., J. Marcilio Ferreira and **J. Albino Aguiar**, Departamento de Física, Universidade Federal de Pernambuco, Av. Prof. Luiz Freire, s/n^o, 50670-901 Recife-PE, Brasil

Niobium thin films with thickness between 100-1000nm have been deposited by magnetron sputtering on dielectric substrates (glasses). The dependence of the deposition rates on the DC/RF power (0-500W), substrate-target distance, and the Ar plasma pressure are studied. The critical temperatures (T_c) were measured by ac susceptibility using a SQUID magnetometer. The DC magnetization was measured using zero field cooling (ZFC) and field cooling (FC) cycles. The irreversibility temperature was determined as been that were the difference between the ZFC and FC curves are less than the mean standard deviation of the measure. The magnetic field-temperature (H-T) diagram reveals a strong dependence of the irreversibility line as function of the film thickness. Thinner films present a more pronounced field dependence on the irreversibility temperature as compared to thicker films. We attribute this behavior to surface pinning effect.

Work supported by the Brazilian Agencies CNPq and FINEP. We acknowledge Centro de Engenharia de Materiais - CEMAR/FAENQUIL Lorena/SP for providing the Nb targets

P1B.24

"On the Thickness Dependence of Irreversibility Line in $\text{YBa}_2\text{Cu}_3\text{O}_{7-x}$ Thin Films," Pablo Menezes and **J. Albino Aguiar**, Departamento de Física, Universidade Federal de Pernambuco, 50670-901, Recife-PE, Brasil

On the most widely studied features of vortex behavior in high-temperature superconductors is the experimentally observed irreversibility line (IL) in the H-T phase diagram that separates the reversible magnetization at high temperatures from hysteric behavior at lower temperatures. In this paper we analyse the IL data of Civale et al. [1] obtained in thin films of $\text{YBa}_2\text{Cu}_3\text{O}_{7-\delta}$ produced by laser ablation. We show that is possible to fit the IL with the function $H_{\text{IRR}} = A(1-t)^\alpha$, where $t = T_{\text{IRR}}/T_c$ and A and α are adjustable parameters for all thickness studied. It is shown that α varies from 1.0 to 1.6 when the film thickness changes from 1000 to 20nm. We argue that surface pinning effects can be responsible for this behavior.

[1]. L. Civale, T. K. Worthington and A. Gupta, Phys. Rev. B43, 5493 (1991).

Work Supported by the Brazilian Agencies CNPq and FINEP.

P1B.25

"Twin Structures in Large Grains of $\text{YB}_2\text{Cu}_3\text{O}_{7-\delta}$ as Affected by the Dispersion and Volume Fractions of Y_2BaCuO_5 ," Manoj Chopra, **Siu-Wai Chan** and V. S. Boyko, Henry Crumb School of Mines, Columbia University, 500 W. 120th St., New York, NY 10027, and R. L. Meng and C. W. Chu, Department of Physics and Texas Center for Superconductivity at the University of Houston, Houston, TX 77205-5932

Quantitative Microscopy studies have been conducted on large grained $\text{YBa}_2\text{Cu}_3\text{O}_{7-\delta}$ (Y123) samples containing various amounts of Y_2BaCuO_5 (211)

particles. Some samples contain 0.05wt% platinum to facilitate the dispersion of the 211 particles. Both the 211 particle size and distribution are analyzed. Transmission electronic microscopy (TEM) studies show that the local twin spacing varies as a function of the local 211 distribution and spacing. It is observed that the mean twin spacing (T_w) decreases linearly with the square root of the local interparticle spacing (S_{211}).

Measurements of the local twin spacing at the Y123/211 interface show that the twin spacing decreases as one approaches the interface. Furthermore, the twin spacing at the interface shows a non-uniform stress field around the 211 particles in the matrix (produced during the $t \rightarrow o$ transformation). This stress is mathematically modeled. Under the parameters of the model the twin spacing at the interface is studied as function of the effective distance R . Twin spacing measurements from various samples are related to the 211 particle shape and distribution. Effects on flux pinning will be discussed.

P1B.26

"Electromagnetic Coupling of Melt-Textured $YBa_2Cu_3O_{6+x}$ Bicrystals," **Michael B. Field** and David C. Larbalestier, University of Wisconsin-Madison, Applied Superconductivity Center, 1500 Engineering Drive, Madison, Wisconsin 53706, and Apurva S. Parikh and Kamel Salama, Department of Mechanical Engineering, University of Houston, Houston, TX 77204

Detailed characterization of five ($5^\circ, 7^\circ, 11^\circ, 14^\circ, 38^\circ$) general misorientation $YBa_2Cu_3O_{6+x}$ bicrystals produced by the melt-texture liquid-phase-removal method shows that the boundaries contain regions of both strong and weak coupling. The ratio of these regions was found to be both a function of crystal misorientation and magnetic field. The role of the macroscopic boundary plane was investigated by sectioning samples with a laser. The electromagnetic properties were not strongly dependent on the macroscopic grain boundary plane orientation for bicrystals of the same misorientation. High-field, high-sensitivity voltage-current characteristics of the inter and intra-grain regions had qualitatively identical properties and confirmed that there was a measurable strongly-coupled component to the boundary. The data suggest that the transition from fully to weakly coupled as a function of crystal misorientation is neither abrupt nor complete.

FRIDAY, MARCH 15

5:40-7:30 p.m., Granger A & B & de Zavala

Poster Session 1B-cont: HTS Theory, Experiment, Material, & Properties

Poster Session 2: HTS Bulk Processing, Characterization & Application

Poster Session 3: HTS Film Processing, Characterization & Application

POSTER SESSION 1B-cont

P1B.27

"Evaluation of Overdoping Effect in $Y_{1-x}Ca_xBa_2Cu_3O_{7-\delta}$ Films," Cheng-Chung Chi, **Chih-Lung Lin** and Yea-Kuen Lin, National Tsing Hua University, Materials Science Center, Hsin-Chu, 30043, Taiwan, ROC, and Weiyuan Guan, Tamkang University, Department of Physics, Tamsui, Taiwan, ROC

Ca-doped $YBa_2Cu_3O_{7-\delta}$ thin films were prepared on MgO substrates using laser ablation method. The XRD measurement showed that single-phase $Y_{1-x}Ca_xBa_2Cu_3O_{7-\delta}$ was obtained up to 50% Ca doping. The resistivity and critical temperature (T_c) of the as-grown samples decreased with increasing Ca content. The films post-annealed under various oxygen pressures result in different oxygen contents and hence different carrier concentrations. The Ca-doped films exhibited an enhancement in T_c with decreasing oxygen contents. The T_c onset can reach a maximum value of $\sim 90K$ by reducing the oxygen content. However, further decrease the oxygen content results in lowering of T_c . We also studied the effects of photoinduced hole doping on these films. The illumination was performed using an Ar-ion laser. We found that the correlation between photoinduced effect and carrier concentration in Ca-doped samples is opposite to that in YBCO. These observations are mainly due to the overdoping effect by the introduction of Ca to YBCO.

P1B.28

"Mixed-State Hall Effect Studies in High- T_c Superconducting $(YBa_2Cu_3O_{7-\delta})_n/(PrBa_2Cu_3O_{7-\delta})_m$ Superlattices," **Kebin Li**^{1,2}, Yuheng Zhang² and H. Adrian³, ¹Institute of Solid State Physics, Academia Sinica, Hefei 230031, China, ²Structure Research Laboratory, University of Science and Technology of China, Hefei 230026, ³Institute of Solid State Physics, Technical University of Darmstadt, Germany

The mixed-state Hall conductivity behavior has been studied systematically on a series of superconducting $(YBa_2Cu_3O_7)_n/(PrBa_2Cu_3O_7)_8$ (here $n=3,8,16,24,45,60$) superlattices in three magnetic fields with H||c-axis and H||J. It was found, for the first time, that the Hall sign anomaly diminishes and even disappears with the decreasing of the YBCO layer thickness, i.e., the increase of the anisotropy parameter ϵ , and the decrease of the pinning strength. The scaling relationship between the Hall resistivity ρ_{xy} and the longitudinal resistivity ρ_{xx} , i.e., $\rho_{xy} \propto \rho_{xx}^\epsilon$ holds for all of the samples with various ϵ . This indicates that the anomalous Hall sign reversal is

independent of the scaling law between ρ_{xy} and ρ_{xx} . The Anomalous Hall sign reversal in relation to the pinning strength, anisotropic characteristics in $(YBa_2Cu_3O_7)_n/(PrBa_2Cu_3O_7)_8$ superlattices will be discussed in the frame of Wang, Dong and Ting theory which argued that the mixed-state Hall sign anomaly originated from the backflow current due to the pinning force and the thermal fluctuations.

P1B.29

"Correlation Between Phonon-Drag Thermopower and T_c in Superconducting (Bi-Pb) SrCaCuO Thin Films," **J. E. Rodríguez**, A. Mariño and J. Giraldo, Department of Physics, Universidad Nacional de Colombia

Thermopower measurement of highly oriented (Bi-Pb)SrCaCuO superconducting thin films showed a monotonic increase in the phonon-drag contribution ($S_p \propto 1/T$), with T_c . This behavior suggests that the carrier-phonon interaction may play an important role in the pairing mechanism.

P1B.30

"Thermoelectric Power of Superconducting Alloys YNi_2B_2C and $LuNi_2B_2C$," J. H. Lee, Y. S. Ha, Y. S. Song and **Y. W. Park**, Department of Physics, Seoul National University, Seoul 151-742, Korea, and Y. S. Choi, Samsung Display Devices Co., Ltd., Energy Research Center, Suwon, Kyungki-Do, 445-970, Korea

The temperature dependent thermoelectric power (TEP) of YNi_2B_2C and $LuNi_2B_2C$ is presented. These borocarbide quaternary intermetallics are prepared by the arc-melting method followed by the thermal annealing process. Both resistivity and TEP measurements show that the superconducting transition temperature T_c is 15K for YNi_2B_2C and 16K for $LuNi_2B_2C$. The sign of the TEP is negative for $LnNi_2B_2C$ ($Ln=Y, Lu$), which implies that the charge carriers are electron-like for these samples. TEP at room temperature is 5.1 $\mu V/K$ for $LuNi_2B_2C$ and 4.7 $\mu V/K$ for YNi_2B_2C . The TEP for both samples shows strong nonlinear temperature dependence and goes rapidly to zero at T_c . Nearly the same behavior of TEP for $YNiBC$ and $LuNiBC$ is simply guaranteed by band structure similarities between these two. The nonlinear temperature dependence of TEP is frequently shown in disordered metal alloys in which the electron-phonon mass enhancement is important. However, the observed nonlinearity seems to be too big to be attributed to the electron-phonon mass enhancement effect. Instead, the present data could be fitted to the formula derived for the description of the mixed valence compounds.

P1B.31

"Electronic Structure and Magnetic Properties of $RENi_2B_2C$ ($RE=Pr, Nd, Sm, Gd, Tb, Dy, Ho, Tm, Er$)," Zhi Zeng, **Elisa Baggio-Saitovitch** and Diana Guenzburger, Centro Brasileiro de Pesquisas Físicas, R. Dr. Xavier Sigaud 150, 22290-150, Rio de Janeiro, Brazil, and D. E. Ellis, Department of Physics and Astronomy and Materials Research Center, Northwestern University, Evanston, IL

The electronic structure and magnetic properties of $RENi_2B_2C$ ($RE=Pr, Nd, Sm, Gd, Tb, Dy, Ho, Tm$ and Er) are studied by using the first principles density-functional theory within the embedded cluster model. Spin-polarization of the conduction electrons by the RE moments is examined in detail and related to the interplay between superconductivity and antiferromagnetic order. A substantial

difference in the extent of the exchange-polarization of the conduction electrons between early and late rare-earth compounds is revealed, due to the decrease of the 4f orbital radius along the lanthanide series. Hyperfine interactions at the Fe site such as electric field gradients and isomer shifts are obtained for Gd, Tb, Dy, Ho and Er in the case of iron substituting Ni with concentrations simulating the experimental $x < 0.1$. Electric quadrupole splittings of these cases are compared with ^{57}Fe Mössbauer experimental results.

P1B.32

"The Magnetic Properties of the Quaternary Intermetallics $RNiBC$ ($R=Er, Ho, Tb, Gd, Y$)," Julio Cesar Trochez and **Elisa Baggio-Saitovitch**, Centro Brasileiro de Pesquisas Físicas, DME, Rua Xavier Sigaud, 150, CEP 22290-180, Urca, Rio de Janeiro, Brazil, and Mohammed El Massalami, Universidade Federal de Rio, Instituto de Física, Caixa Postal 68528, CEP 21945-970, Rio de Janeiro, Brazil

The structural and magnetic features of the $RNiBC$ series of intermetallic compounds ($R=Y, Er, Ho, Tb$ and Gd) were characterized by XRD, resistivity ($1.2K < T < 300K$) and magnetic measurements ($1.5K < T < 300K$) and their properties compared with those of the corresponding superconducting RNi_2B_2C series. The a-parameter reflects the lanthanide contraction (similar to RNi_2B_2C) while c-parameter remains almost constant (different of RNi_2B_2C). The magnetic transition for Ho, Tb and Gd are characterized by $T=9.8(7), 15.8(2)$ and $14.3(5)$ K, respectively, and their magnetic structure, at low temperatures, are presumably collinear antiferromagnetic-like. For $ErNiBC$ the measured critical temperature of 4.7 K is in agreement with recent neutrons diffraction measurement showing a ferromagnetic ordering at 4.5K.

In contrast to the RNi_2B_2C series the magnetic transition temperature are not strictly scaling with the de Gennes factor as observed in the superconducting series RNi_2B_2C and this behavior may be attributed to distinct structural features of $RNiBC$.

P1B.33

"Related Y-Ba-Cu-O Superconducting Oxides Containing Oxyanions," Rosa Scorzelli and **Elisa Baggio-Saitovitch**, Centro Brasileiro de Pesquisas Físicas, Departamento da Materia Condensada e Espectroscopia, Rua Xavier Sigaud 150, CEP 22290-180, Rio de Janeiro, Brazil, and Angel Bustamante Dominguez, Facultad de Ciencias Físicas, Universidad Nacional Mayor de San Marcos, Apartado Postal 14-0149, Lima-14, Perú

It has been observed that carbonate anions (CO_3^{2-}) can be substituted into perovskite structures containing Cu to form samples which can be superconducting. Other oxyanions, e.g., sulphate (SO_4^{2-}), phosphate (PO_4^{3-}) and borate (BO_3^{3-}) have been used to stabilize the $YSr_2Cu_3O_7$ structure at normal conditions, forming new superconductors with T_c in the range 45-60 K. The simultaneous replacement of Y^{3+} by Sr^{2+} and/or Ca^{2+} ions inject holes in the CuO_2 layers, resulting in a change from the antiferromagnetic to superconductor behavior.

Here we report on the effect of partial substitution of Sr and/or Ca in the Y-Ba-Cu-O related materials containing oxyanion groups. The samples were analyzed by X-ray diffraction, electrical resistivity and Mössbauer Spectroscopy. To follow the structural changes induced by the oxyanions through Mössbauer spectroscopy these materials have been doped with ^{57}Fe (partially substituting Cu), showing some Fe species similar to Y-Ba-Cu-O system and others related to the presence of the oxyanions.

P1B.34

"Physical Properties of Infinite-Layer and T^* -Phase Copper Oxides," **John T. Markert**, Ruiqui Tian and Christopher Kuklewicz, University of Texas at Austin, Department of Physics, Austin, TX 78712

The 2-1-4 T^* -phase compounds and the infinite-layer materials are the only two known electron-doped copper-oxide superconductors. We describe the effects of both isoelectronic and n-type doping on superconductivity in these materials; also, attempts to induce hole-doped superconductivity in these structures are discussed. Magnetic, transport, and structural measurements are reported.

For n-type dopings, systematic variation of lattice parameters indicate a common feature, probably indicative of a minimum required CuO_2 plane bond tension for electron-doped superconductivity: in both infinite-layer $\text{Sr}_{1-x-y}\text{Ca}_y\text{La}_x\text{CuO}_2$ (synthesized at 25 kbar) and T^* -phase $\text{Nd}_{2-x-y}\text{Y}_y\text{Ce}_x\text{CuO}_4$, decreasing the in-plane lattice constant a (by increasing the smaller isoelectronic ion substituent concentration y) suppresses superconductivity.

For a material to be amenable to hole-doped superconductivity, CuO_2 plane bond compression is required. Attempts to hole-dope the smallest ambient-pressure T^* -phase material are described. Under ambient oxygen pressure, such doping is accompanied by a compensating oxygen deficiency. Attempts to hole dope the infinite-layer phase will also be discussed. Although magnetic susceptibility and x-ray diffraction data indicate that appreciable p -type substitutions are achievable, transport data exhibit nonmetallic behavior.

P1B.35

"Magnetic and Structural Properties of Nd_2CuO_4 ," **Yurii G. Pashkevich**, Donetsk Phystech, 72 R. Luxemburg Str., Donetsk 340114, Ukraine

Nd_2CuO_4 has the unique magnetic properties caused by exchange-noncollinear magnetic structure of the "cross-like" type. Spin-waves, inelastic neutron scattering [1], two-magnon absorption [2], Raman light scattering on magnons [3], antiferromagnetic resonance [4], spin-reorientation phase transitions in an external magnetic field and unusual manifestations of magnetoelastic coupling in these transitions [5] are considered in this report. The first evidence of the spin-dependent one-phonon absorption from the Brillouin zone boundary was obtained in Nd_2CuO_4 [6]. This absorption is only possible if no structure distortions happened at 300K in Nd_2CuO_4 . Peculiarities of the magnetic structure were manifested in all of these phenomena.

1/V. Sobolev, H. Huang, Yu. Pashkevich, M. Larionov, I. Vitebskii, V. Blinkin, Phys. Rev. B49, 1170 (1994). 2/V. Sobolev, Yu. Pashkevich, H. Huang, I. Vitebskii, V. Blinkin, Phys. Rev. B51, 1010 (1995). 3/Yu. Pashkevich, V. Sobolev, S. Fedorov, A. Eremenko, Phys. Rev. B51, 15898 (1995). 4/V. Blinkin, Yu. Pashkevich, V. Eremenko, S. Zvyagin, V. Pishko, Low Temp. Phys. 18, 848 (1992). 5/V. Sobolev, H. Huang, I. Vitebskii, A. Knigavko, Yu. Pashkevich, Phys. Rev. B48, 3417 (1993). 6/Yu. Pashkevich, V. Pishko, V. Tsapenko, A. Eremenko, Low Temp. Phys. 21, 587 (1995).

P1B.36

"One-Phonon Absorption Caused by Magnetic Ordering in the Nd_2CuO_4 ," **Yurii G. Pashkevich**, Donetsk Phystech, 72 R. Luxemburg Str. Donetsk 340114, Ukraine, Vitalii V. Pishko and Vadim V. Tsapenko, Institute for Low Temperature Physics, 47 Lenina Ave., Kharkov 310164, Ukraine, and Andrei V. Eremenko, Institute for Single Crystals, 60 Lenina Ave., Kharkov 310141, Ukraine

The spin-dependent one-phonon far-infrared absorption from the Brillouin-zone (BZ) boundary of the paramagnetic phase is discovered in Nd_2CuO_4 . Such an absorption is caused by folding effects of the phonon branches after magnetic ordering with quadruplication of the primitive cell. Electro-dipole and magnetodipole mechanisms of absorption from M - and X -points of the BZ which are induced by the magnetic ordering and magnetic field are considered. It is shown by measurement of reflectance at 150K in the magnetic field and by Kramers-Kronig analysis that the lines at 170cm^{-1} and 320cm^{-1} have to belong to M - and X -points of BZ respectively. Positions of these frequencies correspond to those ones obtained from the inelastic neutron scattering by boundaries phonons [1]. The relative contributions of the displacements of magnetic and nonmagnetic ions of the absorption intensity are discussed.

1/L. Pintschovius, N. Pyka, W. Reichardt, A. Yu. Romyantsev, N. L. Mitrofanov, A. S. Ivanov, P. Bourges Physica C, 185-189, 156 (1991).

P1B.37

"Superconducting Phases in the Sr-Cu-O System," **Z. L. Du**, Y. Gao, Y. Y. Sun, L. Gao, Y. Y. Xue and C. W. Chu, Texas Center for Superconductivity, University of Houston, Houston, Texas 77204-5932

Superconductivity at 90 to 110 K observed in samples of the Sr-Cu-O system prepared under high pressure has been attributed to the layered cuprate phases of Sr_2CuO_4 and SrCuO_2 with defects. However, questions have recently been raised if Sr_2CuO_4 and SrCuO_2 are indeed superconducting. We have therefore examined samples with different phase purities of Sr_2CuO_4 , SrCuO_2 , and $\text{Sr}_3\text{Cu}_2\text{O}_5$ prepared under different high pressure conditions. Pure Sr_2CuO_4 samples were obtained and were found not to be superconducting. Up to four superconducting transitions were detected in many of the multiphased samples, at ~ 40 , ~ 60 , ~ 70 , and ~ 90 K. Prolonged annealing in a reduced atmosphere was observed to merge the 70 with the 90 K transition, with no effect on the 90 K transition but suppression of the ~ 40 K transition. The study demonstrates that there are at least two superconducting phases in the Sr-Cu-O system. The exact stoichiometries are yet to be determined; but neither Sr_2CuO_4 nor SrCuO_2 is one of them. $\text{Sr}_3\text{Cu}_2\text{O}_5$ is a possible candidate.

This work is supported in part by NSF, EPRI, the State of Texas through the Texas Center for Superconductivity at the University of Houston, and the T. L. L. Temple Foundation. This material was also prepared with the support of the U. S. Department of Energy, Grant No. DE-FC-48-95R810542. However, any opinions, findings, conclusions, or recommendations expressed herein are those of the authors and do not necessarily reflect the views of DOE

P1B.38

"Superconductivity in $\text{Sr}_2\text{YRu}_{1-x}\text{Cu}_x\text{O}_6$ System," Maw-Kuen Wu¹, **Dah-Chin Ling**¹, Chao-Yi Tai² and Jun-Lin Tseng², National Tsing Hua University, ¹Materials Science Center and ²Department of Physics, Hsinchu, Taiwan

A systematic study on superconducting properties of the $\text{Sr}_2\text{YRu}_{1-x}\text{Cu}_x\text{O}_6$ system with $x=0.0-0.5$ has been carried out. Powder x-ray diffraction patterns suggest that the samples for $x=0.0, 0.1, 0.2,$ and 0.3 are single phase. There are unidentified peaks in the samples with $x=0.4$ and 0.5 . Without Cu-substitution, the system exhibits a semiconductor-like behavior. However, with a small amount of Cu, the system undergoes a phase transition from an insulator to a superconductor. The partial substitution of Ru by Cu seems to vary the Ru valence which might change the carrier concentration and have a significant contribution to superconductivity. Typically the superconducting onset temperature is about 30 K with a width of 20 K. Magnetic susceptibility measurements have shown a similar result with a diamagnetic signal around 30 K. Further investigation is in progress to more fully understand the nature of the transition. The detailed transport and magnetic properties of this system will be presented and discussed.

P1B.39

"Synthesis and Properties of the $\text{La}_{2-x}\text{Cs}_x\text{CuO}_4$ Superconducting Oxides," Maw-Kuen Wu and **Shyang-Roeng Sheen**, National Tsing Hua University, Materials Science Center, Hsinchu, Taiwan, 30043, ROC, and Chen-Hui Hung and Jeng Shong Shih, Department of Chemistry, National Taiwan Normal University, Taipei 117, Taiwan, R.O.C.

We report bulk superconductivity with a maximum critical temperature T_c of 37 K in single-phase $\text{La}_{2-x}\text{Cs}_x\text{CuO}_4$ ($0.00 \leq x \leq 0.20$) synthesized by conventional solid state reaction technique at temperature between 900 and 1000°C. Materials were characterized by X-Ray powder diffraction, magnetic susceptibility and transport measurements. The structure has been determined by X-ray powder diffraction and all the compounds have the K_2NiF_4 -type orthorhombic structure. The effect of cesium substitution of lanthanum resulted in an increase of the free carriers concentration and of the lattice disorder. Superconductivity is observed for the first time in the cesium substituted compound with a maximum T_c of 37 K.

P1B.40

"Magnetic Properties of $\text{HgBa}_2\text{Ca}_{0.86}\text{Sr}_{0.14}\text{Cu}_2\text{O}_{6-\delta}$," **Sung-Ik Lee** and Mun-Seog Kim, Department of Physics, Pohang University of Science Technology, Pohang, 790-784, South Korea, Seong-Cho Yu, Department of Physics, Chungbuk National University, Cheongju, 360-763, South Korea and Nam H. Hur, Korea Research Institute of Standards and Science, Taedok Science Town, Taejon 305-600, South Korea

This study measures the temperature dependence of reversible magnetization of grain-aligned $\text{HgBa}_2\text{Ca}_{0.86}\text{Sr}_{0.14}\text{Cu}_2\text{O}_{6-\delta}$ high- T_c superconductor with external magnetic fields parallel to the c -axis. The magnetization is field independent at $T^* = 114.5$ K, which indicates strong thermal vortex fluctuations. From the vortex fluctuation model, the lower limit of coherence length along the c -axis $\xi_c(0) \cong 2$ and the anisotropy ratio $\gamma \leq 7.7$ has been obtained, which implies that this sample is anisotropic three dimensional superconductor as $\text{YBa}_2\text{Cu}_3\text{O}_{7-\delta}$. These results are

supported by good 3D scaling behavior of high-field magnetization around $T_c(H)$ as a function of $[T - T_c(H)]/(TH)^{2/3}$. The thermodynamic critical field $H_c(T)$ and the Ginzburg-Landau parameter $\kappa = 114.8$ were extracted from the model of Hao et al. Also, the various thermodynamic parameters were obtained; the penetration depth $\lambda_{ab}(0) = 1913 \text{ \AA}$, coherence length $\xi_{ab}(0) = 13.9 \text{ \AA}$, and the zero temperature upper critical field $H_{c2}(0) = 170.4 \text{ T}$.

P1B.41

"Photoexcited Carrier Relaxation in Metallic $\text{YBa}_2\text{Cu}_3\text{O}_{7-\delta}$: A Probe of Electronic Structure," **Tomaz Mertelj**, Faculty of Mathematics and Physics, Physics Department, "Jozef Stefan" Institute, University of Ljubljana, Jadranska 19, 61111 Ljubljana, Slovenia

The temperature dependence of the realization of photoexcited (PE) carriers is used as a probe of the electronic structure of the high-temperature superconductor $\text{YBa}_2\text{Cu}_3\text{O}_{7-\delta}$ ($\delta \approx 0.1$). The relaxation process is studied by "counting" - through measurement of the Raman scattering Stokes/anti-Stokes intensity ratio on the picosecond timescale - the phonons emitted in the process of carrier energy relaxation. The phonon "shake-off" is found to be strongly temperature dependent, implying that the PE carrier relaxation proceeds via a temperature activated process, which can be understood in terms of hopping between localized states. The PE carrier lifetime is in the range of 100 ps at room temperature as deduced from comparison between measurements with 1.5 ps and 70 ps excitation laser pulse lengths. The long PE carrier lifetime and temperature dependence of the relaxation process implies the existence of localized states within a 2 eV band of the Fermi energy also in the normal state of the optimally doped high- T_c superconductor.

P1B.42

"Superstructure of Potential Created by Impurity Oxygen Ions and its Effect on Resistive and Spectral Characteristics of 1-2-3 HTSC," **V. Eremenko**, I. Kachur, A. Ratner and V. Shapiro, Institute for Low Temperature Physics & Engineering 47, Lenin Ave., 310164, Kharkov, Ukraine

It was experimentally and theoretically shown that superstructure of the long-distance potential relief, created in the conductive plane by oxygen ions, incorporated in chain planes CuO_x exerts an essential effect on current characteristics of $Y-Ba-Cu-O$ films. The current-voltage characteristics (CVC) are studied in a wide temperature range. In the low temperature region residual resistivity is observed in some multiphase superconductive samples. Its high sensitivity to photoillumination, affecting the long-distance potential relief, an increase with lowering temperature as well as the CVC shape at helium temperatures give a ground for an assumption about a low-temperature localization of holes in minima of the long-distance potential. Such Anderson-type localization may occur in interphase regions where the structure of copper-oxygen chains can be most irregular. Transitions between the secondary bands of the long distance potential must manifest themselves in anomalous absorption in the nearest infrared region and its dependence on the copper-oxygen chain length and polarization direction within the ab -plane. These inferences are corroborated by literature experimental data.

P1B.43

"Photostimulation of Critical Temperature, Critical Current and Normal State Conductivity in Epitaxial $Y - Ba - Cu - O$ Films Nonsaturated by Oxygen," **V. Eremente**, V. Piryatinskaya, O. Prihod'ko and V. Shapiro, Institute for Low Temperature Physics & Engineering 47, Lenin Ave., 310164, Kharkov, Ukraine

It was shown that photoillumination causing oxygen diffusion in chain planes CuO_x affects current-carrying characteristics of copper-oxygen high-temperature superconductive films Y-Ba-Cu-O in two ways: 1/ Cu-O-Cu chains in CuO_x planes become longer, as a result, additional charge carriers - oxygen holes - are efficiently supplied to conductive planes in the vicinity of the metal-dielectric transition (relatively quick process); 2/ the space distribution of these chains slowly changes creating more or less periodic potential relief in the conductive planes in homogeneous regions of a film. In the present work the influence of these two factors on the density of critical current in Y-Ba-Cu-O films is investigated. The photoinduced increase in a number of holes is shown to improve current-carrying characteristics. For film with $x=0.5$ an increase in critical current is by 5 % for 1.5 hour of irradiation. An influence of the second factor on the critical current density is not so simple, the magnitude and even sign of photoinduced changes are dependent on the rate of increase in transport current. This unusual dependence has been observed when studying the irradiation changes of critical currents in a film with $x = 0.9$ where the factor 1 is inefficient.

P1B.44

"Magnetic Field Effects on Superconducting Nb/Al/Nb Multilayer," Maw-Kuen Wu¹, **Ming-Jye Wang**², Cheng-Chung Chi¹ and Ching-Shuan Huang¹, ¹National Tsing Hua University, Materials Science Center, Hsinchu, Taiwan, ²Institute of Astronomy, Academia Sinica, Taipei, Taiwan

We have studied the magnetic field effects on the resistive transition of the Nb/Al/Nb...multilayer thin films. The multilayer thin films are prepared using the DC sputtering technique. The thickness of the Nb layer keeps constant while the thickness of the Al layer varies for different samples. We observed the resistive transition shifts to lower temperature in proportion to the magnetic field for those samples that the Al layer thickness is less than that of the Nb layer. On the other hand, distinct resistive anomalies in the resistive transition appear in those samples that the Al layer thickness is the same or larger than that of the Nb layer. The observed anomalies are very much similar to the resistive-knee observed in high T_c $YBa_2Cu_3O_7$ single crystals. Details of the experimental results will be presented and discussed.

P1B.45

"Resistive Transitions of HTS Under Magnetic Fields: Influence of Fluctuations and Viscous Vortex Motion," **E. Silva**, Università "La Sapienza," Dipartimento di Fisica - G20, P.le Aldo Moro 2, 00185 Roma, Italy, R. Fastampa and M. Giura, Università "La Sapienza" and INFN, Dipartimento di Fisica, P.le Aldo Moro 2, 00185 Roma, Italy, R. Marcon, III Università degli Studi and INFN, Dipartimento di Fisica "E. Amaldi", Via della Vasca Navale 84, 00146 Roma, Italy, and S. Sarti, Università "La Sapienza" and INFN, Dipartimento di Fisica, P.le Aldo Moro 2, 00185 Roma, Italy

Resistive transitions in magnetic fields in HTS always present a smooth decrease below the (mean-field) critical temperature, in pure as well as in disordered (twinned, irradiated) samples, and a drop of the resistivity close to the irreversibility line, whose sharpness depends on the purity of the specimen.

We present a set of resistive transitions up to high magnetic fields (14 T) in $YBa_2Cu_3O_{7-\delta}$ and $Bi_2Sr_2CaCu_2O_{8+x}$ films. Through a scaling approach we show that fluctuations are responsible for the smearing of the transitions to the extent that, at high fields, up to 80% of the resistance drop can be described in terms of fluctuations.

The lower part of the resistive transitions, down to the noise level, are well described by a phenomenological model that assumes highly viscous flux motion, with an activation energy diverging at a field-dependent glass-to-liquid transition line $T_g(H)$.

Comparison with data in untwinned $YBa_2Cu_3O_{7-\delta}$ crystals show that the fluctuations contribution is essentially independent on the sample purity, while the resistivity in the "viscous motion" region is strongly dependent on the disorder.

P1B.46

"Vortex Phase Transition Critical Parameters in Single Crystals of YBCO – Apparent Translational Order Dependence," **Brandon Brown** and Janet Tate, Department of Physics, Oregon State University, 301 Weniger Hall, Corvallis, OR 97331

We have investigated the current-voltage characteristics of two Au-doped, heavily-twinned, single-crystals of YBCO and found evidence of a second-order phase transition to be manifest in a wide range of applied fields (0.1 T to 2.5 T). Specifically, we examine n , the power-law slope of the E-J isotherm at what is presumed to be the second-order transition (T_g in the vortex glass picture). This quantity, for both samples, is demonstrably field dependent. Furthermore, we estimate a value for the Larkin-Ovchinnikov length, d_{LO} . A plot of n , for each field and sample, versus the corresponding estimate of d_{LO} suggests that n depends directly on the characteristic length of translation order for a pinned vortex lattice. In addition, we show that values of n from both our thin-film data and other E-J measurements from the literature share this dependence on d_{LO} . We discuss these findings in the contexts of the vortex glass theory and the percolative theory of Yamafuji et al.

P1B.47

"Discontinuous Onset of the c -Axis Vortex Correlation at the Melting Transition in $YBa_2Cu_3O_{7-\delta}$," Esteban Righi, **Daniel Lopez**, Gladys Nieva and Francisco de la Cruz, Comisión Nacional de Energía Atómica, Centro Atómico Bariloche and Instituto Balseiro, S. C. de Bariloche, RN, 8400, Argentina, and W. K. Kwok, J. A. Fendrich, G. W. Crabtree and L. Paulius, Materials Science Division, Argonne National Laboratory, Argonne, IL 60439

Transport measurements in untwinned $YBa_2Cu_3O_{7-\delta}$ single crystals using a multiterminal contact configuration have demonstrated that the long-range vortex correlation in the c direction is discontinuously established at the liquid-solid transition. The stiffness of vortices against current-induced cutting becomes nonzero abruptly at the same temperature. These observations mean that in twin-free samples there is no evidence of a disentangled vortex liquid. The correlated vortex motion above the critical point where first-order melting disappears is also discussed.

P1B.48

"Longitudinal Superconductivity and Percolation Transition of the Vortex Lattice,"

C. A. Balseiro and E. G. Jagla, Comisión Nacional de Energía Atómica, Centro Atómico Bariloche, 8400 S. C. de Bariloche, Argentina

We investigate the nature of the resistive transition for a current applied parallel to the magnetic field in high- T_c materials.

We performed numerical simulations on the three dimensional Josephson junction array model with the external magnetic field parallel to the c -axis of the sample. It is shown that for samples with disorder, the critical temperature T_p at which the dissipation becomes different from zero corresponds to a percolation phase transition of the vortex lines perpendicularly to the external field.

The critical temperature T_p is higher than the temperature at which dissipation occurs when the current flows parallel to the ab -plane and decreases with the thickness of the sample and with anisotropy. We predict that the critical behavior around T_p should be observed in experimentally accessible quantities.

P1B.49

"Vortex Phase Transition in $\text{Bi}_2\text{Sr}_2\text{CaCu}_2\text{O}_y$ Single Crystals and the Doping Level Dependence,"

Hiroshi Ikuta, Satoshi Watauchi, Jun-ichi Shimoyama and Kohji Kishio, Department of Applied Chemistry, University of Tokyo, Hongo 7-3-1, Bunkyo-ku, Tokyo 113, Japan

Careful measurements of magnetization and in-plane resistivity were performed on $\text{Bi}_2\text{Sr}_2\text{CaCu}_2\text{O}_y$ single crystals with applying the field along the crystalline c -axis direction. The crystals were prepared by a floating-zone technique and their oxygen contents (y) were adjusted by careful heat treatment under various conditions. High quality samples with doping states varying widely from the underdoped to the overdoped regime were prepared.

We found distinct step structures in the temperature dependence of both of magnetization and resistivity when magnetic field below the so-called "secondary peak" was applied. It is emphasized that the resistivity drop of $\text{Bi}_2\text{Sr}_2\text{CaCu}_2\text{O}_y$ was observed for the first time in this study.

The location of the step structure in the H - T plane depended on the doping level and shifted to higher fields at the same temperature for samples with larger oxygen contents. When measured on the same sample, the position of the step structure observed by magnetization and resistivity coincided well on the H - T phase. We discuss our observations in the context of the vortex lattice melting transition.

P1B.50

"Oxygen Dependence of First-Order Melting Transition Lines in $\text{Bi}_2\text{Sr}_2\text{Ca}_2\text{Cu}_2\text{O}_{8+x}$

Single Crystals," **Ting Wei Li** and Peter H. Kes, Leiden University, Kamerlingh Onnes Laboratory, Nieuwsteeg 18, P. O. Box 9506, 2300RA Leiden, The Netherlands, Boris Khaykovich and Eli Zeldov, The Weizmann Institute of Science, Department of Particle Physics, Rehovot 76100, Israel, and Marcin Konczykowski, École Polytechnique, Laboratoire des Solides Irradiés, 91128 Palaiseau Cedex, France

The vortex-lattice phase transitions in Bi-2212 single crystals with various oxygen stoichiometry are studied using local magnetization measurements. At low fields and high temperature a line is found in the B-T phase diagram, which separates

an ordered Abrikosov vortex lattice from a disordered flux liquid phase. The line represents a first-order phase transition. This phase transition line is strongly dependent on oxygen stoichiometry. It shifts upward from an optimal-doped sample to an overdoped sample. Using the strong layer superconductor melting function [G.Blatter et al.] to fit the experimental data the oxygen dependence of anisotropy γ is obtained.

P1B.51

"Flux Pinning by Ti Doping in $\text{Bi}_2\text{Sr}_2\text{Ca}_1\text{Cu}_2\text{O}_{8+x}$ Single Crystals,"

Ting Wei Li and Peter H. Kes, Kamerlingh Onnes Laboratory, Department of Physics, Leiden University, Nieuwsteeg 18, P. O. Box 9506, Leiden, The Netherlands, Alois A. Menovsky and Jaap J. M. Franse, Van der Waals-Zeeman Laboratory, Department of Physics, Amsterdam University, Amsterdam, The Netherlands, and Henny W. Zandbergen, National Center for HREM, Department of Materials Science, Delft University of Technology, Delft, The Netherlands

We demonstrate for the first time that Ti has been partially substituted in Bi-2212 single crystals by the traveling solvent floating zone method in concentrations of about 1 and 2 at%. From high resolution electron microscopy (HREM) we discovered that a high density of planar defects is created by the Ti doping. The HREM images of these crystals reveal defected areas containing Ti and regions with the structure of pure Bi-2212 in which no Ti could be probed. These defects are parallel to the c -axis and they form effective pinning centers when the field is applied along the c -direction. The increase of flux pinning in the Ti-doped crystals compared to pure Bi-2212 single crystals is evidenced by a comparison of current densities, magnetic relaxation rates and the position of the irreversibility line. Moreover, annealing the crystals in air up to 850°C these defects show to be thermally stable which is essential for application.

P1B.52

"Meissner Holes in Remagnetized Superconductors,"

V. K. Vlasko-Vlasov^{1,2}, U. Welp², G. W. Crabtree², D. Gunet², V. I. Nikitenko¹, V. Kabanov¹ and L. Paulis³, ¹Institute for Solid State Physics, 142432 Chernogolovka, Russia, ²Argonne National Lab, 9700 South Cass Ave., Argonne, IL 60439, ³Western Michigan University, Kalamazoo, MI 49008

Remagnetization of YBCO single crystals in linearly polarized and rotating fields is studied using advanced magneto-optical techniques. Flux distributions on the wide basal and narrow end faces of crystal plates reveal unusual structures corresponding to the appearance of strong current concentrations along certain fronts in the samples. At these fronts the vortex lines bend into closed loops, which then collapse and form flux free cylinders. On the surface of these Meissner holes a strong magnetization current flows which results in a pronounced flux redistribution in its vicinity. Topological considerations requiring the closing of vortices at remagnetization fronts in any finite sample are discussed. Appropriate magnetic induction structures are simulated and experimentally confirmed. The behavior of the Meissner holes presented here has many analogs in the pinch effect of plasmas and can result in a complicated flux structures in superconductors. The effect is shown to be especially important in rotating fields and should be accounted for in the design of motors and other devices which use superconducting parts.

The work was supported by the US DOE, BES-Materials Science under contract #W-31-109-ENG-38 (UW, GWC, LP), the NSF STCS under contract #DMR91-20000 (DG), and ISF (grants #RF100 and RF1300) (VKV-V, VIN, VK).

P1B.53

"Formation of $\text{HgBa}_2\text{Ca}_2\text{Cu}_3\text{O}_{8+\delta}$ with Additions Under Ambient Conditions," **B.**

Hickey, R. L. Meng, Y. Cao, Y. Q. Wang, Y. Y. Sun, Y. Y. Xue and C. W. Chu, Texas Center for Superconductivity at the University of Houston, Houston, TX 77204-5932

A systematic study of the effect of ReO_2 and HgX_2 , where $X = \text{Cl, F and Br}$, has been carried out. We found that the addition of small amounts of ReO_2 and HgX_2 makes it possible to prepare nearly pure Hg-1223 samples using commercially available oxides, without consideration of their age and without the need of handling these oxides in a dry box. While the observed effect of ReO_2 on the compound formation is in agreement with the earlier report by Kishio *et al.*, the addition of HgX_2 promotes the grain growth of Hg-12(n-1)n, reduces the final reaction time to 1 hr, from the 5 hr previously needed, and lowers the reaction temperature for the Re-doped $\text{HgBa}_2\text{Ca}_2\text{Cu}_3\text{O}_x$. The high purity Hg-1223 phase can be routinely obtained under ambient conditions. Samples so prepared are rather stable in air at room temperature.

This work is supported in part by NSF, EPRI, the State of Texas through the Texas Center for Superconductivity at the University of Houston, and the T. L. L. Temple Foundation. This material was also prepared with the support of the U. S. Department of Energy, Grant No. DE-FC-48-95R810542. However, any opinions, findings, conclusions, or recommendations expressed herein are those of the authors and do not necessarily reflect the views of DOE.

P1B.54

"Single Crystals of $\text{HgBa}_2\text{Ca}_{n-1}\text{Cu}_n\text{O}_{2n+2+\delta}$ Compounds: Growth at 10 kbar Gas Pressure and Properties," **Janusz Karpinski**, Hansjörg Schwer, Kazimir Conder, Roman Molinski and Ingmar Meier, Laboratorium für Festkörperphysik, ETH Hönggerberg, CH-8093 Zürich, Switzerland

Single crystals are of a crucial importance for the studies of physical properties but the synthesis is difficult. At the temperatures close to the melting point of $\text{HgBa}_2\text{Ca}_{n-1}\text{Cu}_n\text{O}_{2n+2+\delta}$ compound ($\approx 1060^\circ\text{C}$) decomposition partial pressures of volatile components HgO, Hg and O_2 are very high and reach values of several hundreds bar. Therefore high pressure technique is necessary to stabilize the phase. In a gas-phase high-pressure chamber partial pressures can be controlled by application of well known amount of a precursor and known volume of a crucible. This allows us to grow single crystals for $n=2,3,4,5$ and ∞ of a size up to 1 mm². Crystals have been grown from a flux of BaCuO_2 -CuO as well as PbO. Many important physical studies like electron tunneling spectroscopy, anisotropy, magnetic and transport measurements, structural investigation, have been performed on our crystals. The T_c depends on conditions of crystal growth and n varies from 130 to 70K.

P1B.55

"X-Ray Single Crystal Structure Analysis of $\text{HgBa}_2\text{Ca}_{n-1}\text{Cu}_n\text{O}_{2n+2+\delta}$ Compounds,"

Hansjörg Schwer and Janusz Karpinski, Laboratory of Solid State Physics, ETH Hönggerberg, CH-8093, Switzerland, and Christophe Rossel, IBM Research Division, Zürich Research Laboratory, CH-8803 Rüschlikon, Switzerland

The crystal structure of four members of the homologous series HgPb-12(n-1)n ($n = 2 - 5$) and of the infinite layer calcium cuprate have been determined and refined by X-ray single crystal diffraction. The crystals have maximum transition temperatures of 70 K (1212), 120 K (1223), 130 K (1234), and 115 K (1245), and crystallize with space group $P4/mmm$. In some crystals Hg was substituted up to 50% for Pb in order to increase oxygen content and T_c . Lead is shifted off the ideal Hg position by up to 0.35 Å. Yttrium of the crucible is incorporated to 50% at the Ca site in HgPb-1212, but not in other members of the HgPb-12(n-1)n family. The excess oxygen content varies between 0 and 35%, and oxygen atoms are partly located at the site (0.5, 0.5, 0) and partly are shifted away from this ideal site by about 0.6 Å. Structure refinements of HgPb-1234 and HgPb-1245 show that the crystals contain up to 6% stacking faults of material with one more or one less calcium cuprate layer than the main phase. Much less stacking faults are observed in crystals without Pb.

Structural parameters and bond lengths vary in a systematic way as a function of the number n of CuO layers in the structure. The main changes occur in the rock salt units, whereas CaCuO_2 layers remain almost undistorted.

P1B.56

"Large Bi-2212 Single Crystals Prepared by Traveling Solvent Floating Zone Method,"

Yu Huang, **Kow-Wei Yeh** and Joy Fang, National Tsing Hua University, Material Science Center, Hsinchu, Taiwan, ROC

The effects of the starting compositions of the feed rod and the solvent zone on the crystal growth behavior of Bi-2212 were studied by the traveling solvent floating zone (TSFZ) method. Optimum growth condition was determined. Stable planar growth interface was achieved with a 0.2 mm/h velocity. Large single crystal of 1 mm thickness along the c -axis was grown without inclusion. Homogeneous single crystals with composition $\text{Bi}_{2.01}\text{Sr}_{2.03}\text{Ca}_{0.93}\text{Cu}_{2.03}\text{O}_8$ were obtained from a solvent of nominal composition $\text{Bi}_{0.325}\text{Sr}_{0.29}\text{Ca}_{0.145}\text{Cu}_{0.24}\text{O}_y$. $T_{c(\text{onset})}$ is 89 K for as-grown crystals. Laue X-ray measurement showed that the quality of the single crystal is good.

P1B.57

"Growth and Characterization of $\text{Bi}_2(\text{Sr}_{1-x}\text{Ca}_x)_3\text{Cu}_2\text{O}_8$ Single Crystals with Various x -Values," **Yu Huang**, Kow-Wei Yeh and Joy Fang, Material Science Center, National Tsing Hua University, Sec. 2, Kuang-Fu Rd., Hsinchu, Taiwan, ROC

Crystal growth experiments were conducted by the traveling solvent floating zone (TSFZ) method on the high- T_c superconducting Bi-2212 phase. The influences on the crystal growth process with various Sr/Ca ratios in the feed rod and the solvent zone were studied. The optimum growth conditions and compositions of the starting materials were determined. The physical properties of inter-substitution between Sr and Ca in a single crystal specimen were studied. Homogeneous single crystals with Sr/Ca ratios 2.25, 1.78 and 1.67 were grown with 0.2 mm/h velocity. The superconducting transition temperature T_c measured by AC magnetic susceptibility

in a magnetic field of 2 G is 89 K for Sr/Ca=2.25, while for higher Ca-content single crystals the superconducting transition is slightly suppressed. Powder X-ray and Laue X-ray measurements were performed in order to measure their variations in the lattice parameters and to check the quality of the crystals.

P1B.58

"Study of the Crucible Reactivity in the BSCCO Melt," Maw-Kuen Wu, **Mei-Hui Huang** and Yu Huang, National Tsing Hua University, Materials Science Center, Hsin-Chu, Taiwan, 30043, R.O.C.

Crucible corrosion problem have always been disturbing crystal growth of the HTSC materials. In this study, various ceramic crucible materials were test in the crystal growth of Bi-Sr-Ca-Cu-O system in order to understand their reactivity with BSCCO melt. Economic alumina crucible was not severely corroded for long duration of soaking, but the reactant $(\text{Sr,Ca})_3\text{Al}_2\text{O}_6$ was easily formed on the crystal surface. As zirconia crucible reacts with BSCCO and forms a SrO-ZrO₂ solid solution, we tried the SrZrO₃ crucible synthesized ourselves. However, its reaction rate was too fast to disturb a crystal growth experiment. In our comparisons, CeO₂ crucible appears to be a better candidate for the growth of BSCC crystals. Ce may be dissolved in the Bi-2212 phase, but it does not destroy the superconductivity nor disturb the surface morphology of single crystals.

*Supported by the National Science Council of ROC under grant no. NSC84-2112-M-007-50-PH

P1B.59

"Preparation and Structure Characterization of the PrBa₂Cu₄O₈ Compound," Shyang-Roeng Sheen¹, **Ju-Chun Huang**², Maw-Kuen Wu¹ and Tsong-Jen Lee³, National Tsing Hua University, Materials Science Center¹, Department of Chemistry² and Department of Physics³, Hsinchu, Taiwan, 30043, ROC

The compound PrBa₂Cu₄O₈ has been prepared under ambient oxygen pressure by oxalate coprecipitation method. The crystal structure of PrBa₂Cu₄O₈ has been refined from X-ray powder diffraction data by the Rietveld method and confirms this compound has the 124 structure. Refined parameters for the orthorhombic (space group Ammm) unit cell are a=3.888 Å, b=3.903 Å and c=27.33 Å. Characterization of this compound by electrical resistivity and magnetization are reported.

* Supported by the National Science Council of ROC under grant No. NSC84-2212-M0005PH

P1B.60

"Intercalation and Staging Behavior in Superoxygenated La₂CuO_{4+δ}," **Barrett O. Wells**¹, Robert J. Birgeneau¹, Fang-Cheng Chou², Marc A. Kastner¹, Young S. Lee¹, Gen Shirane³, John M. Tranquada³, David C. Johnson⁴, Yasuo Endoh⁵ and Kazu Yamada⁵, ¹Department of Physics and ²Center for Materials Science and Engineering, Massachusetts Institute of Technology, 77 Massachusetts Avenue, Cambridge, MA 02139, ³Department of Physics, Brookhaven National Laboratory, Upton, NY, ⁴Ames Laboratory and Iowa State University, Department of Physics and Astronomy, Ames, IA, ⁵Department of Physics, Tohoku University, Aramaki Aoba, Sendai, 980-77, Japan

A high temperature electrochemical process has been used to produce large single crystals of La₂CuO_{4+δ} suitable for neutron scattering experiments. Below room temperature the oxygen-rich phases have structural superlattice peaks which indicate new periodicities ranging from 2 to 7 layers perpendicular to the Cu-O planes. A model structure originally proposed for La₂CuO_{4+δ} can account for the superlattice peaks as a result of anti-phase domain boundaries between different tilt directions of the CuO₆ octahedra, induced by segregated layers of interstitial oxygen which order in a manner similar to intercalants in graphite. This structural model clarifies earlier work and gives further insight into the phase diagram of La₂CuO_{4+δ} and the macroscopic phase separation of the excess oxygen. Most importantly, this work establishes La₂CuO_{4+δ} as a unique lamellar superconducting system with annealed rather than quenched disorder.

This work was supported by the MRSEC Program of the National Science Foundation under award number DMR 94-00334 and by the NSF under award number DMR 93-15715.

P1B.61

"In-Plane Ordering in Phase-Separated and Staged Single Crystal La₂CuO_{4+δ}," **Xiozhong Xiong**¹, Peter Wochner² and Simon C. Moss¹, ¹Department of Physics, University of Houston, 4800 Calhoun, Houston, TX 77204-5506, ²Department of Physics, Brookhaven National Laboratory, Bldg. 510B, Upton, NY 11973

Neutron scattering has revealed a periodic one-dimensional modulation of the in-plane ordering through a splitting of the staging satellites (h,k,ℓ±0.16; with h even, k odd, ℓ even) along the a* direction in a phase-separated and well-staged (213K) single crystal, La₂CuO_{4.015}, during a long annealing from 213K to 185K. The modulation period decreases on cooling and is 69Å at 185K. We suggest that an ordering into laterally separated (vertically offset), and thus phase shifted, Daumas-Herold or related domains is responsible for the splitting of the staging satellites. These split peaks are broad (FWHM is 0.09 in r.l.u. along h), indicating a distribution of in-plane domain sizes. Analytical calculations of the structure factor are consistent with the experimental results in which the central staging satellite vanishes and is replaced by the split-peak sidebands.

*Research at Houston sponsored by NSF (DMR-9208420) and the Texas Center for Superconductivity; at BNL on DOE (DE-AC-02-76CH000160).

P1B.62

"Microstructural Changes of YBCO Induced by Lanthanide Doping," **Irene Rusakova**, Ruling Meng, Pierre Gautier-Picard and C. W. Chu, Texas Center for Superconductivity and Department of Physics at the University of Houston, Houston, TX 77204-5932

We have observed that partial substitution of Y in melt-textured YBCO by rare earth ions such as Sm, Eu, Gd, Ho, and De, respectively, results in increasing values of J_c. The structure of YBCO after doping with these rare elements was studied by SEM and TEM. The TEM study was performed using a JEOL 2000 FX operating at 200 kV. The chemical composition of the samples was checked using EDS and the concentration of lanthanides was determined to be ~1.8 at.%. We found that J_c

P1B.63 - P2.2

increases with increasing magnetic moment of substitutional ions. This might be due to the random distribution of the magnetic atoms which act as effective pinning centers. We also observed some structural changes after doping that could be responsible for enhancing pinning. The d-spacing of twins decreased and twin boundaries had more steps after doping with all the mentioned elements. In addition, arrays of long parallel dislocations have been observed after doping with Ho and Dy that could explain the much higher values of J_c obtained in these samples.

P1B.63

"Formation Mechanisms of Y124 Stacking Fault and Ba-Cu-O Platelet Structure in Melt-Textured Y-Ba-Cu-O System," Chang-Joong Kim, **Gye-Won Hong**, Ki-Baik Kim and Il-Hyun Kuk, Superconductivity Research Laboratory, Korea Atomic Energy Research Institute, P. O. Box 105, Yuseong, 305-600, South Korea

The Y124 stacking faults and Ba-Cu-O platelets were observed around the Y211 trapped within the melt-textured Y123 domain, which were initiated at the Y123/Y211 interface and extended into the Y123 matrix. The Y124 stacking fault has a lenticular shape, with a width about a few ten nanometers and a length about a few hundred nanometers and developed along the [100] and [010] direction of the Y123. The formation mechanism of the Y124 stacking fault the Ba-Cu-O platelet structure is discussed on the basis of the oxygenation-induced decomposition of the Y123 phase. Prolonged oxygenation heat treatment inducing the tetragonal-to-orthorhombic phase transformation is responsible for the formation of the platelet structure and the stacking faults.

P1B.64

"Fractal Grain Boundaries in Composite $YBa_2Cu_3O_{7-\delta}/Y_2O_3$ Resulting from a Competition Between Growing Grains: Experiments and Simulations," Nicolas Vandewalle, **Marcel Ausloos**, N. Mineur and R. Cloots, SUPRAS, Institut de Physique B5, Université de Liège, B-4000 Liège, Belgium

Fractal grain boundaries are found in $YBa_2Cu_3O_7$ melt-textured compounds grown in presence of some Y_2O_3 oxide additions. The nature of this "no-scale" geometry in such a compound is found to result from the competition between different grains surprisingly growing from one single "nucleation center" in the melt. The grain boundary fractality was investigated for several samples. The fractal dimension D_f of the boundaries is found to be close to $4/3$ and this result is reproducible. Fractal scaling is valid from $5\mu m$ to $500\mu m$, i.e. roughly ranging from the 211 particle size to the grain size. This value of D_f is predicted by a simple multicomponent Eden growth model. This work opens new ways of investigations for the synthesis and the patterning of superconducting and non-superconducting ceramics.

P1B.65

"TEM Study of Low-Angle Grain Boundaries in Polycrystalline YBCO," **Maria Mironova**, Guoping Du, Sathyamurthy Srivatsen, Irene Rusakova and Kamel Salama, Texas Center for Superconductivity, University of Houston, 4800 Calhoun Rd., Houston, TX 77204

Grain boundaries are extremely important for the ability of High Temperature Superconductors to carry high currents. In polycrystalline melt-textured YBCO, grain

boundaries are found to have current densities up to $30000 A/cm^2$ at 77 K in self field. In this paper, the results of TEM study of 25 low-angle grain boundaries in polycrystalline melt-textured YBCO are presented. The samples were fabricated by Liquid Phase Removal Method. The grain boundaries in these samples are observed to be clean, their chemical compositions are the same as that of the bulk and inner boundary structure consists of dislocation arrays. The grain boundaries lie on the *ab*-plane, and their density is estimated to be $\sim 10^8 cm^{-2}$. The total misorientation angles for these boundaries are within the range of $0.2-5^\circ$ and contain tilt and twist components with prevailing tilt component. The rotation axes are of [110] or $[\bar{1}10]$ type. Analysis of large areas containing low-angle grain boundaries revealed that they maintain the alignment of the bulk as a whole to within $\pm 6^\circ$. These results are found to be useful to explain the possibility for high-angle grain boundaries to carry large currents.

POSTER SESSION 2

P2.1

"Phase Relations in the Bi_2O_3 -CaO-CuO and Bi_2O_3 -CaO-SrO Systems at 750° to 1000° in Pure Oxygen at 1 atm," Chi-Fo Tsang, **James K. Meen** and Don Elthon, Texas Center for Superconductivity, University of Houston, Houston, TX 77204

Phase relations in Bi_2O_3 -CaO-CuO (BCC) and Bi_2O_3 -CaO-SrO (BCS) are outlined by a series of isothermal sections in 50° increments from 750° to $1000^\circ C$. (All experiments conducted in a pure oxygen atmosphere with total pressure of 1 atm). At $750^\circ C$, these systems are both subsolidus; at $1000^\circ C$, liquids coexist with a limited number of binary oxides. Most of the complications in the super-solidus phase relations occur at temperatures in the studied range.

The lowest-temperature liquids are Bi-rich in each system. Those in BCC form at temperatures just above $750^\circ C$ and are in equilibrium with Bi_2CuO_4 and a Bi_2O_3 s.s. At higher temperatures, liquids coexist with Bi_2CuO_5 and CuO and with the several solid solutions between Bi_2O_3 and CaO. At $1000^\circ C$, the liquids coexist only with CaO, Ca_2CuO_3 , $Ca_3Cu_7O_{10}$ and CuO.

The melting relations in BCS are complicated by the extensive solid solutions between Ca and Sr compounds. The lowest-temperature liquids form from the Bi_2O_3 s.s. and liquids at temperatures up to $900^\circ C$ are essentially confined to the Bi_2O_3 -CaO join. At $1000^\circ C$, liquids coexist only with CaO-SrO solid solutions and with two Sr-rich Bi-Sr binary oxides.

P2.2

"Subsolidus Pressure-Temperature Phase Relations in CaO-CuO to 30 kbar," Jürgen Sander, Arne Schmitz, **James K. Meen** and Don Elthon, Texas Center for Superconductivity, University of Houston, Houston, TX 77204

At 1 atm, two binary phases exist on the solidus in the system CaO-CuO; $Ca_3Cu_7O_{10}$ and Ca_2CuO_3 . Ca_2CuO_3 and CuO react at $977^\circ C$ to form $Ca_3Cu_7O_{10}$. We have conducted a series of experiments from 8 to 30 kbar in the system CaO-CuO for the temperature range 950° to $1200^\circ C$. $Ca_3Cu_7O_{10}$ is, however, not stable under any conditions investigated. At lower temperatures, Ca_2CuO_3 is stable (as at 1 atm) but CuO and Ca_2CuO_3 react at $\sim 1050^\circ C$ at 10 kbar and $\sim 1160^\circ C$ at 30 kbar to form

CaCuO_2 . Presumably, an invariant point at which the compounds $\text{Ca}_3\text{Cu}_7\text{O}_{10}$, Ca_2CuO_3 , and CaCuO_2 coexist occurs at a pressure below 8 kbar and at a temperature of 1000-1040°C.

Phase relations were determined using electron-probe microanalysis and the structure of the phase CaCuO_2 is not currently known. Structural studies of monophasic experimental run products are aimed at determining the structure of this phase.

The eutectic at which $\text{Ca}_3\text{Cu}_7\text{O}_{10}$ and CuO melt at 1 atm (pure oxygen) at 1045°C. Melting experiments at higher pressures are greatly hindered by the reaction of the liquid with the Pt capsules used to contain the reactants.

P2.3

"Liquidus Phase Relations in the Bismuth-Rich Portion of the Bi_2O_3 -SrO-CaO-CuO System at 1 Atm in Pure Oxygen," **Marie-Laure Carvalho, Karine L. Senes, James K. Meen and Donald Elthon**, Department of Chemistry and Texas Center for Superconductivity at the University of Houston, Houston, TX 77204

Liquidus phase relations in Bi_2O_3 -SrO-CaO-CuO and its subsystems are being investigated by synthesis-type experiments. Liquid and solid compositions are determined after quenching in liquid nitrogen by use of electron-probe microanalysis that gives precise analyses of micron-scale parts of the sample.

The binary eutectic where Bi_2O_3 and Bi_2CuO_4 coexist with a liquid is at 784°C. Addition of alkaline earth oxides (AEO) to the system results in a slight freezing point depression. The marked solubility of AEO's in Bi_2O_3 coexisting with liquids has two results:

1- The primary phase field of Bi_2O_3 (ss) greatly expands with respect to that of Bi_2CuO_4 compared with its size in Bi_2O_3 -CuO so that univariant lines representing the composition of a liquid in equilibrium with Bi_2O_3 and Bi_2CuO_4 are at an acute angle to the join Bi_2O_3 -CuO.

2- The lowest temperature liquids in Bi_2O_3 -AEO-CuO systems exist at minima rather than at eutectics. The minimum in Bi_2O_3 -CaO-CuO occurs between 750 and 760°C indicating a freezing-point depression of only about 30°C relative to the Bi_2O_3 -CuO binary.

P2.4

"Phase Equilibria in the La_2O_3 -SrO-CuO System at 950°C and 10-30 kbar," **Joel Geny, James K. Meen, and Don Elthon**, Department of Chemistry and the Texas Center for Superconductivity, University of Houston, Houston, TX 77204

Phase equilibria in La_2O_3 -SrO-CuO were determined at 950°C and 10-30 kbar. Electron-microprobe analyses were used to determine the phase compositions. Powder X-ray diffraction studies were used to determine the crystal structures. At this temperature, the stable phases at the apices of the ternary phase diagram are CuO, La_2O_3 , and SrO over a pressure range of 1 atm to 30 kbar. Stable binary phases in CuO-SrO are Sr_2CuO_3 , SrCuO_2 , and $\text{Sr}_{14}\text{Cu}_{24}\text{O}_{41}$. The only binary phase in $\text{LaO}_{1.5}$ -CuO from 1 atm to 10 kbar is La_2CuO_4 ; it is joined by $\text{La}_2\text{Cu}_2\text{O}_5$ at 30 kbar. No binary compounds exist on the La_2O_3 -SrO join. The $\text{La}_{2-x}\text{Sr}_x\text{CuO}_{4-\delta}$ solid solution has an essentially constant compositional range ($0.0 \leq x \leq \sim 1.3$) over this pressure interval. The extent of the $\text{La}_{2-x}\text{Sr}_{1+x}\text{Cu}_2\text{O}_{6+\delta}$ solid solution ($0.0 \leq x \leq 0.2$) and of the $\text{La}_x\text{Sr}_{14-x}\text{Cu}_{24}\text{O}_{41}$ solid solution ($0 \leq x \leq 6$) also appears to be essentially independent

of pressure. From 1 atm to 10 kbar, the $\text{La}_{8-x}\text{Sr}_x\text{Cu}_8\text{O}_{20-\delta}$ solid solution is stable for $1.3 \leq x \leq 2.7$, but it is stable for a much wider range ($0 \leq x \leq 4.3$) at 30 kbar. A phase with the composition $\text{La}_{1-x}\text{Sr}_{2+x}\text{Cu}_2\text{O}_{5.5+\delta}$ is stable for $0.04 \leq x \leq 0.16$ at 1 atm to 10 kbar but this phase is not stable at 30 kbar.

P2.5

"Y123 Superconductor via in-situ Reaction/Deoxidation of a Submicrometer Precursor Containing $\text{BaCuO}_{2.5}$," **Shome Sinha**, CME Department, University of Illinois at Chicago, 842 W. Taylor, Chicago, IL 60607

Orthorhombic Y123 is synthesized without the oxygenation of tetragonal Y123 by in-situ reaction of a submicrometer precursor, NEPTH that contained Y_2O_3 , CuO, and $\text{BaCuO}_{2.5}$ phases (and AG) and had an oxygen content of 7.4-7.6 ($Y=1$) compared to theoretical value of 7.5. Absence of intermediate tetragonal Y123 was confirmed by (1) DTA/TGA analyses, (2) weight loss of sample during the formation of Y123 and (3) qualitative analyses of the intermediate phases while chemical reactions occurred, and provided the technological advantages: almost no dependence of (i) oxygen partial pressure and (ii) sample geometry, and (iii) ability to form melted Y123 within solid silver. Compared to conventional approaches, rate of formation of Y123 was 2-3 orders of magnitudes faster and it took only 15 minutes to form 0.55 mm thick and melted Y123 superconductors at 950-55°C and 0.55 Kpa oxygen partial pressure. Melted Y123 superconductor was contained in solid silver casing while it formed during which it was in equilibrium with $\text{BaCuO}_{2.5}$. Despite no attempts for texturing, the samples exhibited 001 texturing and attained a J_c (transport) of 40-45 A/mm² and J_c (magnetization) of > 100 KA/mm² at 77K.

P2.6

"Stability Study of $\text{Hg}_{1-x}\text{Ba}_2\text{Ca}_{n-1}\text{Cu}_n\text{O}_{2n+2+\delta}$ With $n \leq 6$," **Q. M. Lin, Y. Y. Sun, Y. Y. Xue and C. W. Chu**, Department of Physics and Texas Center for Superconductivity at the University of Houston, Houston, TX 77204-5932

It has been shown that the phase stability of $\text{Hg}_{1-x}\text{Ba}_2\text{Ca}_{n-1}\text{Cu}_n\text{O}_{2n+2+\delta}$ decreases, and thus the difficulty of the compound formation increases, with the number of CuO_2 -layers per unit cell (n). We have therefore investigated the formation of $\text{Hg}_{1-x}\text{Ba}_2\text{Ca}_{n-1}\text{Cu}_n\text{O}_{2n+2+\delta}$ with different Hg-deficiency (x) under pressure. We have found that as n increases, the compounds form more easily with increasing x and increasing synthesis temperature (T_s), leading to an increase in carbon-contamination derived from the graphite-furnace. For instance, pure samples have been made for $n = 3, 4$, and 5, respectively, for $x = 0.25, \sim 0.25$, and 0.35. The observations suggest that the incorporation of carbon into the Hg-site helps stabilize the structure. A systematic annealing study shows the same maximum T_c for the $n = 3$ samples with different carbon-contents, in contrast with previous reports.

This work is supported in part by NSF, EPRI, the State of Texas through the Texas Center for Superconductivity at the University of Houston, and the T. L. L. Temple Foundation. This material was also prepared with the support of the U. S. Department of Energy, Grant No. DE-FG-48-95R810542. However, any opinions, findings, conclusions, or recommendations expressed herein are those of the authors and do not necessarily reflect the views of DoE.

P2.7 - P2.11

P2.7

"Synthesis of Hg-1212 Using the Precursor Prepared by Sol-Gel Technique,"
Arumugam Thamizhavel, Ramasamy Jayavel and C. Subramanian, Crystal Growth Centre, Anna University, Madras 600 025, India

The recent discovery of superconductivity in the homologous series of the Hg-based superconductors has attracted considerable interest not only because of their high transition temperature but also due to their structural simplicity. Here we report on the synthesis of the Hg-1212 by the two step process, with the precursor prepared by sol-gel technique. A homogenous gel was prepared by complexing the aqueous solution of the respective metal nitrates with ammonia and properly adjusting the pH. The gel was initially dried at 100° and finally decomposed at 850°C in oxygen atmosphere. The resulting black mixture of the nominal composition $Ba_2CaCu_2O_{5+\delta}$ was mixed immediately with HgO and pressed into pellets. This pellet together with a precursor pellet were sealed in a quartz tube and the final reaction was carried out at 810°C for 10 hours. The powder XRD revealed that the sample is phase pure. Final annealing in oxygen atmosphere exhibited the superconducting property.

P2.8

"Effects of Heating Process on the Superconducting Property and Microstructure of BPSCCO Materials*," **Yi-Da Chiu**, Chin-Hai Kao and Maw-Kuen Wu, National Tsing Hua University, Materials Science Center, Hsin-Chu, 30043, Taiwan

The effects of heating process on the superconducting properties of $Bi_{1.7}Pb_{0.3}Sr_{1.6}Ca_{2.4}Cu_{3.6}O_y$ bulk materials were studied. Results indicated that the decomposition of the high- T_c phase was observed when samples were sintered at 840-859 °C. The low- T_c phase and non-superconducting phases such as 2201, CuO, CaO, Ca_2PbO_4 , and $(Sr,Ca)_2CuO_3$ were found to be in these samples. However, the high- T_c phase could be recovered by two-step sintering process. It was also observed that the irreversible lines for the two-step sintering samples are positioned at higher temperature than that for the normal processed samples, and indicating that the improvement of flux pinning in the two-step sintering processed samples is higher than the normally sintered samples. This could explain why the critical current density of the BPSCCO pellets was strongly improved by this two-step heating process.

*Supported by the National Science Council of ROC under grant no. NSC84-2212-M-007-005PH.

P2.9

"Control of 211 Particle Dispersion And J_c Property In Melt-Textured YBCO Superconductor," **Yuh Shiohara** and Akihiko Endo, Superconductivity Research Laboratory, ISTEK, Div. 4, 1-10-13, Shinonome, Koto-ku, Tokyo, 135, Japan

Macrosegregation in dispersion of Y_2BaCuO_5 (211) particles in Pt-added $YBa_2Cu_3O_{7-\delta}$ (123) crystals were grown by isothermal solidification method and continual cooling method. It was found that entrapped 211 distribution in 123 crystals depended on the growth direction and the growth rate (R) as a function of undercooling (ΔT). The amount of 211 particles in the 123 crystal grown at small ΔT (i.e. small R) were smaller than those at large ΔT (i.e. large R), especially in c-direction growth. The smaller 211 particles in size were entrapped in the 123 grown

at large R. Further, it was noted that the 211 distribution in the 123 samples grown by continual cooling changed continuously with growing time. These phenomena could be qualitatively explained by the prevalent inclusion trapping theory. From SQUID measurements, the J_c values were shown to vary with the 211 distribution even though the nominal composition was constant. These results indicated that the J_c properties of the 123 crystals were affected by the trapping phenomena of 211 particles as well as the amount of 211 addition in the nominal composition.

This work was supported by NEDO.

P2.10

"Partial-Melt Processing of Bulk MgO-Whisker Reinforced $(Bi,Pb)_2Sr_2Ca_2Cu_3O_{10-x}$ Superconductor," J. S. Schön* and **S. S. Wang**, Department of Mechanical Engineering and Texas Center for Superconductivity, University of Houston, Houston, TX 77204-5932, *Currently with Swedish Institute of Aeronautics, Stockholm, Sweden

Like most oxide-based ceramics, monolithic high-temperature superconductors (HTS) are recognized to have weak mechanical properties. In order to sustain thermomechanical stresses and associated deformations resulting from coupling/interactions among thermal, electrical, and magnetic fields, the HTS materials need to be strengthened and toughened, capable of sustaining long-term thermomechanical loading, while retaining satisfactory superconducting properties. In our laboratory, a comprehensive study of processing the BPSCCO HTS material with high-strength/high-modulus MgO whiskers has been conducted. The $(MgO)_w$ /BPSCCO composites have been shown to possess a promising combination of superconducting and mechanical properties suitable for bulk HTS applications. In this paper, a partial-melt processing method has been studied to improve further the performance of the $(MgO)_w$ /BPSCCO composite. This method consists of repeated hot pressing/annealing and short-period partial melting to achieve the desired grain texturing and additional pinning centers. Fabrication studies of both monolithic BPSCCO and $(MgO)_w$ /BPSCCO composites have been made to investigate the effects of various processing variables. Relationships among the bulk processing parameters, associated microstructures and grain texturing are summarized. Also, improved composite properties and mechanisms of the $(MgO)_w$ /BPSCCO by the partial melt processing are discussed.

P2.11

"Strain Tolerance of Superconducting Properties of Bulk MgO-Whisker-Reinforced HTS BPSCCO Composite," **G. Z. Zhang**, M. S. Wong and S. S. Wang, Department of Mechanical Engineering and Texas Center for Superconductivity, University of Houston, Houston, TX 77204

High-temperature superconductors (HTS) have been demonstrated to possess excellent superconducting properties at cryogenic temperatures. Like many other oxide-based ceramics, monolithic HTS materials are also recognized to have inherently weak mechanical properties. The weak mechanical properties cause severe technical barriers for potential applications of the bulk HTS materials. Among various concerns is the critical issue of limited strain tolerance of their superconducting properties. The HTS deformability during processing and in service may have a significant impact on their current-carrying capability. The HTS materials need to

be physically strengthened so that they will be capable of sustaining deformations during thermomechanical loading and meanwhile retaining desirable superconducting properties. In this study, a monolithic HTS BPSCCO material is reinforced by MgO whiskers to improve its thermomechanical properties. The detailed mechanical behavior of the $(\text{MgO})_w/\text{BPSCCO}$ composite at 77K is studied for the first time. The strain tolerance of the critical current density of the MgO-whisker reinforced BPSCCO is found to be improved significantly. The unique cryogenic electromechanical experiment as well as the detailed electromechanical properties of the $(\text{MgO})_w/\text{BPSCCO}$ composite at cryogenic temperatures are reported.

P2.12

"Electro-Mechanical Properties of Jointed BPSCCO Composites," C. Vipulanandan^{1,2} and G. Yang², ¹Department of Civil Engineering and ²Materials Engineering Laboratory, Texas Center for Superconductivity, University of Houston, Houston, TX 77204-4791

For BPSCCO tapes and bulk materials to be used in magnets and other applications, it is important to produce high current materials with long lengths. Joining is one method of producing such high current carrying long elements. Also, these jointed materials must have good mechanical properties. Several methods are being investigated to improve the joining of BPSCCO bulk composites without significant losses at the joints. Some of the joining methods currently being investigated are uniaxial and isostatic pressing coupled with hot-pressing.

In this study, methods to improve the mechanical properties and joining BPSCCO composites to produce long lengths of good quality materials were investigated. Both metal and polymers were used to improve the mechanical properties of the bulk material. Two methods of joining bulk BPSCCO material were investigated in this study. Electro-mechanical properties of the BPSCCO joints have been characterized at 77 K while the critical current was measured in situ. Also, metal powder and metal fibers were used for reinforcing the joints. XRD and transition temperature tests were performed on the jointed section to evaluate the purity of the 2223 phase. Unlike lap joint the butt-joint showed well textured grain structure at the joint. Stress-strain-critical current relationships have been developed for the joints in the composite bulk materials. The current capacity at the joints varied from 50 to 85% of the bulk material (depending on the processing parameters).

P2.13

"Magnetic Levitation Transportation System by Top-Seeded Melt-Textured YBCO Superconductor," In-Gann Chen, Jen-Chou Hsu and Gwo Jamn, Department of Materials Science and Engineering, National Cheng Kung University, 1-Ta-Hsueh Rd., Tainan, Taiwan, R.O.C.

High Temperature Superconductor (HTS) material exhibits attractive potential application with its magnetic levitation and suspension properties, i.e. Meissner effect. Recently, with the advance of materials processing techniques, such as Top-Seeding and Melt-Texturing (TSMT) methods, very large single grain Y-Ba-Cu-O (YBCO) samples up to several centimeters in diameter can be produced. Each sample is capable of levitating several kilogram of weight. A TSMT-YBCO magnetic levitation (MagLev) transportation system has been constructed to validate the concept of HTS-MagLev system based on Meissner effect. This HTS-MagLev is a stable levitation system, unlike

traditional MagLev systems which require sensors and feed-back circuits to dynamically adjust their unstable levitation position. In this report, the preliminary results with various magnetic levitation parameters, such as different permanent magnet configurations, relative levitation stability, levitation force, as well as their correlation with TSMT-YBCO sample's superconducting properties, magnetic field intensity and distribution, etc. will be discussed.

This work was supported by the National Science Council, Taiwan, R.O.C., under contract No. NSC84-2112-M006-020.

P2.14

"High- T_c Ceramic Superconductors for Rotating Electrical Machines: From Fabrication to Application," Athanasios G. Mamalis¹, Ildiko Kotsis², Istvan Vajda³, Andras Szalay⁴ and George Pantazopoulos¹, ¹Department of Mechanical Engineering, National Technical University of Athens, 42, 28th October Ave., 10682 Athens, Greece, ²Department of Silicate Chemistry and Technology, Veszprem University, Veszprem, Hungary, ³Department of Electrical Machines and Drives, Technical University of Budapest, Budapest, Hungary, ⁴Metalltech Ltd., Budapest, Hungary

Explosive compaction and subsequent multiple-pass warm extrusion were employed to fabricate silver/Y(Ba,K)₂Cu₃O₇ composite rods. The soundness of the product at the various stages of the fabrication, i.e. the macro- and microscopical defects, microstructural and stoichiometric changes, as well as the induced superconducting properties are discussed. In relation to the warm-extrusion as a post-compaction forming technique, most of the characteristic defects of the extruded component, such as intense radial/longitudinal cracking and shear fracturing were reduced, as compared to the cold-extrusion defects reported in a previous work, mainly due to the improvement of the plastic flow and the formability of the material at higher temperatures.

These high- T_c superconducting components were used in the construction of a HTSC synchronous generator model, designed by the authors; the generator is excited with SmCo₅ rare-earth permanent magnets placed in the rotor to obtain high enough magnetic fields, whilst rod-shaped HTSC materials were placed in the stator.

The magnetic field and forces between the HTSC and the permanent magnet were calculated employing a finite-difference method developed by the authors. This superconductor model involves also the hysteresis of the material, accounting for its magnetic history.

POSTER SESSION 3

P3.1

"Molecular Level Control of the Interfacial Properties of High- T_c Superconductor Structures and Devices," John T. McDevitt, Rung-Kuang Lo, Jianai Zhao and Jason Ritchie, Department of Chemistry and Biochemistry, The University of Texas at Austin, Austin, TX 78712, and Chad A. Mirkin and Kaimen Chen, Department of Chemistry, Northwestern University, 2145 Sheridan Rd., Evanston, IL 60208

Following a survey of the surface coordination chemistry of high- T_c phases such as YBa₂Cu₃O_{7- δ} and Tl₂Ba₂Ca₂Cu₃O₁₀, it has been established that molecules

P3.2 - P3.6

containing alkylamine and arylamine functionalities bind tenaciously to the cuprate superconductor interfaces. Cyclic voltammetry, atomic force microscopy, contact angle and x-ray photoelectron spectroscopy measurements provide strong evidence for the spontaneous adsorption of the amine molecules onto the superconductor structures. This paper will focus on studies on the monolayer derivatization of bulk ceramic and thin film samples of $\text{YBa}_2\text{Cu}_3\text{O}_{7-\delta}$ using amine-tagged hydrocarbon and fluorocarbon molecules that are capable of self-assembly onto the cuprate materials. The formation and performance properties of corrosion protection barriers and polymer adhesive layers formed from these self-assembled monolayers will be described. The newly described methods provide for the first time a precise procedure through which interfacial properties of superconductors can be controlled in a simple manner. Through appropriate choice of adsorbate molecule, superconductor surfaces can now be tailored from the molecular level so as to suit a variety of applications. These new methods may have important implications for the processing of high- T_c films structures.

P3.2

"Crystal Engineering of Chemically Stabilized, Cation Substituted $\text{YBa}_2\text{Cu}_3\text{O}_{7-\delta}$ Thin Film Structures," **John T. McDevitt** and Ji-Ping Zhou, Department of Chemistry and Biochemistry, The University of Texas at Austin, Austin, Texas 78712

In order to produce stable forms of $\text{YBa}_2\text{Cu}_3\text{O}_{7-\delta}$ superconductors, a series of cation substitution reactions have been completed. Here it is found that the corrosion resistance increases with increasing substitution level in systems of $\text{Y}_{1-y}\text{Ca}_y\text{Ba}_{2-y}\text{La}_y\text{Cu}_3\text{O}_{7-\delta}$. Interestingly, the composition of $\text{Y}_{0.6}\text{Ca}_{0.4}\text{Ba}_{1.6}\text{La}_{0.4}\text{Cu}_3\text{O}_{6.96}$ ($T_c = 80$ K) is found to be at least 100 times more stable than the parent compound, $\text{YBa}_2\text{Cu}_3\text{O}_{6.94}$. Similar stable cuprate systems with transition temperatures above 85K have been prepared suggesting that the surface reactivity, processability and superconducting properties can be tailored with the use of the appropriate cation composition. Using these compounds and the pulsed laser ablation method, the preparation of the chemically robust superconductor films has been accomplished. Detailed studies of the corrosion mechanism for these samples suggest that changes in the lattice stress and strain features as well as minor changes in the oxygen ordering properties are responsible for the enhanced stability. Importantly, oxygen mobility within the modified structures is suppressed also making these systems quite attractive from a processing perspective. The crystal engineering methods developed here may help to facilitate the development of more reliable processing methods and foster better performance characteristics for high- T_c thin film devices.

P3.3

"Electrochemical Molten Salt Deposition of 77K Superconducting $\text{EuBa}_2\text{Cu}_3\text{O}_{7-x}$," **Horng-Yi Tang**, Chuen-Shen Lee and Jeng-Lin Yang, National Tsing Hua University, Materials Science Center, Hsinchu, Taiwan

Many different techniques such as doctor blade, spray pyrolysis or electrophoresis are used for thick film preparation. However, these techniques require high temperature treatment to enhance grain-grain and grain-substrate bonding strength. Here we report a low temperature, isothermal electrochemical technique for the rapid deposition of $\text{EuBa}_2\text{Cu}_3\text{O}_{7-x}$ superconductor. Orthorhombic $\text{EuBa}_2\text{Cu}_3\text{O}_{7-x}$ crystallite thick film can be deposited at electrode surface by electrochemical deposition from a

molten hydroxide solution. After 2 hours of reaction, the average crystal size is approximately 100 microns. The SQUID measurement of harvested crystals shows the 77K T_c onset with wide range transition width. X-ray diffraction studies indicate that the sample contains $\text{EuBa}_2\text{Cu}_3\text{O}_{7-y}$ phase. This technique performed under 450° C, so far, achieves a lowest temperature that can directly deposit superconducting oxide thick layers with transition temperature onset within liquid nitrogen regime.

P3.4

"An Improved Procedure for Fabricating YBCO Step-Edge Junctions on MgO Substrates," **Hsiao-Mei Cho**, Hong-Chang Yang and Heng-Er Horng, Department of Physics, National Taiwan University, 1, Sec. 4, Roosevelt Rd., Taipei, Taiwan, 10764, R.O.C.

An improved procedure for fabricating YBCO step-edge junctions on MgO substrates is described. It is based on the sharpness of step-edge by using metal mask instead of photoresist. The characterization of step-edge junctions, fabricated by two different process, is compared and reported. We found that the metal masks can improve the sharpness of step-edge of MgO as well as the qualities of junctions.

P3.5

"Directly Coupled DC-SQUIDS of YBCO Step-Edge Junctions Fabricated by a Chemical Etching Process in Mixed Acids," **Junho Gohng**¹, Christelle Dosquet² and Jo-Won Lee¹, ¹New Materials Laboratory, Samsung Advanced Institute of Technology, P. O. Box 111, Suwon, 440-600, South Korea, ²Department of Polymer Chemistry, Ecole Nationale Supérieure de C.P. Bordeaux, Avenue Pey Berland, B. P. 108, Talence Cedex, 33402, France

High T_c directly coupled DC-SQUIDS have been successfully fabricated on chemically etched MgO substrate steps. The chemical etching was performed in a mixed acid solution in H_3PO_4 and H_2SO_4 for the best control of etched surface and roughness. YBCO thin films were deposited epitaxially on the step-edged MgO substrate by a KrF laser ablation method. Characteristics of the directly coupled DC-SQUID have been studied following the patterning and fabrication of the device.

The chemically etched steps show sharper edges at the top as well as at the bottom of the step unlike those from ion milling. The result is a good quality junction even at a relatively low step angle. AFM and Raman spectroscopy studies on the YBCO thin film deposited and patterned on the chemically etched arcs show no sign of appreciable degradation. Directly coupled DC-SQUIDS that are fabricated with this process show typical sweeping voltages of 160 μV at 4.2 K, and 6 μV at 77 K respectively.

P3.6

"Growth of Epitaxial LaAlO_3 and CeO_2 Films Using Sol-Gel Precursors," **Shara S. Shoup**, Mariappan Parantharam, David B. Beach and Eliot D. Specht, Chemical and Analytical Sciences, Oak Ridge National Laboratory, Box 2008, MS-6110, Oak Ridge, TN 37831-6110

Sol-gel techniques have emerged as viable non-vacuum methods for the fabrication of long-length conductors. Buffer layers such as LaAlO_3 and CeO_2 are of interest because critical current densities exceeding 10^6 A/cm² have been repeatedly

observed from superconductors grown on these layers. Also, the lattice mismatch between LaAlO_3 or CeO_2 and Y-123 or Tl-1223 are quite small.

We present here in detail the successful growth of LaAlO_3 and CeO_2 films using sol-gel precursors. LaAlO_3 precursor solution has been prepared from a metal alkoxide route and spin-coated on a SrTiO_3 (100) single crystal to yield an epitaxial film following pyrolysis at 800°C in a rapid thermal annealer. A CeO_2 precursor solution has been made using an aqueous route, and an alkoxide route is being studied. Attempts will be made to grow superconductors on these epitaxial buffer layers.

Research sponsored by the U. S. Department of Energy, Division of Materials Sciences, Office of Basic Energy Sciences and Office of Energy Efficiency and Renewable Energy, Office of Utility Technology-Superconductivity program, managed by Lockheed Martin Energy Research Corporation under contract # DE-AC05-96OR22464. Supported in part by an appointment to the ORNL Postdoctoral Research Associates Program administered jointly by ORNL and by Oak Ridge Institute for Science and Education.

P3.7

"Study of the In-Plane Epitaxy of Bi-Epitaxial Superconducting Grain Boundary Junctions," Maw-Kuen Wu¹, Mei-Yen Li¹, Hui-Ling Kao² and Cheng-Chung Chi¹, ¹National Tsing Hua University, Materials Science Center, Hsin-Chu, 30043, Taiwan, R.O.C., ²Chang-Gung College of Medicine and Technology, Department of Electrical Engineering, Taoyuan, Taiwan, R.O.C.

We have previously obtain 45° grain boundary between $\text{YBCO}/\text{CeO}_2/\text{MgO}$ and YBCO/MgO . A small percentage of $\text{CeO}_2[110]/\text{MgO}[100]$ seems to be always present according to ϕ -scan X-ray diffraction. The inevitable presence of $\text{CeO}_2[110]/\text{MgO}[100]$ causes mixtures of in-plane rotation of 0° and 45° between $\text{YBCO}/\text{CeO}_2/\text{MgO}$ and YBCO/MgO . To overcome this problem, we have further developed a new structure, namely $\text{YBCO}/\text{CeO}_2/\text{YSZ}/\text{MgO}$ and YBCO/MgO boundary, so that 100% in-plane rotation of 45° can be routinely obtained. The atomic structure of the interface between the YSZ and MgO investigated by X-ray rod scan and high-resolution transmission electron microscopy (HRTEM). The results also gives us a hint to study the epitaxial growth of oxide thin films. A photolithographically defined grain-boundary junction showed weak link behavior with critical current density (J_c) of $3 \times 10^3 \text{ A/cm}^2$ at 77K, while J_c reaches 10^6 A/cm^2 in the YBCO films on both sides. The better epitaxy of our new structure can lead to a better control of grain boundary critical current density.

*Supported by the National Science Council of ROC under grant no. NSC84-2212-M-00005PH.

P3.8

"*in situ* Deposition of Thallium Cuprate and Other Thallium-Containing Oxides," Kirsten E. Myers¹, Dean W. Face² and Dennis J. Kountz², DuPont Superconductivity, Experimental Station E304/¹C110 and ²C131, Wilmington, DE 19880-0304

DuPont has developed processes for the *in situ* growth of thallium and thallium/lead cuprate superconductors. Our method comprises off-axis sputter deposition in the presence of thermally-generated thallos oxide vapor. This process is unique in

that the crystal structure of the desired thallium cuprate phases is formed during growth. As a result, the films are very smooth and well-oriented. Recent work has exploited these advantages to produce multilayer thallium cuprate composites. For example, we have made SNS trilayer structures with superconducting $(\text{Tl,Pb})\text{Sr}_2\text{Ca}_{0.8}\text{Y}_{0.2}\text{Cu}_2\text{O}_7$ and non-superconducting $(\text{Tl,Pb})\text{Sr}_2\text{CuO}_5$. Our current work is aimed at expanding the number and range of materials that can be made by, or are compatible with, the *in situ* thallium growth process. Most recently, we have deposited thallium tantalate, an insulator with the pyrochlore structure, epitaxially on YSZ. In this talk I will discuss the growth of $\text{Tl}_2\text{Ta}_2\text{O}_6$ thin films and multilayers with the cuprates.

P3.9

"Growth of Superconducting Epitaxial $\text{Tl}_2\text{Ba}_2\text{CuO}_{6+\delta}$ Thin Films with Tetragonal Lattice and Continuously Adjustable Critical Temperature," Zhifeng Ren, Chang An Wang and Jui H. Wang, Superconductive Materials Laboratory, SUNY/Bufalo, P. O. Box 835, NSM Complex, Buffalo, NY 14260-3000

High quality epitaxial $\text{Tl}_2\text{Ba}_2\text{CuO}_{6+\delta}$ thin films on single crystalline SrTiO_3 substrate have been synthesized for the first time by RF magnetron sputtering followed by a two-step post-deposition annealing process. The as-deposited films were amorphous. The epitaxial growth was obtained by post-deposition annealing at 810°C for 20 min. The post-annealed films were superconducting at T_c (zero resistance) of 11-12 K, presumably due to over-doped oxygen. Annealing at 450°C for 6.0 hours in flowing 1 atm Ar only raised T_c to 52 K. However, annealing at $350\text{--}400^\circ\text{C}$ for 2.0 h under reduced pressure of flowing Ar raised T_c to 83.5 K. The T_c increases with the increase of annealing time from 0 to 2.0 h, then decreases with further increase of annealing time. A T_c of 65 K was observed for the 6.0 h annealed sample. T_c of the same film can be increased or decreased continually and reversibly in the 11-83.5 K range by annealing in argon or air, with no change in tetragonal lattice symmetry. X-ray diffraction data show that the film is c-axis oriented (θ - 2θ scan) with full width at half maximum of rocking curve (FWHM) of 0.265° (ω -scan) and alignment in the ab-plane (ϕ -scan).

P3.10

"Transport Critical Currents of Bi-2212 Tapes Prepared by Sequential Electrolytic Deposition," Lelia Schmirgeld-Mignot, Fabrice Legendre and Pierre Régnier, C.E.A. Saclay, SRMP/DECM, F91191 Gif Sur Yvette Cedex, France, and Hugo Safar and Martin Maley, Los Alamos National Laboratory, Superconductive Technology Center, Mail Stop K763, Los Alamos, NM 87545

The transport critical currents of Bi-2212 tapes prepared by oxidation of metallic precursors have been measured as a function of temperature, between 4 and 77K, and as a function of magnetic field, for fields up to 9T applied perpendicular and parallel to the ab planes. The tapes have been prepared by a technique, developed with the aim of manufacturing long lengths, and is based on the sequential electrolytic deposition of Bi, Cu, Sr, and Ca onto polycrystalline silver ribbons followed by thermal treatments. Optimisation of the deposition sequence and of the thermal treatments have lead to highly textured specimens having transport J_c values of $35\,000 \text{ A/cm}^2$ at 77K, and of $2.6 \times 10^5 \text{ A/cm}^2$ at 4 K, both under self field, after only 4 hours total processing time (starting from salts of the metallic constituents and not from already

P3.11 - P3.14

synthesised superconductor powders). Values of the order of 4×10^4 A/cm² remain under magnetic fields of the order of 10T at 4 K.

P3.11

"Role of Constituents on the Behavior of Composite BPSCCO Tapes," **S. Salib**², M. Mironova² and C. Vipulanandan^{1,2}, ¹Department of Civil Engineering and ²Materials Engineering Laboratory, Texas Center for Superconductivity, University of Houston, Houston, TX 77204-4791

In order for BPSCCO tapes to be used in commercial applications, their irreversible strain of approximately 0.2% must be further improved. Several methods are being investigated to improve the irreversible strain in tapes. Some of the methods include changing the sheath material or using multifilament tapes instead of monocoil tapes. In this study methods to improve the ceramic core and the failure mechanism for the tapes were investigated.

BPSCCO tapes with silver sheath were reinforced with metal powder, flakes and fibers to improve the irreversible strain of the tapes. Due to processing conditions and mismatch in the coefficient of thermal expansion of the BPSCCO core and the metal reinforcements, residual stresses developed in the core. XRD was used to evaluate the residual stresses in the metal sheath and ceramic core and to determine the residual compressive and tensile stress distribution in the tapes. Results from the TEM study are also discussed in terms of variation in dislocation densities within the tape. A constitutive model was developed to investigate the role of each of the components in the tape. The model predicted the experimental trends accurately. By core modification, tapes with irreversible strain over 0.4% in direct tension were produced.

Due to chemical/physical incompatibility between the core and the different reinforcements, some reaction products were produced around the reinforcements. These reaction products were identified using EPMA coupled with WDS and their distribution within the ceramic core was also determined.

P3.12

"Ion Channeling Studies in YBCO Thin Film at Low Temperature," **Xingtian Cui**, Zuhua Zhang, Quark Chen, Jiarui Liu and Wei-Kan Chu, Texas Center for Superconductivity, University of Houston, 3201 Cullen Blvd., Houston, TX 77204-5932

High quality epitaxially grown YBCO thin films have been used for ion channelling investigation in a wide range of temperatures below and above the superconducting transition temperature (T_c). Channeling width changes of Cu atoms, which reflect the amplitude of lattice vibration, were observed across T_c . The width transition, if it does exist, would suggest a phonon-mediated superconducting mechanism. Thin film YBCO superconductors have the advantages over their bulk counterparts for the larger sample area and flexibility in choosing crystal orientations. Particularly interesting is the anisotropic behaviors of the channeling width transitions along the c- and ab-directions.

P3.13

"Current Transport Across YBCO-Au Interfaces," **Regina Dömel Dittmann**, Matthias Grove and Michael Bode, Research Center Jülich (KFA), Institute of Thin Film and Ion Technology, D-52425 Jülich, Germany

We have developed a fabrication process which for the first time allowed us to independently measure current-voltage-characteristics of the two SN-interfaces in YBCO / Au / YBCO step-edge SNS-junctions.

For both currents smaller than a characteristic current, the I-V-characteristics of both interfaces showed an excess conductivity, due to contributions from Cooper pairs to the charge carrier transport.

From the good correlation of the experimental data with the theory of Zaitsev [1] can be concluded, that both proximity effect and Andreev reflections at the SN interfaces contributed to the current transport across interfaces and thus the SNS junction.

Furthermore, the two YBCO-Au interfaces had nearly the same transparency, even though transmission electron microscope micrographs suggested c-axis coupling at the bottom interface and (a-b)-axis coupling at the top interface.

This work was supported by the German BMBF contract 13N6411/9.
[1] A. I. Zaitsev, JETP Lett. 61, 771 (1995)

P3.14

"Surface Characterization of Superconductive Nd₁Ba₂Cu₃O_y Thin Films Using Scanning Probe Microscopes," **Wu Ting**, M. Badaya, R. Itti, T. Morishita, N. Koshizuka and S. Tanaka, Superconductivity Research Laboratory, International Superconductivity Technology Center (ISTEC), 1-10-13 Shinonome, Koto-ku, Tokyo 135, Japan

For device applications and surface sensitive scientific researches, a clean, stable, and well characterized surface of high temperature superconductors (HTSC) is often required. In the past few years, it has been realized that most of the HTSC are unstable in air. They react with the constituents of air, forming an insulating layer on the top. Recently, high quality superconductive Nd₁Ba₂Cu₃O_y (Nd123) thin films have been successfully fabricated at our institute employing the standard laser ablation method. In this paper, we report the results of surface characterization of the Nd123 thin films using an ultrahigh vacuum scanning tunneling microscope/spectroscopy (UHV-STM/STS) and an atomic force microscope (AFM) system operated in air. Following several physical properties of the thin films are investigated:

- 1) Surface morphology
- 2) Thin film growing mechanism
- 3) Surface atomic images and the atomic images of surface adsorbates
- 4) Surface electronic properties.

Our results indicate that the surfaces of the Nd123 thin films grown under optimal conditions are highly smooth and free from serious degradation when exposed to ambient air.

*: This work was supported by the New Energy and Industrial Technology Development Organization (NEDO) for R&D of Industrial Science and Technology Frontier Program.

P3.15

"Direct Measurement of the Magnus Force in YBCO Films," **X-M. Zhu**, Eric Bäckström and Bertil Sundqvist, Umeå University, Experimental Physics, Umeå, S-90187, Sweden

The debate over the Magnus force in type-II superconductors has been active for more than thirty years and regained momentum since the discovery of the Hall anomaly in both HTc and some of the conventional superconductors. While this topic has attracted so much attention theoretically, there was not a single experimental attempt to measure this force directly in the previous decades. We present here the first experiment to measure the Magnus force in type-II superconductors using YBCO films. The force measurement is done mechanically. We hope our effort will contribute towards a conclusion on the Magnus force in type-II superconductors and help to filter out the various theoretical models for the Hall anomaly.

P3.16

"Interface Roughness Effect on Differential Conductance of High- T_c Superconductor Junctions," **Jian-Xin Zhu** and Z. D. Wang, Department of Physics, University of Hong Kong, Pokfulam Road, Hong Kong, and D. Y. Xing, National Laboratory of Solid State Microstructures, Nanjing University, Nanjing 210093, People's Republic of China

Within the framework of Blonder-Tinkham-Klapwijk (BTK) model and taking into account the interface roughness, we calculate the differential conductance of normal metal-insulator- d -wave superconductor junctions. We find that the tunneling spectrum depends strongly on both the incident angle of electrons and the crystalline axis orientation of the superconductor, and exhibits the zero-bias anomaly under suitable arrangements. Interestingly, even in the absence of the insulating layer, the tunneling spectrum of normal metal- d -wave superconductor junctions differs significantly from that for normal metal- s -wave superconductor due to the interface roughness. Moreover, both the tunnel conductance peak at the energy gap and the zero-bias conductance peak are suppressed by the interface roughness. Our results can explain many experimental measurements on the tunneling spectra of high- T_c superconductors.

P3.17

"Modern Magneto-Optical Techniques for Superconductors," **V. I. Nikitenko**¹, V. K. Vlasko-Vlasov¹, G. W. Crabtree² and U. Welp², ¹Institute for Solid State Physics RASc, 142432 Chernogolovka, Russia, ²Argonne National Laboratory, 9700 South Cass Avenue, Argonne, IL 60439

Advantages and perspectives of magneto-optical observations using iron garnet films with in-plane anisotropy for studies and nondestructive quality control of superconducting materials and parts are presented.

Recent results of magneto-optical investigations of defects serving as pinning centers and as sources of weak links in single crystals, films and bulk samples of HTSC are reviewed.

The role of sample shape, grain boundaries and twins in YBCO crystals and melt processed ceramics is discussed. A difference between magnetization and transport current trajectories observed in YBCO bulk samples and BSCCO tapes is emphasized.

Also possibilities of application of the garnet indicators for estimation of the magnetic materials are shown.

The work was supported by the ISF (grants #RF100 and RF1300: VIN and VKVV) and by the US DOE, BES-Materials Science (contract #W-31-109-ENG-38: GWC and UW)

P3.18

"Magneto-Optical Study of Flux Penetration and Critical Current Densities in [001] Tilt $\text{YBa}_2\text{Cu}_3\text{O}_{7-\delta}$ Thin Film Bicrystals," **A. A. Polyanskii**^{1,2}, A. Gurevich¹, A. E. Pashitski¹, N. F. Heinig¹, R. D. Redwing¹, J. E. Nordman^{1,3} and D. C. Larbaestier^{1,4}, ¹Applied Superconductivity Center, University of Wisconsin, Madison, WI 53706, ²Institute of Solid State Physics, Russian Academy of Sciences, Chemogolovka, Moscow District, 142432, Russia, ³Department of Electrical and Computer Engineering and ⁴Department of Material Science and Engineering, University of Wisconsin, Madison, WI 53706

Magneto-optical (MO) imaging has been used to visualize and calculate magnetic flux and current distributions at temperatures T ranging from 7 K to 80 K in thin film [001] tilt $\text{YBa}_2\text{Cu}_3\text{O}_{7-\delta}$ bicrystals with misorientation angles $3^\circ \leq \theta \leq 10^\circ$. A characteristic cusp in the flux distribution $B_z(x,y)$ was observed for $5^\circ \leq \theta \leq 7^\circ$, which is shown to indicate that the critical current density J_b across the boundary is smaller than the intragrain J_c . We use the Bean model for thin-film superconductors to calculate the observed features of the $B_z(x,y)$ distribution and to separate both the intragrain J_c and intergrain $J_b(\theta)$ independently from the MO data. The study of angular and temperature dependences of $J_b(T,\theta)$ in bicrystals with different θ shows that $J_b(\theta)$ strongly decreases with θ above $\theta \approx 5^\circ$. The decrease of $J_b(T,\theta)$ with temperature becomes weaker as the misorientation angle θ is increased, so the substantial difference in J_b for 5° and 7° boundaries at low T turns out to be less pronounced at nitrogen temperatures. In addition, the ratio $J_b(\theta,T)/J_c(T)$ for low-angle grain boundaries is shown to exhibit an anomalous increase with T , thus indicating that the grain boundaries can provide additional flux pinning. This is plausibly associated with the grain boundary dislocations that accommodate the misorientation of the grains.

P3.19

"Monolithic Terminations for Multifilamentary BSCCO Wires," **Yuan Kai Tao**, Teco Electric & Machinery Co. Ltd, 11 An-Tung Road, Chung-Li City, Taiwan, ROC, and Chin-Hai Kao and Maw-Kuen Wu, National Tsing Hua University, Materials Science Center, Hsin-Chu, Taiwan, 30043, ROC

For applications of superconductors based on persistent current, it is necessary to have separate superconducting components linked together by superconducting joints. By using the powder in tube method, long length Ag-sheathed BSCCO wires that can carry a large critical current (I_c) have been prepared. A technique has also been developed which allows for single core Ag-sheathed BSCCO wires to be jointed with no degradation in current carrying capacity. The technique is not quite successful, however, in jointing multifilamentary BSCCO wires. The I_c across joint is only 50-70% of that measured on individual wires. This reflects the difficulty in forming joints between filaments in multifilamentary BSCCO wires. One possible solution to this problem is to prepare monolithic terminations at the ends of the multifilamentary

P3.20 - P3.23

wires. Our preliminary results show that the transition from multifilamentary section to monolithic termination is structurally smooth, and I_c in the transition zone is basically the same as in the wires.

P3.20

"A Preliminary Study of the Joining of BPSCCO Superconducting Tape," **Chin-Hai Kao**¹, Yuan Kai Tao² and Maw-Kuen Wu¹, ¹National Tsing Hua University, Materials Science Center, Hsin-Chu, Taiwan, 30043, ROC, ²Teco Electric & Machinery Co. Ltd, 11 An-Tung Road, Chung-Li City, Taiwan, ROC

In this work, we report the difference in critical current through and within the pressed regions of the BPSCCO/Ag superconducting tapes at the joint. The difference in thickness between the normal and pressed region of these tapes increases with increasing of the uniaxial pressing. It was found that critical current through the transition region decreases with increasing of the pressing. Besides, critical current within the pressing regions of tape is 15-17 A, that of regular tape is 17 A. Non-superconducting phase, $(\text{Sr}_{1-x}\text{Ca}_x)\text{O}$, was found to be between BPSCCO and silver in the pressed regions of tape. The correlations of superconducting properties with microstructures of these materials are discussed.

P3.21

"Mutual High-Frequency Interaction of High T_c Josephson Junctions," **Marian Darula**, Gerhard Kunkel and Stephan Beuven, Research Center (KFA), Institute of Thin Film and Ion Technology, D-52425 Jülich, Germany

We report about recent development in study of mutual high-frequency interaction between high T_c (HTS) Josephson junctions integrated in different types of arrays. In particular, three system are considered: two junctions arrays shunted by common load, series arrays biased in parallel and arrays which form multi-junction superconducting loops (MSL). The mutual interaction showing phase-locking has been observed up to THz frequency region and up to 50 K. In two-junction arrays besides classical behaviour known from low T_c Josephson junctions systems the enhancement of mutual interaction has been observed due to internal cavity resonances in junctions. Series arrays consisted of up to 10 junctions and biased in parallel have shown radiation output using both out-of-chip (in W band) and on-chip detection techniques. Voltage locking of all junctions in MSL with four and six step-edge and bicrystal junctions in loop has been observed up to 1 THz.

We have shown applicability of HTS Josephson junctions in active high-frequency devices applications e.g. as submillimeter-wave oscillators.

P3.22

"Magnetocardiography in an Unshielded Clinical Environment Using High- T_c SQUIDS," **Nilesh Tralshawala**¹, James R. Claycomb¹, John H. Miller, Jr.¹, Krzysztof Nesteruk², Ji-Hai Xu¹ and David R. Jackson³, ¹University of Houston, Texas Center for Superconductivity, 4800 Calhoun Road, Houston, Texas 77204-5932, ²Institute of Physics of Polish Academy of Sciences, Department of Magnetic Materials, Al. Lotnikow 32/46, 00 662 Warsaw, Poland, ³University of Houston, Department of Electrical and Computer Engineering, 4800 Calhoun Road, Houston, Texas 77204-4793

We report on experimental and theoretical aspects of our high- T_c SQUID magnetocardiography (MCG) system. We have fabricated and tested an MCG system that reduces ambient field noise using a combination of novel, localized high- T_c superconducting shields, active noise compensation and digital signal processing. A simple nonmetallic gantry was designed to obtain vibration isolation and to reduce the microphonics noise. A digital finite impulse response comb filter was implemented to remove powerline related noise. Adaptive noise cancellation techniques are being employed to further alleviate effects of vibrations, and to compensate for the imperfections in the mechanical and electronic alignment between the sensor and reference SQUIDS. Both planar and axial electronic gradiometers have been assembled and tested in an unshielded laboratory and clinical environment. Thus far we have reduced noise levels by several orders of magnitude, sufficient to observe the QRS complex. One of the prototypes has been used to obtain an adult human MCG signal in an unshielded clinical environment of a catheterization laboratory at Texas Children's Hospital.

P3.23

"High- T_c Superconducting *rf* Receiver Coils for Magnetic Resonance Imaging," **Jaroslaw Wosik**^{1,2}, Krzysztof Nesteruk⁴, Lei-Meng Xie¹, Piotr Gierlowski⁴, Cheng Jiao¹ and John H. Miller, Jr.^{1,3}, ¹Texas Center for Superconductivity, ²Department of Electrical and Computer Engineering and ³Department of Physics, University of Houston, 4800 Calhoun Road, Houston, TX 77204-5932, ⁴Institute of Physics of Polish Academy of Sciences, Al. Lotnikow 32/46, 00-662 Warsaw, Poland

We report on the results of our development of low-loss high-temperature superconducting (HTS) *rf* receiver surface probes for high-resolution magnetic resonance imaging (MRI). Our HTS surface probes are designed to replace implanted copper receiver coils currently being used in animal research on spinal cord injuries. We have calculated the signal-to-noise ratio as a function of coil-to-spine distance, coil size, and coil resistance. Our calculations predict that the HTS probe should yield an MR image, obtained noninvasively, with a resolution comparable to or better than that obtained with the implanted copper coil.

Each HTS probe was designed with a virtual ground plane, thus reducing coil-to-ground losses and making the resonant frequency less sensitive to the probe's proximity to the body. A resonant circuit for this probe is created by sandwiching a dielectric (sapphire) between the two faces of the planar coils in order to achieve capacitive coupling. Each coil was fabricated by depositing YBCO onto 2 x 2" LaAlO₃ substrates using our large-area pulsed laser deposition system. Two different probes were tested in a 2 Tesla (84.4 MHz) MRI scanner. Both the signal-to-noise ratio and the field-of-view were measured. The results are in agreement with our theoretical calculations. The images of a rat spine, obtained with copper and HTS receiver coils, will be compared and discussed.

P3.24

"Investigation of the Microwave Power Handling Capability of High- T_c Superconducting Thin Films," **Jaroslav Wosik**^{1,2}, Dawei Li^{1,2}, Lei-Meng Xie¹, Irene Ruskova¹, John H. Miller^{1,3} and Stuart A. Long², ¹Texas Center for Superconductivity, ²Department of Electrical and Computer Engineering and ³Department of Physics, University of Houston, Houston, TX 77204

We report on experimental and theoretical investigations of the microwave power-dependence of the surface impedance Z_s in YBCO thin films. The goal of these experiments was to optimize the choice of deposition conditions, thickness, and substrate, such that the HTS films can ultimately be utilized for reproducible fabrication of HTS microwave devices with high power handling capability and/or well-characterized nonlinear performance.

The measurements were carried out at 14 GHz using a TE₀₁₁ mode dielectric cavity. A microwave pulsed set-up with a 150 W Varian TWT amplifier was used, and both the Q and the frequency were determined by analyzing a decay signal from the cavity. Thin films were deposited onto LaAlO₃, NdGaO₃ and 24° bicrystal YSZ substrates by pulsed laser ablation. Three regions in the Z_s power-dependence were observed: low-field (weak link dominated region), intermediate (linear), and high-field (hysteretic losses). No significant differences in Z_s vs. temperature dependence were found for all samples at low *rf* power levels. However, at higher power levels, substantial discrepancies in $Z_s(T)$ were noted. A nonlinear RSJ model¹ combined with a vortex motion model were used to describe the dependence of Z_s on *rf* magnetic field.

[1] J. Wosik, L.-M Xie, M. F. Davis, N. Tralshawala, P. Gierlowski, J. H. Miller, Jr., In: J. D. Hodge, editor, *SPIE Proceedings Series*, Vol. 2559, *High- T_c Microwave Superconductors and Applications*, 10 July 1995, San Diego, CA, pp. 76-84.

PRESENTING AUTHOR INDEX

- Aeppli, G.** A.6(16)
Agafonov, A. B. PIB.5(45)
Aguiar, J. A. PIB.22(49),
 PIB.23(49), PIB.24(49)
Ando, Y. A.1(15)
Ao, P. P1A.26(44)
Ausloos, M. PIB.64(58)
Baggio-Saitovitch, E.
 PIB.31(51), PIB.32(51),
 PIB.33(51)
Bahcall, S. R. P1A.11(40)
Balachandran, U. E9(25)
Balakirev, F. F. PIB.12(47)
Balseiro, C. A. PIB.48(55)
Bill, A. P1A.10(40), P1A.9(40)
Birgeneau, R. J. I.10(31)
Blumberg, G. E. C.4(18)
Boebinger, G. S. PIB.4(45)
Bolza, A. F. B.2(16)
Bozovic, I. H.1(28)
Brown, B. PIB.46(54)
Budnick, J. I. K.9(36)
Bulut, N. P1A.3(39)
Campuzano, J. C. J.1(32)
Cao, Y. PIB.16(47)
Cardona, M. A.4(15)
Carvalho, M.-L. P.2.3(59)
Cava, R. J. D.7(21)
Chan, S.-W. PIB.25(49)
Chen, C. C. L.3(37)
Chen, F. J.9(33)
Chen, I. G. P.2.13(61)
Chikumoto, N. E.2(24)
Chiu, Y. D. P.2.8(60)
Cho, H.-M. P.3.4(62)
Choi, H.-Y. P1A.14(41)
Christen, D. K. K.8(35)
Chu, C. W. PL.1.2(11)
Chu, W. K. B.5(16)
Clarke, J. L.1(36)
Clayhold, J. A. I.6(31)
Clem, J. R. K.2(34)
Coffey, M. W. PIB.19(48)
Crabtree, G. W. PL.7.1(14)
Cui, X. T. P.3.12(64)
Cyrot, M. G.6(27)
Dagotto, E. R. E.8(23)
Darula, M. P.3.21(66)
de la Cruz, F. K.5(35)
Demircan, E. P1A.27(44)
Derro, D. J. PIB.1(44)
Ding, H. PIB.2(44)
Dittmann, R. D. P.3.13(64)
Dow, J. D. P1A.22(43)
Driscoll, D. B.3(16)
Du, Z. L. PIB.37(52)
Dynes, R. C. C.1(17)
Edwards, P. P. D.9(21)
Emery, V. J. E.5(22)
Eremenko, V. PIB.42(53),
 PIB.43(54)
Eremin, M. P1A.19(42)
Face, D. W. L.9(38)
Fan, J. D. E.11(23)
Ferraz, A. G.9(27)
Field, M. B. PIB.26(50)
Fischer, Ø. C.5(18)
Franz, M. C.10(19)
Freeman, A. J. G.4(26)
Frenkel, D. P1A.23(43)
Freyhardt, H. C. H.6(29)
Gammel, P. L. K.3(34)
Geny, J. P.2.4(59)
Gohng, J. H. P.3.5(62)
Goldman, A. M. C.6(19)
Goldschmidt, D. PIB.18(48)
Gooding, R. J. PIB.13(47)
Gor'kov, L. P. G.8(27)
Guan, W. Y. PIB.20(48)
Gubser, D. B.4(17)
Hardy, W. N. J.2(32)
Henning, P. F. PIB.8(46)
Hermann, A. M. D.4(20)
Hickey, B. PIB.53(56)
Hong, G.-W. PIB.63(58)
Hor, P.-H. D.6(21)
Houssa, M. PIB.9(46)
Hu, C.-R. P1A.28(44)
Huang, J.-C. PIB.59(57)
Huang, M.-H. PIB.58(57)
Huang, Y. PIB.57(56)
Hussey, N. E. PIB.11(46)
Ignatiev, A. H.2(28)
Ikuta, H. PIB.49(55)
Johnston, D. C. A.5(16)
Jorgensen, J. D. J.10(34)
Junod, A. R. J.4(32)
Kallio, A. P1A.17(41),
 P1A.18(42)
Kao, C.-H. P.3.20(66)
Kapitulnik, A. L.5(37)
Karpinski, J. PIB.54(56)
Kirtley, J. R. L.2(37)
Kitazawa, K. D.10(21)
Kohno, H. P1A.6(40)
Kresin, V. Z. G.5(27)
Kroeger, D. M. F.10(26)
Kruchinin, S. P. P1A.7(40),
 P1A.8(40)
Ku, H.-C. PIB.21(49)
Lane, N. Keynote(10)
Larbalestier, D. C. PL.5.1(13)
Laughlin, R. B. E.3(22)
Lee, S.-I. PIB.40(53)
Lee, T. K. P1A.1(39)
Leggett, A. J. PL.4.1(12)
Leung, E. M. W. B.6(17)
Leung, P. W. P1A.2(39)
Levin, K. C.9(19)
Li, K. PIB.28(50)
Li, M.-Y. P.3.7(63)
Li, T. W. PIB.50(55),
 PIB.51(55)
Likharev, K. K. H.3(28)
Lin, C.-L. PIB.27(50)
Lin, J. G. L.6(37)
Lin, J. T. PIB.3(45)
Lin, Q. M. P.2.6(59)
Ling, D.-C. PIB.38(53)
Lopez, D. PIB.47(54)
Loram, J. W. J.5(33)
Luther, A. H. E.9(23)
Maeno, Y. D.5(21)
Maki, K. G.2(26)
Maley, M. P. I.1(30)
Malozemoff, A. P. B.1(16)
Malozovsky, Y. M. P1A.20(42)
Mamalis, A. G. P.2.14(61)
Mannhart, J. C.8(19)
Maple, M. B. K.4(35)
Marezio, M. J.11(34)
Markert, J. T. PIB.34(52)
McDevitt, J. T. L.4(37),
 P.3.2(62)
Meen, J. K. P.2.1(58), P.2.2(58)
Meng, R. L. F.4(24)
Mertelj, T. PIB.41(53)
Miller, J. H., Jr. L.7(38)
Mironova, M. PIB.65(58)
Moler, K. A. J.3(32)
Mook, H. A. I.11(31)
Moss, S. K.10(36)
Müller, K. A. PL.1.1(11)
Myers, K. E. P.3.8(63)
Nagaosa, N. E.7(23)
Nikitenko, V. I. P.3.17(65)
Osofsky, M. S. A.2(15)
Park, Y. W. PIB.30(51)
Pashkevich, Y. G. PIB.35(52),
 PIB.36(52)
Peterson, D. E. F.3(24)
Pines, D. E.2(22)
Polyanskii, A. A. P.3.18(65)
Putikka, W. P1A.5(39)
Raveau, B. D.2(20)
Ravikumar, S. PIB.17(48)
Reiter, G. P1A.15(41)
Ren, Z. F. P.3.9(63)
Rice, T. M. E.4(22)
Ritchie, J. P.3.1(61)
Rodríguez, J. E. PIB.29(51)
Rosner, C. PL.4.2(13)
Rossel, C. L.8(38)
Rowell, J. M. PL.3.1(12)
Rusakova, I. PIB.62(57)
Salama, K. E.8(25)
Salib, S. P.3.11(64)
Sánchez, D. R. PIB.14(47),
 PIB.15(47)
Sato, K.-I. F.1(24)
Scalapino, D. J. E.1(22)
Schilling, A. L.10(38)
Schmirgeld-Mignot, L.
 P.3.10(63)
Schrieffer, J. R. PL.2.1(11)
Schwer, H. PIB.55(56)
Selvamanickam, V. E.7(25)
Senes, K. L. P.2.3(59)
Sharma, R. P. I.5(30)
Shaw, D. T. B.7(17)
Sheen, S.-R. PIB.39(53)
Shen, Z.-X. C.7(19)
Shimoyama, J.-I. D.8(21)
Shiohara, Y. F.5(24), P.2.9(60)
Shoup, S. S. P.3.6(62)
Si, Q. M. P1A.4(39)
Silva, E. PIB.45(54)
Simon, R. H.8(29)
Sinha, S. P.2.5(59)
Smalley, R. Banquet(10)
Sridhar, S. H.4(28)
Suenaga, M. I.4(30)
Sugahara, M. PIB.10(46)
Tahir-Kheli, J. P1A.13(41)
Takano, M. D.3(20)
Tallon, J. L. J.8(33)
Tanabe, K. C.3(18)
Tanaka, S. PL.2.2(11)
Tang, H.-Y. P.3.3(62)
Tao, Y. K. P.3.19(65)
Terasaki, I. J.6(33)
Thamizhavel, A. P.2.7(60)
Timusk, T. I.8(31)
Ting, C. S. G.3(26)
Ting, W. P.3.14(64)
Tralshawala, N. P.3.22(66)
Tsuei, C. C. C.2(18)
Uchida, S. A.3(15)
Uemura, Y. J. A.7(16)
Uher, C. J.7(33)
van der Marel, D. L.7(31)
van Otterlo, A. I.2(30)
Varma, C. M. G.1(26)
Vlasko-Vlasov, V. K.
 PIB.52(55)
Wang, M.-J. PIB.44(54)
Wang, S. S. P.2.10(60)
Wang, Z. D. I.3(30),
 P1A.25(43)
Weber, H. W. E.6(25)
Weger, M. E.10(23)
Weinstein, R. K.7(35)
Wells, B. O. PIB.60(57)
Weng, Z. Y. E.6(22)
Wheatley, J. M. P1A.16(41)
Wolf, S. A. PL.6.1(14)
Wosik, J. P.3.23(66), P.3.24(67)
Wu, J. Z. H.7(29)
Xiong, Q. H.5(29)
Xiong, X. Z. PIB.61(57)
Xu, W. P1A.12(41)
Xue, Y. Y. D.1(20)
Yang, G. P.2.12(61)
Yang, I.-S. K.6(35)
Yeh, K.-W. PIB.56(56)
Zeldov, E. K. I.3(34)
Zhang, G. Z. P.2.11(60)
Zhou, D. P1A.21(42)
Zhou, J.-S. G.7(27)
Zhou, T. PIB.6(45)
Zhou, X. J. PIB.7(46)
Zhu, J.-X. P1A.24(43),
 P.3.16(65)
Zhu, X.-M. P.3.15(65)

10th Anniversary HTS Workshop Schedule

	Monday, March 11	Tuesday, March 12	Wednesday, March 13	Thursday, March 14	Friday, March 15	Saturday, March 16
7:30 a.m.						
8 a.m.			Press Room Open, 7:30 a.m. - 8:30 p.m., Fannin			
8:30 a.m.		Exhibits Open 8 a.m., de Zavala	Continental Breakfast, 8-8:30 a.m., Granger Foyer (Wednesday), La Salle Pre-Function Foyer (Thursday-Saturday)			
9 a.m.		Continental Breakfast 8-9 a.m., Granger Foyer	Gen. Ann., 8:30-8:40 a.m., La Salle A & B	Plenary Session 5 8:30-9:10 a.m. La Salle Ballroom A & B	Plenary Session 6 8:30-9:10 a.m. La Salle Ballroom B	Gen. Ann., 8:30-8:40 a.m., La Salle B Plenary Session 7 8:40-9:20 a.m. La Salle Ballroom B
9:30 a.m.		Opening Ceremonies 9-10:00 a.m. La Salle Ballroom A & B	Plenary Session 4 8:40-10 a.m. La Salle Ballroom A & B	Break, 9:10-9:20 a.m.	Break, 9:10-9:30 a.m.	Break, 9:20-9:40 a.m.
10 a.m.		Break, 10:00-10:20 a.m.	Break, 10-10:20 a.m.	Concurrent Sessions 9:20 a.m. - 1 p.m.	Concurrent Sessions 9:30 a.m. - 12:30 p.m.	Concurrent Sessions 9:40 a.m. - 1 p.m.
10:30 a.m.		Plenary Session 1 10:20-11:40 a.m. La Salle Ballroom A & B	Concurrent Sessions 10:20 a.m. - 12:40 p.m.	E: HTS Theory I La Salle Ballroom A & B	G: HTS Theory II La Salle Ballroom A	K: Vortex, etc. Granger B
11 a.m.			A: HTS Properties La Salle Ballroom B	F: HTS Processing Granger A & B	H: Film & Applications La Salle Ballroom B	L: Film & Properties de Zavala
11:30 a.m.			B: Bulk Applications Granger A & B			
12 noon		Box Lunch Pick-Up 11:40 a.m. - 1:20 p.m. Nautile Room, 1st Floor	Box Lunch Pick-Up, 12:40-1 p.m. Nautile Room, 1st Floor		Box Lunch Pick-Up 12:30-1:30 p.m. Nautile Room, 1st Floor	
12:30 p.m.			Press Briefing: Conf. Co-Chairs/Panel 1-1:30 p.m., La Salle Ballroom A & B	Box Lunch Pick-Up 1-2 p.m. Nautile Room, 1st Floor		Luncheon & Closing Ceremony, 1-2:30 p.m. La Salle Ballroom A & B
1 p.m.		Plenary Session 2 1:20-2:40 p.m. La Salle Ballroom A & B	Keynote Address 1:30-2:20 p.m. La Salle Ballroom A & B		Concurrent Sessions 1:40-5:40 p.m.	
1:30 p.m.		Break, 2:40-3 p.m.	Individual Interviews, 2:20-2:40 p.m.		I: Properties & Theory La Salle Ballroom B	
2 p.m.		Plenary Session 3 3-3:40 p.m. La Salle Ballroom A & B	Concurrent Sessions 2:40-6:20 p.m.	Optional Afternoon Activities	Break, 3:40-4 p.m.	
2:30 p.m.			C: Symmetry La Salle Ballroom B		J: Materials & Properties La Salle Ballroom A	
3 p.m.		Poster Sessions 1A & 1B 4-6 p.m. Granger A & B	Break, 4:20-4:40 p.m.			Optional Afternoon & Evening Activities
3:30 p.m.			D: HTS Materials Granger A & B		Poster Sessions 1B-cont, 2 & 3 5:40-7:30 p.m. Granger A & B & de Zavala	
4 p.m.						
4:30 p.m.						
5 p.m.						
5:30 p.m.						
6 p.m.						
6:30 p.m.		Welcome Reception 6-7:30 p.m. La Salle Ballroom A & B				
7 p.m.						
7:30 p.m.						
8 p.m.						
8:30 p.m.						
9 p.m.						
9:30 p.m.						
10 p.m.						

Hotel Check-In, 2 p.m. - on

Early Registration, Check-In & Manuscript Submission, 3-6 p.m., Pre-Function Foyer

Exhibitor Registration & Set-Up & Poster Sessions 1A & 1B Set-Up, 4-8 p.m.
Poster Set-Up continues Tuesday, March 12, 7:30 a.m. - 12 noon

Early Registration, Check-In & Manuscript Submission 7-9:30 p.m., Pre-Function Foyer

Poster Sessions 1B-cont, 2 & 3 Set-Up, 9-10 p.m.
Granger A & B & de Zavala
Poster Set-Up continues Friday, March 15, 7 a.m. - 12 noon

APR 190-12
STINGO

Approved for public release,
distribution unlimited